Design and Synthesis of Temperature Switchable Non-ionic Block Copolymers for Application to Oil Sands Extraction

by

Chao Han

A thesis submitted in partial fulfillment of the requirements for the degree of

Master of Science

in
Chemical Engineering

Department of Chemical and Materials Engineering
University of Alberta

Abstract

Based on the analysis of typical warm water oil sands extraction process, we investigated the use of a novel temperature switchable non-ionic block copolymer, poly (ethylene glycol)-*b*-poly (N-isopropyl acrylamide) (MPEG-*b*-PNIPAM), to enhance the bitumen recovery and the recycle of the polymer after the extraction through the temperature change in the extraction process. The temperature switchable polymer was designed to lower the interfacial tension between bitumen and water at high temperature for enhancing the bitumen liberation. When the temperature goes down, the copolymer can be recovered with process water for reuse in liberation and extraction. Two temperature switchable non-ionic block copolymers, MPEG2000-*b*-PNIPAM$_{50}$ and MPEG750-*b*-PNIPAM$_{35,}$ were synthesized and characterized by IR spectroscopy and ^{1}HNMR to elucidate the chemical structure of the two copolymers. The polymers synthesized showed good interfacial activity with temperature switchable properties. Investigations using a home-built on-line bitumen liberation analyzer showed that the synthesized polymer enhanced bitumen liberation process. The Denver flotation cell extraction tests showed an enhanced bitumen recovery by the addition of the synthesized polymers. A home-built induction timer was used to evaluate the induction time between air bubble and bitumen surfaces. The results showed that the polymer with short chain length helped reduce the induction time and could help aeration while the polymer with longer chain made aeration less favorable. By using toluene as the oil phase, we demonstrated a good recoverability of the polymer when temperature reduced to 25 ℃. It is proved that the polymer can be reused in liberation and extraction to reduce the operating cost of the process.

Preface

Part of the research conducted in this thesis forms part of a paper to be submitted to related journal.

Acknowledgement

I would like to thank my gracious supervisor Dr. Zhenghe Xu for his guidance and support throughout my project. In the past two-year, I really learned a lot from him in doing research. And he really expanded my knowledge and view of research.

I would also like to thank Dr. Qingxia Liu, Dr. Zifu Li and Dr. Lan Liu, for their insightful discussions and valuable suggestions which facilitated the progress of this project.

I am very thankful to Mr. Chen Wang, Mr. Yuechao Tang, Ms. Xurui Zhang, Mr. Rui Li, Mr. Peiqi Qiao, and Dr. Fan Yang for giving kindly help during my research, offering valuable discussions and explaining results.

I appreciate the help from Mr. Jim Skwarok, Ms. Jie Ru and Ms. Lisa Carreiro for their excellent assistance with my work. And I also would like to thank the entire oil sands extraction research group for their help and suggestions.

Finally, I appreciate the NSERC Industrial Research Chair in Oil Sands Engineering and AITF (Alberta Innovate Technology Futures) for financial support.

Nomenclature

CHWE: Clark Hot Water Extraction

CSS: Cyclic Steam Stimulation

SAGD: Steam Assisted Gravity Drainage

WWBE: Warm Water Bitumen Extraction

PSV: Primary Separation Vessel

PSC: Primary Separation Cells

IFT: Interfacial Tension

EDL force: Electric Double Layer force

VDW force: Van der Waals force

NIPAM: N-isopropyl acrylamide

PNIPAM: poly (N-isopropyl acrylamide)

$PNIPAM_{50}$: poly (N-isopropyl acrylamide) with 50 repeating units

$PNIPAM_{35}$: poly (N-isopropyl acrylamide) with 35 repeating units

MPEG: methyl poly ethylene glycol mono ether

MPEG2000: methyl poly ethylene glycol mono ether with a molecular weight of 2000

MPEG750: methyl poly ethylene glycol mono ether with a molecular weight of 750

DBL: Degree of Bitumen Liberation

ATRP: Atom Transfer Radical Polymerization

Table of Contents

List of Figures

List of Tables

List of Schemes

Chapter 1. Introduction

1.1 Introduction to Alberta Oil Sands

Oil sands, which are also known as tar sands or bituminous sands are a type of unconventional petroleum deposit.[1] Oil sands are either loose sands or partially consolidated sandstones containing sands, clays, water and extremely viscous petroleum technically referred to as bitumen (Figure 1).[2-4] Canada has the largest oil sands reserve in the world which takes 97% of Canadian's total crude oil reverse and makes Canada the third largest crude oil proved reserve in the world by the end of 2013, only after Saudi Arabia and Venezuela.[5]

Figure 1. Oil sands Ore (left); Oil sands structure schematic (right).[2, 3]

Canadian oil sands are mainly located in the Athabasca region in Alberta, with the rest in Peace River and Cold Lake area (Figure 2).[6] In 2013, the crude oil production from oil sands in Canada has exceeded 1.9 million barrels/day comparing 1.5 million barrels/day from conventional crude

oil. Alberta's crude oil production took 76% of total crude oil production in Canada.[5] It is also predicted that the total crude oil produced from the oil sands in Alberta can grow to 3 million barrels/day by 2020.[7]

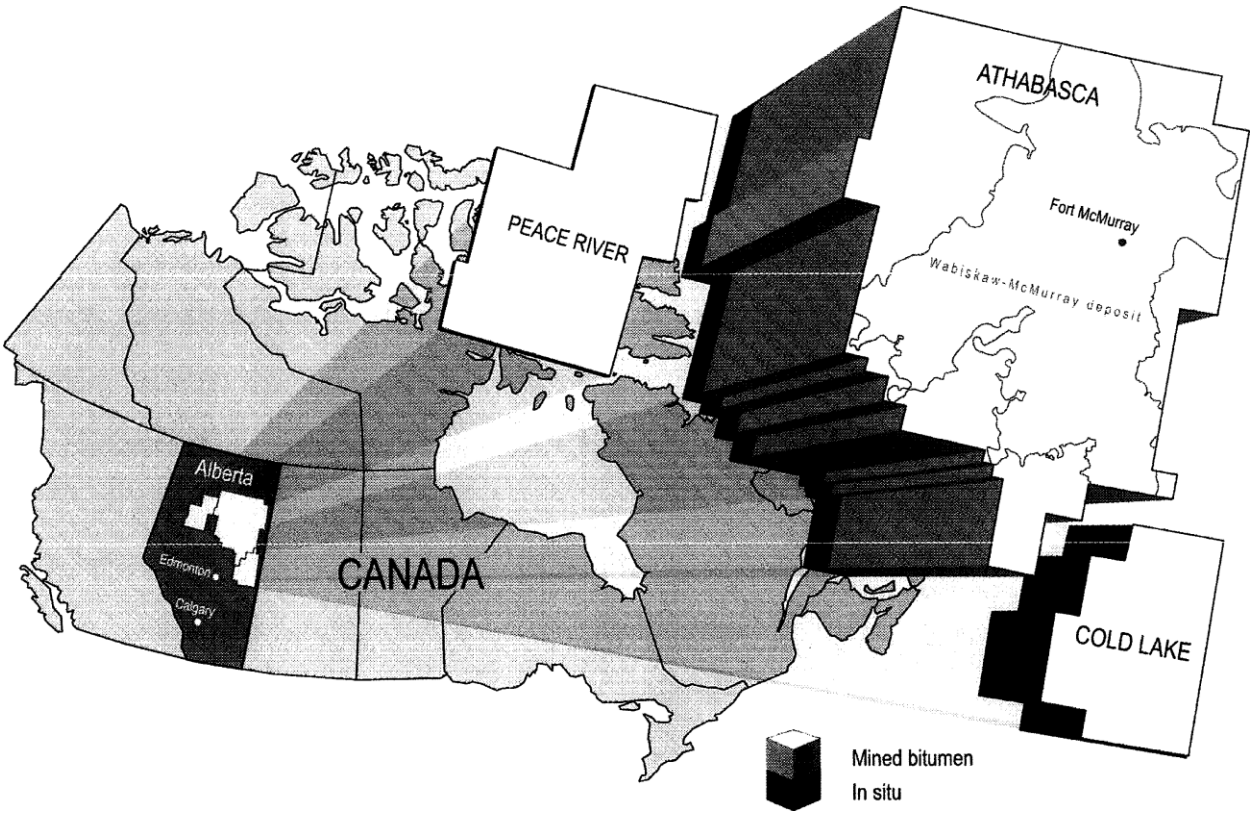

Figure 2. Map of oil sands reserve in Alberta.[6]

1.2 Overview on Oil Sands Extraction

The bitumen from oil sands is basically recovered by two major methods: surface mining (open-pit mining) process and *in-situ* technology. Surface mining process requires the removal of forest and layers of overburden (muskeg and topsoil) to expose the oil sands, and is usually applied to the deposits less than 75 m under the ground.[1, 7] And Clark Hot Water Extraction (CHWE) process

and its modified processes are used to extract bitumen from the mined oil sands.[8-12] For the *in-situ* extraction process, two major technologies are widely and commercially used, Cyclic Steam Stimulation (CSS) and Steam Assisted Gravity Drainage (SAGD), and the depth of the deposits is usually more than 100 meters.[13-15]

1.2.1 Surface Mining

Clark Hot Water Extraction (CHWE) process was developed by Dr. Karl Clark and his colleagues at Alberta Research Council in 1920s and it is widely implemented in commercial operations by different oil sands operators for open-pit mining process.[4, 8-12]. Considering the reduction of energy cost and cut of greenhouse gas emission, the process temperature is now reduced to around 45 to 55 ^{o}C from around 80 ^{o}C, which is referred to as warm water bitumen extraction (WWBE) process.[16] A general scheme for oil sands processing of surface mining is shown in Figure 3.

Generally, shovels and trucks are used to dig oil sands up and transport ores from sites to extraction plants. Then the oil sands lumps are crushed and mixed with hot steam/hot water in mixing boxes, stirred tanks, cyclo-feeders (Syncrude) or rotary breakers (Suncor and Albian).[4] Usually, at this stage the chemical additives are added to enhance the bitumen extraction process. Then the slurry is fed to hydrotransport pipelines or tumblers to further reduce the ores' size and apply shear force to the sand grains. The main idea of this stage is to separate bitumen droplets from sand grains, so the liberated bitumen can be attached to the entrained or introduced air bubbles. Typically, 40 to 55 ^{o}C is the operation temperature of the slurry. Then the slurry is pumped into the so called primary separation vessel (PSV), separation cells (Sep Cell) or primary separation cells (PSC), and the froth formed can float to the top (the bitumen's density is reduced due to the attachment to air bubbles and increasing temperature). Then the froth is skimmed out for

froth treatment. As some un-aerated bitumen droplets remain in slurry, mechanical floatation cells, cyclo-separators or hydrocyclones are used to recover more bitumen from the slurry. The unrecovered bitumen, water and solids are referred as tailings and pumped to the tailings ponds.[17]

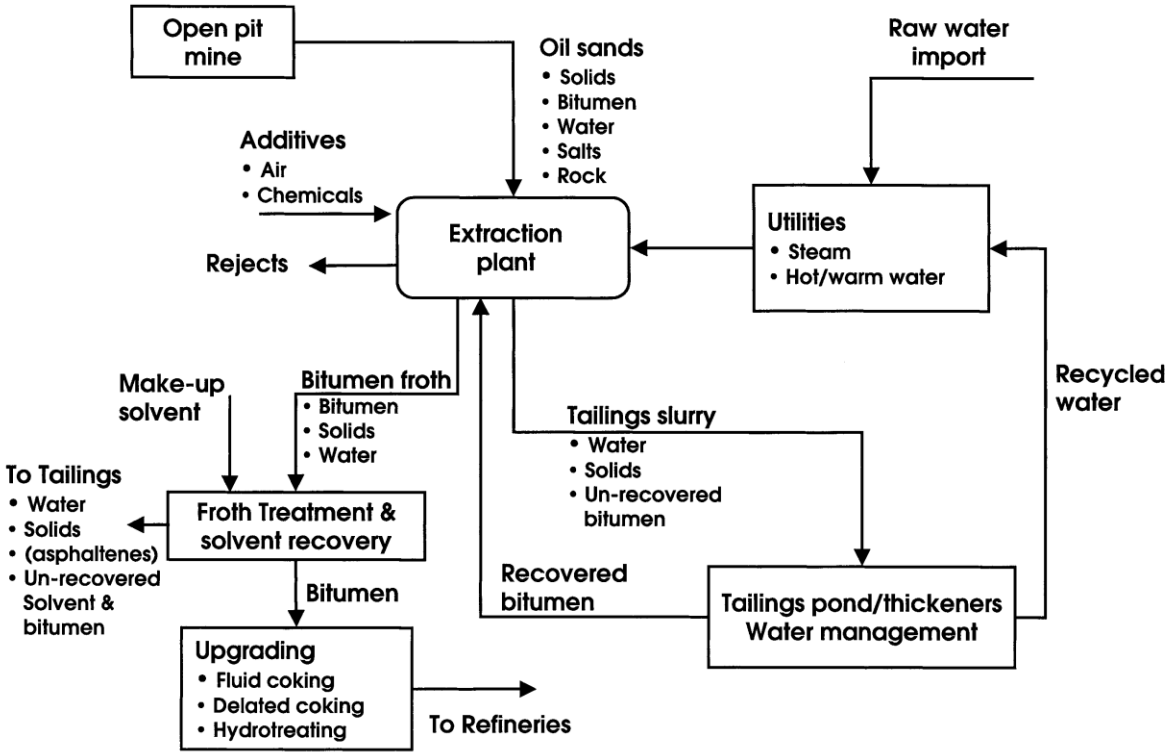

Figure 3. A generalized scheme for oil sands processing in surface mining process.[4]

Typically, bitumen froth from PSV contains 60% bitumen, 30% water, and 10% solids. Further froth treatment is needed to get rid of the water and solids since both solids and water are detrimental for downstream upgrading processes. The collected bitumen froth is first de-gassed and then diluted with organic diluents (naphtha or paraffinic solvent) to introduce enough density difference among bitumen, water and solids, so the water and solids can be separated from diluted

bitumen solution by using inclined plate settlers, centrifuges or cyclones. Presently, naphtha is used by Suncor, CNRL and Syncrude for froth treatment while Albian uses paraffinic diluent in their froth treatment plants.[18] At a certain ratio of bitumen to paraffinic diluent, about 30% to 50% of the asphaltenes inside the bitumen with fine solids and emulsified water can be precipitated out.[17] The unrecovered bitumen, water, and solids (might contain asphaltenes) after the froth treatment are pumped into tailings ponds as well and the water there can be recycled for further process after settling.

In water based oil sands extractions process, the tailings slurry produced is an alkaline aqueous suspension that contains 55 wt% solids, of which 82 wt% is sand, 17 wt% are fines smaller than 44 μm and 1 wt% bitumen residue.[19] The tailings slurry comes from both the separation vessels and froth treatment stage and are discharged into tailings ponds (Figure 4). As the intake amount of fresh water is strictly limited by legislation, the tailings need to be treated and the process water can be recycled and reused, also, the tailings ponds can be reclaimed.[19, 20]

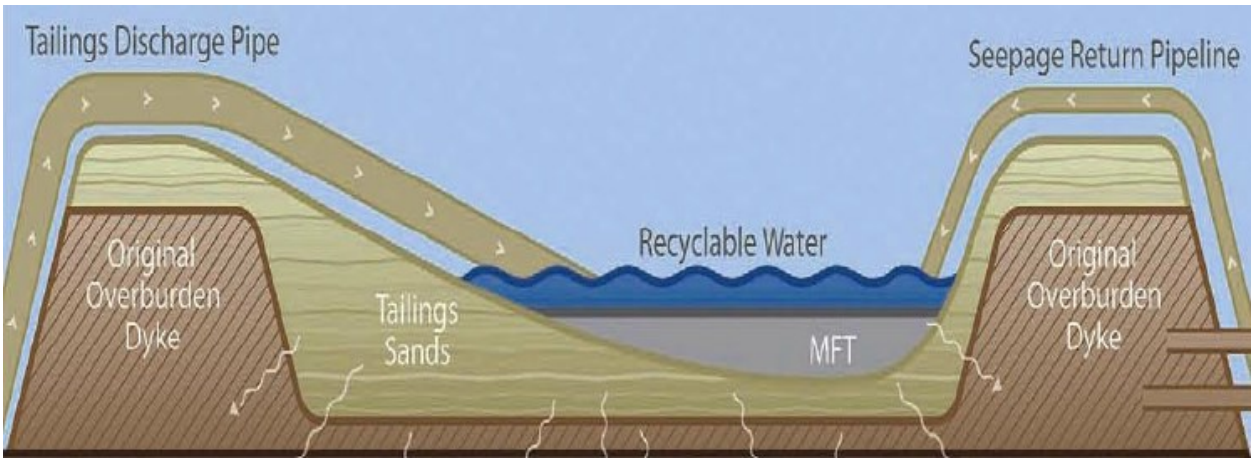

Figure 4. A schematic diagram of tailings pond.[16]

1.2.2 *In-situ* Extraction Processes

For the ores located underground with a depth more than 100 meters, *in-situ* methods such as CSS and SAGD are commercially used to recover the bitumen from Alberta's oil sands.

In CSS process, high pressure and high temperature steam is injected into oil sands deposits. Then the oil sands underground are fractured by the high pressure of the high temperature steam and the bitumen contained in the ores is melt. With the soaking effect of the steam, the mixture of bitumen and water can flow to the producing well and is collected and pumped up to the ground surface (Figure 5).[21] Typically, the process is preferred for thick, high-quality reservoirs.[22]

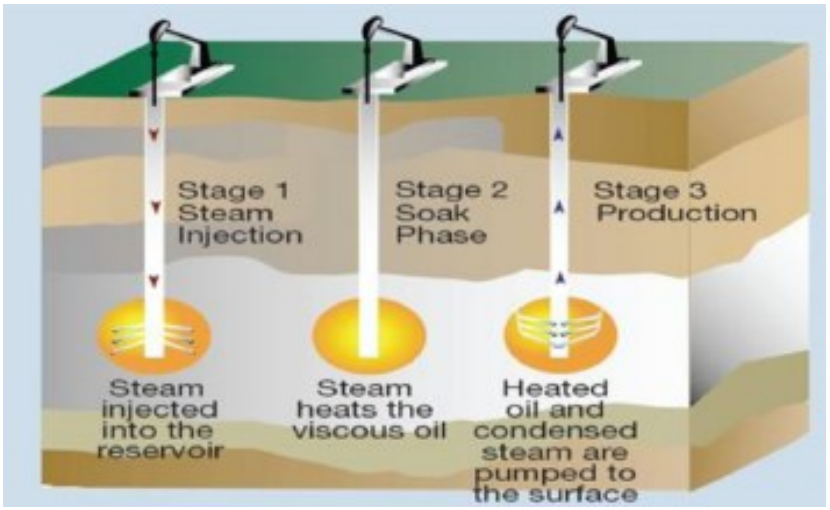

Figure 5. Schematic of cyclic steam stimulation (CSS) process.[21]

SAGD process is the most popular enhanced oil recovery technology adopted by Canadian heavy oil producers currently.[7] It requires drilling two parallel wells horizontally in the oil sands formation. The high temperature steam is injected into the formation through the upper well and form a high-temperature steam chamber. And the lower well is located below and parallel to the steam injection well to collect the melt bitumen and condensed water (Figure 6, 7, 8).[7, 23, 24]

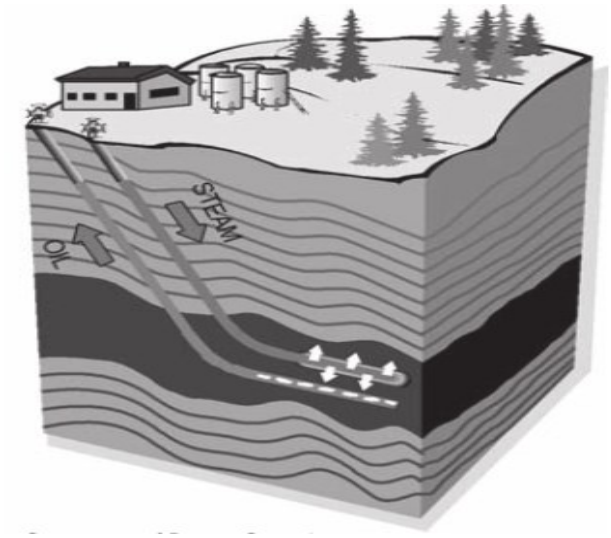

Figure 6. Schematic diagram of SAGD process.[7]

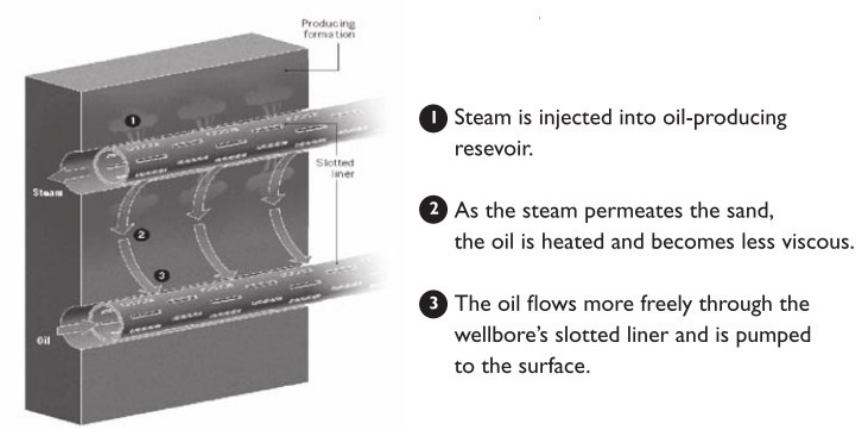

Figure 7. Schematic diagram of three steps of SAGD.[7]

Usually around 25% to 75% of the bitumen is recovered by using SAGD process, though the recovery is lower than typical surface mining process. However, 90 % of the water can be recycled and the water is injected into the bitumen-drained area to maintain the stability of the deposit.[7] One of the advantages of SAGD process is it doesn't produce tailings pond, which is a huge problem for open pit mining process.

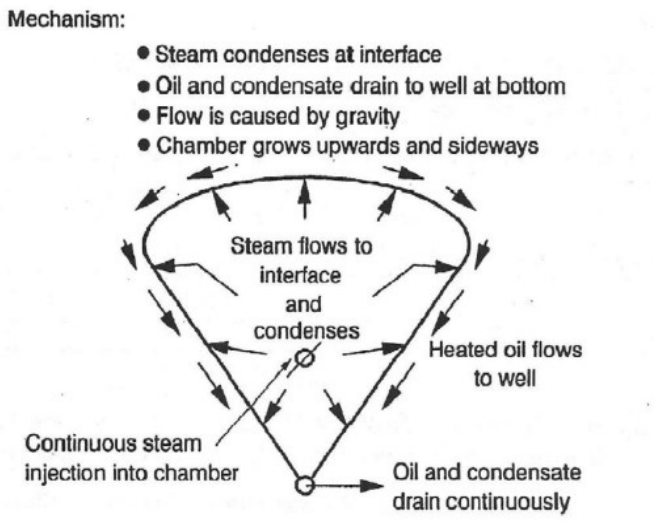

Figure 8. Mechanism of SAGD process.[23, 24]

Other *in-situ* extraction methods of oil sands like Vapor Extraction Process,[25] Toe to Heel Air Injection[26] and Supercritical Fluid Extraction[27] are also available.

1.3 Problems and Project Objectives

To maximize the bitumen recovery efficiency is one of the main tasks in oil sands surface mining extraction process since the higher the efficiency is, the more profits for oil sands operators. Much efforts have been made to achieve high bitumen extraction efficiency by invoking different chemical aids that will be discussed in Chapter 3.

In our project, we designed, synthesized and characterized a type of non-ionic temperature responsive block copolymer which can help facilitate the bitumen recovery of oil sands extraction and can be potentially used and recycled in surface mining process with water. As the polymer can be reused and can increase the extraction efficiency, it would help the operators to reduce the environment impact from oil sands industry.

Chapter 2. Review on Colloid Science Involved in Oil Sands Extraction

2.1 Basics on Colloid Science

Colloids are usually defined as disperse systems in which one phase has dimensions in the order of 1 *nm* to 1 μm.[28, 29] A colloids system usually consists of grains or droplets of one phase in a matrix of the other phase. Different kinds of colloid systems can be formed such as aerosol, foam, emulsion, sol, solid emulsion *etc.* During the oil sands extraction process, several colloids systems are formed such as oil-in-water emulsion, water-in-oil emulsion, middlings and fine tailings. Understanding the basic principles in colloid science is very important to ones dealing with the extraction condition and related processes.[16]

2.1.1 Surface/Interfacial Tension

Surface tension, or surface free energy is usually defined as the increase in the Gibbs free energy per increase in surface area of liquid-gas interface at constant temperature (T), pressure (P) and molecules (N_i).[30] When it refers to a liquid-liquid or solid-liquid system, it is called interfacial tension.

$$\frac{\partial \mathrm{G}}{\partial \mathrm{A}}\Big|_{T,P,N_i} = \gamma \qquad [1]$$

It should be noted that the dimension of surface or interfacial tension is given in unit of energy per unit area (J/m^2), which is the same as the unit of force per unit length (N/m).[29, 30]

2.1.2 Young's Equation

It is quite common in real colloid system that three different phases are present, *e. g.* bitumen, sand grains and water all exist in slurry during extraction process. Interesting phenomena can be

observed at the line where the three phases meet, which is referred to as three phase boundary. This situation is the main case when bitumen recesses from sand grains during the extraction process. One can consider the force balance at the three-phase contact line, where the net force acting on the contact line should be zero (Figure 9). If we assign $\gamma_{B/W}$, $\gamma_{B/S}$ and $\gamma_{S/W}$ as the interfacial tension of bitumen/water, bitumen/sand grains and sand grains/water, and θ is the contact angle, we can get equation 2.[29,30]

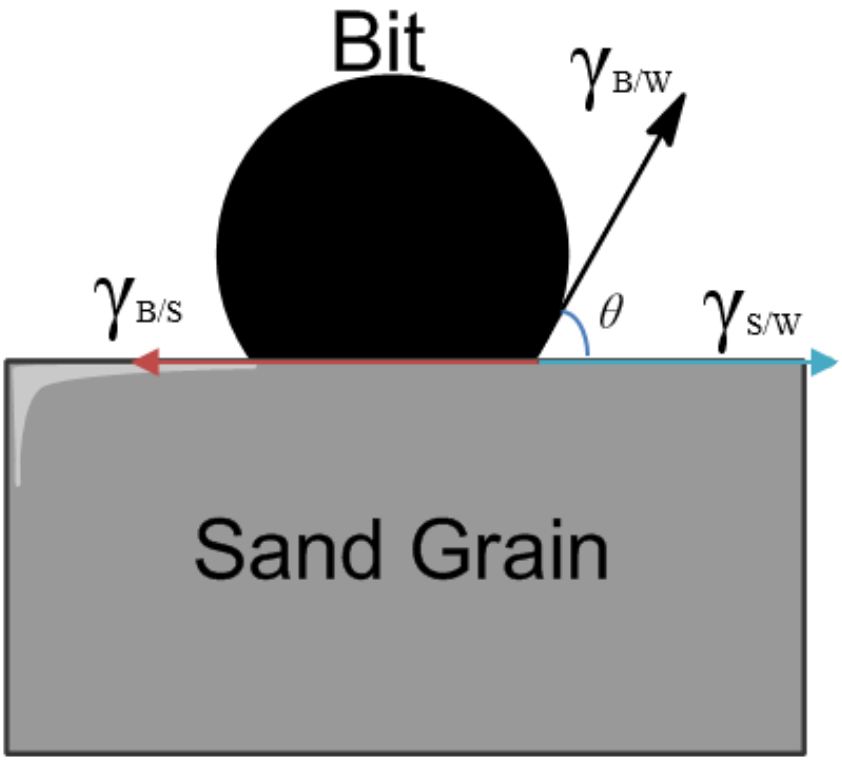

Figure 9. Contact angle (θ) of bitumen on sand grain in water phase.

Equation 2 is named as Young's equation, after Thomas Young, who first introduced it in 1805.[29-31]

$$\gamma_{B/S} = \gamma_{B/W} \cdot \cos\theta + \gamma_{S/W} \quad [2]$$

2.1.3 Electric Double Layer

The surfaces between phases are electrically charged, which can be originated from several different reasons like the adsorption of ions from neighboring solution on an initially uncharged solid surface, dissociation of surface groups, *etc.* As we are mostly interested in bitumen extraction from oil sands, we deals with the charged interfaces like oil and water, solid and water, or air bubbles and the phases mentioned above.

If we take the sand grains immersed in water phase as an example, we would have the equilibrium at the interface between SiO_2 and water shown in Scheme 1.

$$(SiO)_s + H_2O \rightleftarrows (H_2SiO_3)_s \rightleftarrows (HSiO_3^-)_s + H^+$$

Scheme 1. Reaction of silica with water.

The scheme shows that the sand grains surface can react with water and form silicic acid. And the dissociation will release proton into water phase and leave a negatively charged surface behind. As we know that the bulk mixture is neutral, the surface charge of the sand grains' surface should be neutralized in the solution.

Briefly, surface charges on the sand grains cause an electric field, which attracts counter ions. The layer of surface charges and counter ions is called "electric double layer". In the years 1910–1917, Gouy and Chapman revised the double layer model by considering the thermal motion of the ions, which is not considered in Ludwig Helmholtz model.[32-35] In Helmholtz model, the counter ions are pictured as a layer of ions binding to the charged surface directly, while by taking the thermal motion of the ions into account, Gouy and Chapman proposed that the thermal fluctuations tend to drive the counter ions away from the surface and form a diffuse layer, which is more extended than a molecular layer shown in Figure 10.

Later, Debye and Hückel calculated the potential and ion distribution around spherical surfaces.[29] Based on their research, when two charged colloidal particles approach to each other in a medium containing ions, they interact with each other through their double layers. The potential energy of interactions (per unit area) resulting from double layer overlapping is repulsive if they are made of same materials, further detailed calculations can be found elsewhere.[29, 36]

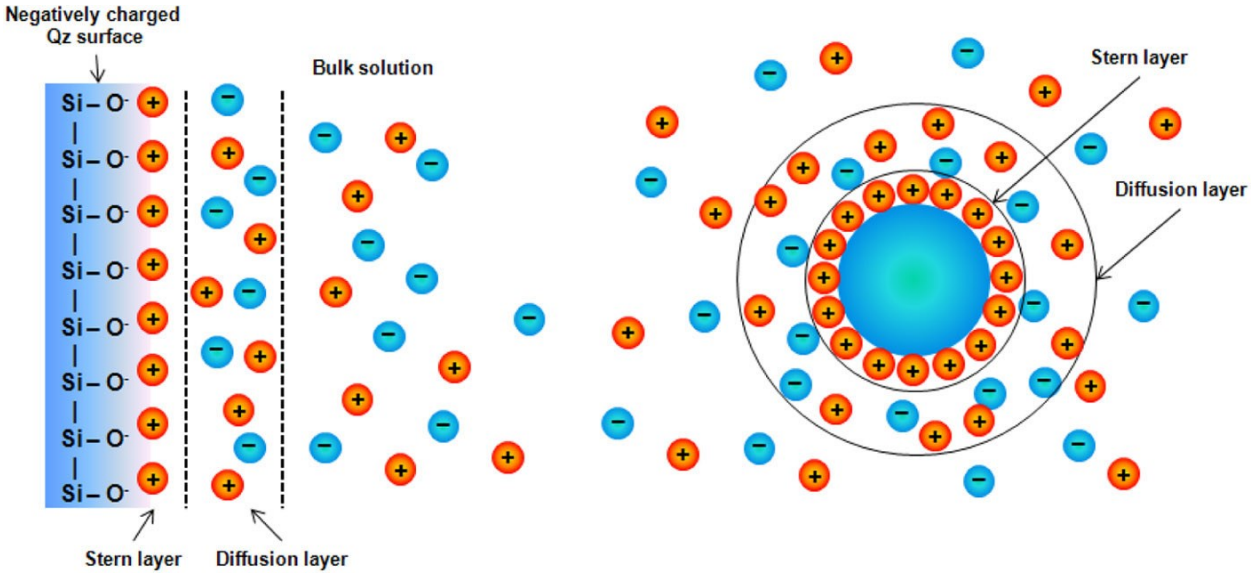

Figure 10. Electric double layer model for negatively charged surface.[37]

2.1.4 Van der Waals Force

Van der Waals force, also known as intermolecular forces, typically includes dipole-dipole interaction, dipole-induced dipole interaction and dispersive interaction.[36]

Dipole-dipole interaction originates from the molecules that have permanent electric dipole moments. Averaging the dipole-dipole interaction energy over all possible orientations results in

the net dipole-dipole attraction $V_{d-d} = -\beta_{d-d} r^{-6}$, β_{d-d} is the characteristic constant depends on the dipole strength, and r is the distance between the two dipole centers.[36]

Dipole-induced dipole interaction is the interaction between a molecule with permanent dipole and a non-polar molecule. The non-polar molecule is polarized by the first one and gets an induced dipole. The overall interaction of dipole-induced dipole is $V_{d-id} = -\beta_{d-id} r^{-6}$, β_{d-id} depends on the first molecules dipole strength and the second molecule's polarizability.[36]

Dispersive interaction originates from the fluctuation of electron position in each molecule. The transit dipole moment can be formed for a very short time, but it creates induced dipole moments and results an overall attraction.[36]

All these three components of intermolecular attraction energy decays with the sixth power of the distance $V = -\beta r^{-6}$, where β is a constant.[36] For simple geometries, the van der Waals energy can be expressed by formula with a constant called Hamaker constant. Briefly, when the effective Hamaker constant is positive, the interaction between two particles is attractive.

In the case of the interaction of a bitumen droplet with an air bubble through water, the expression of an effective Hamaker constant takes the form $A_{123} = \left(\sqrt{A_1} - \sqrt{A_2}\right)\left(\sqrt{A_3} - \sqrt{A_2}\right)$, where A_1 and A_3 stand for bitumen and air, respectively; A_2 is the Hamaker constant for medium water.[36] As $A_1 \approx 5.4 \times 10^{-20}\ J, A_2 = 3.7 \times 10^{-20}\ J, A_3 = 0\ J$, we have $A_{132} < 0$. This indicate when air bubbles interact with bitumen through water, the van der Waals force repel the bitumen from the bubbles.

2.1.4 DLVO Theory

As described in 2.1.1, the increase of interfacial area increases the total energy of the system. Intrinsically, colloids system are thermodynamically unstable and should be spontaneously evolve and the dispersed phase should aggregate to lower the entire energy of the whole system.[36] However, we can still encounter many colloid systems that are highly stable for a very long period, for example, the mature fine tailings (MFT) from the tailings ponds of oil sands industry can be extremely stable for tens of years that makes the MFT's settling a huge problem to oil sands open-pit mining industry. DLVO theory is the first successful theory to explain the colloids stability named after Derjaguin, Landau, Verwey and Overbeek.[38-40]

In DLVO theory, the coagulation of dispersed particles is explained by the interplay between two forces: the attractive van der Waals force and the repulsive electrostatic double-layer force.[29]

$$E = E_{vdW} + E_{DL} \qquad [3]$$

The van der Waals interaction energy, the double layer repulsion, and the total interaction energy for two identical spherical particles are shown in Figure 11.

The van der Waals interaction energy between two identical particles are always attractive regardless of the medium. The double layer force are repulsive and decays quickly with increasing distance. The total interaction energy is weakly attractive when the distance between the two particles are relatively large. The attractive energy gets stronger and stronger when the two particles approach to each other and reaches the secondary minimum of the total energy. This secondary energy minimum can lead to a weak, reversible coagulation without leading to direct molecular contact between the particles.[29] After that, the double layer repulsive force becomes

override the van der Waals force and the total energy goes up to make the total energy repulsive at intermediate distances. Finally, if the two particles have the energy to jump across the repulsive energy barrier, the van der Waals force dominates again and makes the two particles strongly attractive to each other (primary energy minimum), which leads to precipitation. In addition, the surface potential usually decreases with increasing salt concentration that can lower the energy barrier of the repulsive double layer force. More detailed calculations can be found elsewhere.[36, 41-43]

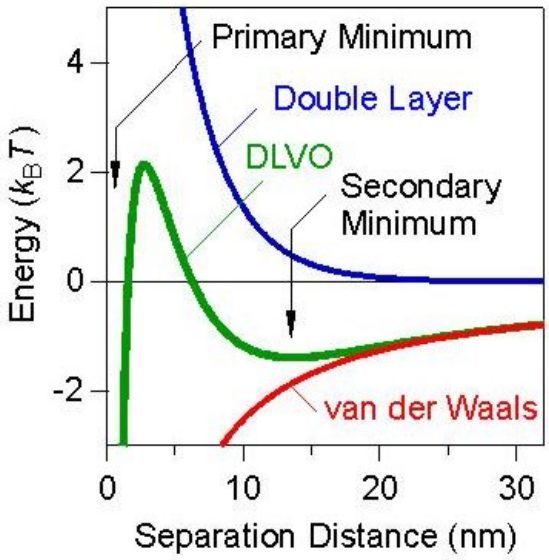

Figure 11. Schematic of van der Waals attraction, double layer repulsion, and total interaction energy for two identical spherical particles.[36, 41-43]

2.2 Elementary Steps in Water-based Bitumen Extraction

As mentioned in Chapter 1, the micro structure of oil sands ores is proposed to be each sand grain surrounded by a thin film of water and a thin film of bitumen. In order to recover bitumen from the oil sands-water slurry, the ores have to be disintegrated and the bitumen has to be first separated from the sand grains and then get collected.[44] The separation of bitumen from sand grains is

referred to as bitumen liberation. The dispersed bitumen droplets can collide and fuse into bigger ones which is referred to as coalescence. As the bitumen droplets can collide with air bubbles, some of these collisions result in bitumen aeration. These bitumen-air bubble aggregates can float to the surface of separation vessel due to the sufficient buoyancy force, which is known as flotation process. Basically, liberation, aeration are the elementary process in bitumen recovery. However, there is no reason to believe that the aforementioned steps occur sequentially. It is quite likely that air engulfing or entrainment could assist bitumen liberation.[4]

2.2.1 Bitumen Liberation

Bitumen liberation is a key step in bitumen extraction process, which is defined as the detachment or separation of bitumen from sand grains in aqueous phase. With detailed investigation of the liberation, it can be broken down to two sub-steps: bitumen recession on the sand grain surface, and bitumen separation from the sand grain.[44]

Bitumen recession on sand grains refer to the process that the decreasing of contact area between bitumen film and sand grains as shown in Figure 12.

Figure 12. Bitumen recession and liberation.

As the change of interface area of bitumen-water is negligible and the interface of bitumen-sand interface ($\gamma_{B/S}$) is replaced by the water-sand interface ($\gamma_{W/S}$). We can easily get the Gibbs free energy change (ΔG) for a given interfacial area (ΔA) during recession is:

$$\frac{\Delta G}{\Delta A} = \gamma_{W/S} - \gamma_{B/S} \quad [4a]$$

Input Young's equation,

$$\gamma_{B/S} = \gamma_{B/W} \cdot \cos\theta + \gamma_{S/W} \quad [2]$$

we can get:

$$\gamma_{B/S} - \gamma_{W/S} = \gamma_{B/W} \cos\theta \quad [4b]$$

So we have:

$$\frac{\Delta G}{\Delta A} = -\gamma_{B/W} \cos\theta \quad [4c]$$

Equation 4 shows: in order to make the recession process spontaneously, we should make the contact angle θ smaller than 90°. Otherwise, the Gibbs free energy of the recession process would be positive and the process is thermodynamically unfavorable. As we aforementioned in Chapter 1, caustics are often added in bitumen extraction process, and the alkaline condition and high pH can hydrolyze the surface of sand grains and make sands more hydrophilic, which reduce the contact angle θ and lead to more negative Gibbs free energy to facilitate the recession process. However, we should also notice that the addition of caustic helps release surfactants in bitumen and reduced the interfacial tension between bitumen and water ($\gamma_{B/W}$), which is not favorable for recession.[44] The entire effect of using caustics is a comprehensive result.

After the bitumen recesses to a certain shape, the bitumen droplets will detach from sand grains as shown in Figure 12. In the process, the bitumen-sand grain interface changed into bitumen-water and sand-water interface. By considering the Gibbs free energy (ΔG) associated with the

detachment process, we can get Gibbs free energy change for the interface change of a given area (ΔA):

$$\frac{\Delta G}{\Delta A} = \gamma_{S/W} + \gamma_{B/W} - \gamma_{B/S} \quad [5]$$

According to Young's equation, we can get:

$$\frac{\Delta G}{\Delta A} = \gamma_{B/W}(1 - cos\theta) \geq 0 \quad [6]$$

As the Gibbs free energy of bitumen detachment is positive, it is thermodynamically unfavorable. If we want bitumen liberate from sand grains at static condition, the sand grains have to be complete hydrophilic and have a 0^o contact angle. However, the lumps and sand grains can get the compensate energy of the interfacial energy gained from mechanical shear in practical production.

In order to facilitate the detachment of bitumen droplets from sand grains thermodynamically, we should consider reducing both $\gamma_{B/W}$ and contact angle θ. Usually, the addition of caustics can help extract natural surfactant from bitumen bulk phase. Naturally existing carboxylic acids and acidic compounds can be deprotonated and turn to correlated anion, which are usually more interfacial active than their neutral forms. So with the presence of caustics, the natural surfactants help reduce the interfacial tension between bitumen and sand grains $\gamma_{B/W}$. At the same time, high pH hydrolyzed the sand grain surfaces, which increase the wettability of sand grains and lower the contact angle θ.

In reality, the liberation rate of bitumen from sand grains not only depends on the interfacial tension $\gamma_{B/W}$ and contact angle θ, but also on temperature, shear rate, bitumen original layer's shape and electric surface potential, *etc.*[16, 45]

2.2.2 Bitumen Aeration

The aeration of bitumen is another key step in bitumen extraction and is the process of attachment between bitumen and air bubbles. As bitumen has similar density with water, after bitumen liberated into water phase, the bitumen droplets still suspended in slurry if there are no air bubbles attached to them. The aerated bitumen would have lower density and can float to the surface of separation vessel as froth. However, aeration is not a sequential process that has to occur after bitumen liberation. There is report that aeration of bitumen can assist bitumen liberation.[44, 46]

As shown in Figure 13, the aeration process can be analyzed from thermodynamically view as follows.

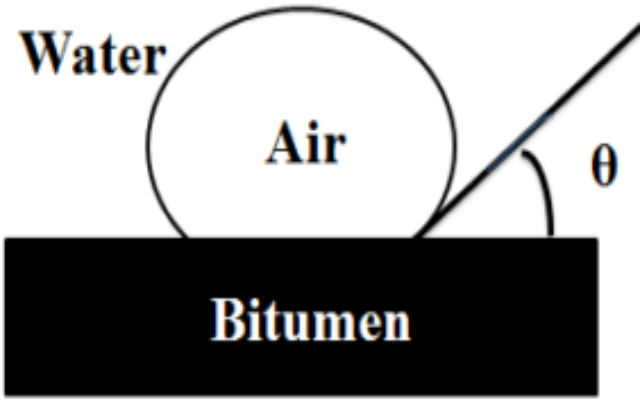

Figure 13. Contact angle of air bubble on bitumen surfaces.

The Gibbs free energy change in the process can be described in equation 7, where the subscripts A, B, and W represent air, bitumen and water, respectively.

$$\frac{\Delta G}{\Delta A} = \gamma_{B/A} - (\gamma_{B/W} + \gamma_{A/W}) \quad [7]$$

If we input Young's equation into equation 7, we can get Gibbs free energy change of aeration using equation 8:

$$\frac{\Delta G}{\Delta A} = \gamma_{A/W}(\cos\theta - 1) \quad [8]$$

As $\cos\theta \leq 1$, we can easily conclude that the aeration process is thermodynamically favorable when $\theta > 0$. However, reducing of surface tension and smaller contact angle would be less favorable for aeration process.[44]

Further investigation shows that the contact angel of water and bitumen is related with solution's pH.[47] The increase of pH would decrease the contact angle of water on bitumen and the surface tension of water. These two factors would be undesirable for bitumen aeration thermodynamically.[44]

2.3 Bitumen Flotation

In oil sands extraction, flotation technic is used to float fine, fugitive bitumen droplets in primary separation vessel. In bitumen flotation step, air bubbles are generated and used as carriers to attach to bitumen droplets and bring the bitumen droplets to the top of separation vessels.[44]

For a stable attachment of air bubble to bitumen droplets, the time required for thin film rupture to form three phase contact line is referred to as induction time of bubble-bitumen attachment. The collision time of air bubble and bitumen droplets has to be longer than induction time to make attachment happen.

As discussed in section 2.2.2, the total Gibbs free energy change of aeration is negative when we have $\theta > 0$. It's thermodynamically favorable for air bubble attach to bitumen droplet. However, there is a thin intervening water film between air bubble and bitumen surface when they approach to each other. In order to achieve attachment of air bubble to bitumen, the thin film has to be ruptured. The energy barrier of thinning the liquid film plays a critical role in determining the induction time upon contact.

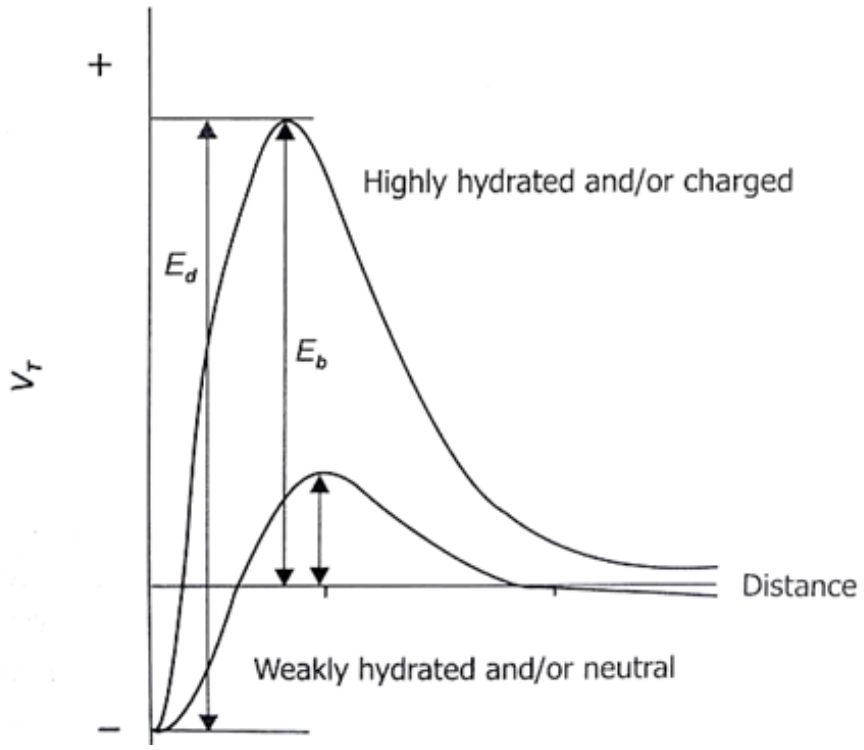

Figure 14. Schematic diagram of the energy profiles (V_T) between a bitumen droplet and an air bubble as a function of distance between the two in aqueous solution. E_b stands for energy barrier, E_d for detachment energy.[44]

A schematic diagram of the energy barrier, E_b, for the thinning of the intervening liquid film is shown in Figure 14. The energy barrier can be calculated by DLVO theory, which solely considers

the double layer force and van der Waals force. Both the double layer force and van der Waals force are repulsive between bitumen droplets and air bubbles.[36, 48]

However, DLVO theory is inadequate to describe the bubble-bitumen attachement as there is a high energy barrier for negatively charged bubbles and bitumen surface. In fact, attractive force originating from surface hydrophobicities is the only driving force for bitumen-bubble attachment, which is referred as hydrophobic force.[44, 48, 49]

In 1992, Luttrell and Yoon proposed the probability of bubble-particle adhesion P_A by using an analogue of the chemical reaction rate theory.[48]

$$P_A = \exp(-\frac{E_b}{E_k}) \quad [9]$$

E_k stands for the kinetic energy imparted on colloidal particles by mixing while E_b represent the energy barrier. From the equation we can see the lower E_b, the higher the possibility of bitumen-bubble attachment. For calculation of energy barrier of E_b, classical DLVO expression cannot be applied, and the expression based on extended DLVO theory considering the hydrophobic force should be used and the theory detail can be found elsewhere.[48]

In terms of increasing the probability of bubble-bitumen attachment, it is usually a comprehensive consideration of multi-faceted effects. Typically, decreasing surface potential will lower the double layer repulsive force; a higher electrolyte concentration will reduce the repulsive force; smaller bubbles lead to a high collision rate and facilitate bubble-bitumen attachment upon collision; addition of surfactant can usually help generate smaller air bubbles but an additional force is required to push the surfactant molecules away from the contact area, which would increase the energy barrier.[36, 44, 48, 50]

Chapter 3. Review on Chemical Aids Used to Enhance Bitumen Recovery

In order to enhance the recovery of bitumen from water-based oil sands extraction in industry, especially for the low grade ores (high fine solids content, low bitumen content), different chemical aids were used during the bitumen extraction process.[51-56]

3.1 Caustics

Caustics are the most commonly and widely used chemical additives to increase bitumen recovery by enhancing the liberation process.[57]

3.1.1 Sodium Hydroxide

For typical caustic like NaOH, it can enhance the bitumen liberation stage by: (i) increasing the pH of slurry, deprotonating and ionizing the natural surfactants, (ii) helping the natural surfactants released from the bitumen, (iii) improving the wettability of sand grains by hydrolyzing the sand grain's surface layer, (iv) dispersing the clays by imposing negative charges on the edge of clays, (v) scavenging the divalent cations inside the process water and form related carbonate.[51]

At high pH, the natural surfactant can be extracted to the bitumen-water interface and be negatively charged. The ionized surfactants become more surface active and attach to the interface between bitumen droplets and water, which help lower the interfacial tension (IFT) and hence, improve the liberation process. The sand grain surface is highly hydrolyzed due to the base and create mostly hydroxyl groups (-OH) and negatively charged sites ($-O^-$), leading to a small contact angle and helping the bitumen to detach from the sand grain. The more hydrophilic sand grain surfaces would less favor to stick to bitumen, which would enhance the liberation process.

However, the increasing of pH by addition of NaOH is detrimental to aeration of bitumen droplets. The ionized natural surfactants such as naphthenic acid with negative charges generated by caustic addition could make bitumen droplets and air bubbles more hydrophilic, which makes it more difficult for attachment by increasing of double layer repulsive force, imposing a stable liquid film between bitumen and air bubbles.[51, 58, 59] The released surfactants also help reduce the contact angle of air bubble which makes it harder for air bubbles to attach to bitumen droplets.

In order to get high recovery of bitumen, a trade off both liberation and aeration was made in oil sands extraction. The optimized pH with addition of NaOH is around 8.5 to 9.0, which could give fairly good bitumen liberation. And at the same time, it gives acceptable efficiency of air bubble/bitumen attachment.

3.1.2 Ammonium Hydroxide

Ammonium hydroxide was investigated as caustic and its effect on the sub-processes in oil sands extraction was analyzed.[51] Comparing with NaOH, ammonium hydroxide showed continuous increase of bitumen recovery when the pH of slurry goes higher.[51] More detailed study showed that the ammonium hydroxide addition made the bitumen surface more hydrophobic, less negative charges on air bubbles and bitumen droplets which is beneficial to the extraction process.

3.1.3 Lime

Lime (CaO or $Ca(OH)_2$) was also reported to promote the liberation of bitumen from sand grains and the detachment of clay particles from bitumen droplet.[60] The attachment of bitumen to air bubbles was enhanced when the dosage is between 30-200 ppm based on the ores at the slurry pH around 8-9.[61] Inside the patent, the author explained the mechanism as follows: the water soluble

asphaltic acids are surface active and they exist at bitumen-water interface as surfactants. They can reduce or eliminate the activity of Ca^{2+} and Mg^{2+} ions binding to the clay particles and bitumen droplets.[60] The detachment of clay particles promotes the attachment of air bubbles to bitumen droplets, which enhances the bitumen recovery.[60]

3.2 Amine Compounds

3.2.1 Short Chain Amines

Three types of short chain amines, *n*-propylamine, *n*-butylamine and *n*-pentylamine were tested to improve the bitumen recovery from weathered/oxidized oil sands ores.[56] Xu *et al.* found that the amines can reduce the induction time between bitumen surface and air bubbles, which may be the key reason for facilitating bitumen recovery. 10 mM of *n*-butylamine solution at pH 8.5 gave the minimum induction time and resulted in the best bitumen recovery enhancement around 20%.[56]

3.2.2 Alkanol Amines

The alkanol amines are a type of chemicals having a formula R_xNH_{3-x} where R is a hydroxyl alkyl and x is 1-3.[62] Klimpel and Fee found that monoethanolamine and diethanolamine are particularly useful as flotation promoters to enhance bitumen recovery. The amines can be used alone or in combination with sodium hydroxide. The dosage of NaOH and alkanol amine required is determined by ores' quality.[61, 62]

3.3 Organic Solvent and Other Chemical Mixture

3.3.1 Liquid Hydrocarbon and Alkali Metal Bicarbonate/Alkali Metal Carbonate Mixture

In 1999, Humphreys patented an extraction method of oil sands by using the mixture of alkali

metal carbonate, alkali metal bicarbonate and liquid hydrocarbon at conditioning step.[61] This new modification in conditioning stage substantially eliminates the production of sludge while improving or maintaining the bitumen recovery. The process allows for hot conditioning solution to be recycled in the process by use of a recycle storage tank.[63]

3.3.2 Using Kerosene and Methyl-isobutyl-carbinol (MIBC) in Cold Water Slurry Process

In 1990, Sury patented a cold water extraction process (2 - 15 °C) by use of a mixture of a collector (kerosene or diesel) and a froth agent (methyl-isobutyl-carbinol).[64] It is believed that the added kerosene spreads and form a thin coating on the surface of bitumen and promote their attachment to air bubbles. On the other hand, MIBC is added and promotes the formation of stable air bubbles. Allcock *et. al* also patented a similar method, and it is reported that the total bitumen recovery using low grade ore can gets to 91% vs. 64% for the blank when the chemical aid is used at a dosage of 200 - 400 ppm.[61, 65]

3.4 Surfactant

3.4.1 Surfactants Produced from Oxidation or Sulfonation of Bitumen Asphaltenes

Ozum utilized the naturally present bitumen asphaltenes treated with selective chemical agents such as air or ozone and sulfonation agents such as sulphur dioxide, sodium sulfite and sodium bisulfite to produce surfactants that reduce surface and interfacial tension and promote the production of bitumen water emulsion, thus facilitate the bitumen production and recovery.[61, 66] The asphaltenes react with the aforementioned reagents by oxidation, sulfonation, sulfoxidation, or sulfomethylation reactions, or by a combination of such reactions. It is believed that the methods of the invention improved the stability of bitumen-water emulsions to facilitate

transportation of the emulsions by pipeline, and to enhance the recoverability of bitumen from oil sands.[66] However, it may be detrimental for later froth treatment to demulsify the water in oil emulsion in froth treatment.

3.4.2 Sulfonated Fatty Acids

In 1990, Hall and Russo patented a chemical combination of sodium silicate (7% by weight), liquid caustic soda (50%, 8% by weight), sodium salt of sulfonated oleic acid (6%), anionic surfactant (5%), non-ionic surfactant (5%), liquid potassium phosphate (10%), tetrahydrofurfuryl alcohol (11%), ethylene glycol monophenyl ether (5%), defoamer (such as silicone oil), which was used to separate bitumen from the sand in water based extraction process.[67] The chemicals can be used and recovered, and it is claimed that the hydrocarbon content in the remained sands after the extraction is lower than that in other process.[61]

3.4.3 Non-ionic Surfactant or Zwitterionic Surfactant with Potassium Bicarbonate

In 1978, Globus patented a method to recover bitumen from oil sands ores by using potassium bicarbonate combined with a non-ionic surfactant.[68] Many types of non-ionic surfactant (*e.g.* polyoxyethylene) and zwitterionic surfactant (*e.g.* betaines and sulfobetaines) are stated in the patent. However, only one example with addition of 1-(lauryldimethylammonio-acetate) (0.5% by weight) was shown in the patent and it needs 2% of potassium bicarbonate by weight of the sand and water mixture.[68]

3.5 Addition of Polymer Flocculant

3.5.1 Anionic Polymer Flocculant Hydrolyzed Polyacrylamide (HPAM)

In 2005, Beetge *et al.* patented a method to improve the bitumen extraction recovery by use of

hydrolyzed polyacrylamide (HPAM).[52, 69] They also found the polymer aid can help reduce divalent ions and increase the tailings settling rate. The highest bitumen liberation and recovery were obtained at a HPAM dosage of about 15 - 30 ppm. This synergetic role of HPAM was investigated by AFM and it showed that the improvements were attributed to the selective flocculation of clay fines by HPAM after addition of appropriate dosage. Based on the results, it was suggested to directly add HPAM into the bitumen extraction process, rather than to tailings, to facilitate both bitumen recovery and tailings treatment in production operations.[52] However, the addition of HPAM led to poor bitumen froth quality, *e.g.* high solids content in the recovered aerated bitumen.[52, 53]

Further studies showed that both molecular weight and polymer charge density have impact on the performance of extraction and tailings settlement.[54] High molecular weight (MW) HPAM improved both bitumen recovery and tailings settling but it was detrimental to froth quality. In order to achieve high bitumen recovery and fast tailings settling, a HPAM polymer must have a low to medium charge density (~30%) and a high MW (17.5 million Daltons).[54]

3.5.2 Combination of $Al(OH)_3$-polyacrylamide (Al-PAM) and HPAM

In 2008, Masliyah *et al.* published their work on processing low grade oil sands ores by use of hybrid Al $(OH)_3$-polyacrylamide (Al-PAM) combined with partially hydrolyzed polyacrylamide as chemical aid.[55] According to the results, it was found that Al-PAM was capable of improvinge bitumen froth quality and tailings settling. But it led to decrease in bitumen recovery due to the formation of large bitumen lumps during the bitumen extraction process. The problem was solved by combination of HPAM with Al-PAM in the extraction process. The use of the dual system at a low dosage achieved a holistic improvement in bitumen recovery, froth quality, and tailings

settling.[55]

3.5.3 Non-ionic Poly (N-isopropylacrylamide) (PNIPAM)

In 2011, Long *et al.* published their work of improving bitumen recovery by use of temperature sensitive polymer PNIPAM.[53] PNIPAM is a well-known temperature-sensitive polymer in aqueous solutions. It can undergo a thermally reversible conformational change with temperature variation when crossing their lower critical solution temperature (LCST).[70, 71] The polymer is hydrophilic and soluble in aqueous solutions when the temperature is below LCST (for pure PNIPAM around 31°C) and becomes hydrophobic and insoluble when the temperature is above LCST.[70] As the slurry temperature changes at different stages in the extraction process, they explored the possibility of using thermal-sensitive polymer for improving the processing ability of poor processing oil sands ores. When the extraction process was carried out at 23 °C, the polymer showed negative impact to both bitumen recovery and froth quality. However, when the extraction process was carried out at 40 °C, which is above the LCST of PNIPAM, the addition of PNIPAM polymer in the extraction significantly improved bitumen recovery and tailings settlement, but it deteriorated the forth quality. The author explained the results by the change of the polymer's conformation from a long, extended structure to a coiled conformation, which resulted in the formation of compacted floccules of fine solids.[53]

3.5.3 Non-ionic Block Copolymer

Recently, Yang *et al.* published their work on facilitating oil sands recovery by utilizing thermoresponsive block polymer combined with toluene in water based extraction process.[72] PEG_{113}-*b*-$PMEO_2MA_x$ (x = 48 to 80) was synthesized by atom transfer polymerization and it

showed LCST around 34 ℃. When the polymer and toluene were mixed with oil sands in bottle test at 45 ℃ or 50 ℃, it helped improve the bitumen recovery based on the vial test. The author stated that the polymer can dissolve back into water phase when the temperature went down, so the polymer can be recycled and reused. According to the paper, the polymer can be reused for 5 times. However, the related vial tests require longtime of mixing, more importantly, there is no Denver flotation cell tests have been done with this method yet.

Chapter 4. Design of Temperature Switchable Non-ionic Block Copolymer

The chemical aids aforementioned in Chapter 3 can help increase the bitumen recovery based on different design concept. However, they are typically one-off reagents and cannot be recycled while the cost and associated environmental concerns could be a problem for large scale bitumen production. It would be ideal if the additive can be recycled in extraction process.

As the extraction process contains two essential sub-processes: liberation of bitumen from sand grains and aeration of liberated bitumen droplet in slurry,[73] the efficiency of bitumen extraction process largely depends on the degree of bitumen liberation (DBL) and the induction time which is defined as the time needed for attachment of air bubbles with a layer of bitumen when they are in contact.[59, 73-75]

As caustics are added during the extraction in currently commercial plants, they help the liberation process by: (i) increase the pH of slurry, and hence, deprotonate and ionize the natural surfactants, (ii) help release the natural surfactants inside bitumen, (iii) improve the wettability of sand grains by hydrolyzing the sand surface layer. The ionized surfactants become more surface active and attach to the interface between bitumen droplets and water, which helps lower the interfacial tension (IFT) and hence, improve the liberation process. However, ionized natural surfactants with negative charges generated by caustic addition could also make bitumen droplets and air bubbles more hydrophilic, leading to an increase of double layer repulsive force, imposing a stable liquid film between bitumen and air bubbles, and reducing bitumen–bubble attachment which leads to poor aeration.[51, 58, 59] Furthermore, in real process water, calcium ions and fine solids can bind to carboxylate anions, which would also be detrimental to aeration.[59] It would be ideal if one chemical additive can enhance both liberation and aeration processes.

To address the two problems aforementioned, we need a type of chemical additive which can help liberation without negative impact on aeration process; also the chemical should be recycled during the whole extraction process to reduce cost.

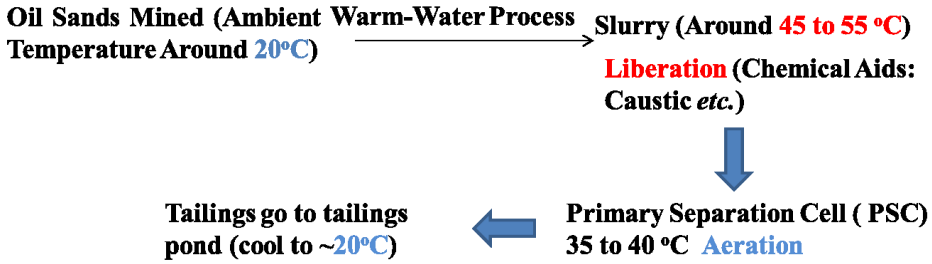

Figure 15. Temperature change in oil sands extraction process.

If we have a careful look into the overall situation of the bitumen extraction, we can easily find that there are temperature changes in the process (Figure 15): the ores are mined at ambient temperature around 20 °C and mixed with hot water or steam to make slurry at 45 ~ 55 °C. After the extraction, the tailings (most solids, water.) go to tailings pond and the temperature again cools to ambient temperature around 20 °C. After the settling, the process water is reused for extraction again. If a chemical additive have temperature switchable property, which can enhance the bitumen extraction process at around 50 °C, and then it can go back to aqueous phase with tailings when temperature cools down to around 20 °C. Then the chemical can be reused for next batch of extraction together with process water, which in turn reduces cost and environmental impact while increasing the bitumen recovery.

Although copolymers based on similar design were synthesized by Yang *et al.* recently and used to oil sands liberation vial test,[72] it still requires organic diluent such as toluene to help the liberation which is not the practical water-based extraction process used in industry. The invoked vial tests require long time mixing which cannot be utilized by practical extraction plant. In our design, for

the sake of improving both liberation and aeration process, we designed and synthesized temperature switchable non-ionic block copolymers to achieve the goals by considering the following aspects.

Firstly, to enhance liberation of bitumen from sand grains, the polymer designed should be highly interracially active which can help lower the IFT between bitumen and water phase at 50 °C. As polyethylene glycol (PEG) is soluble in water in a wide range of temperature (0 ~ 98 °C) and PNIPAM is very hydrophobic above its LCST (lower critical solution temperature) around 32 °C, we can intuitively expect the block copolymer is amphiphilic and could lower the IFT between bitumen and water phase at 50 °C (Figure 16). [71, 76-78]

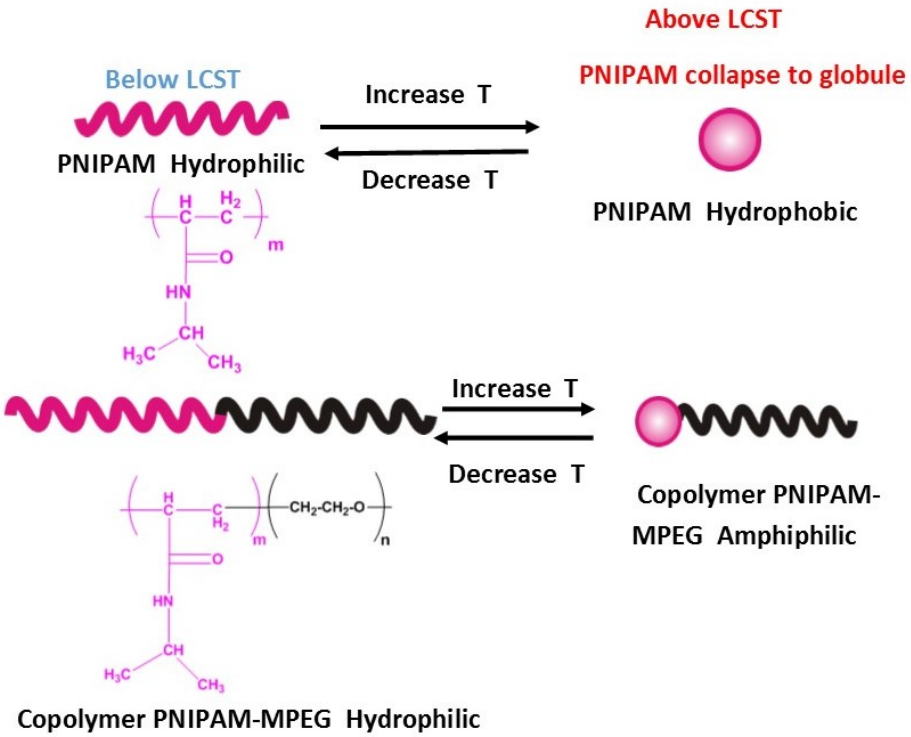

Figure 16. Designed block copolymer structure and its switching with temperature.

Secondly, the designed copolymers should be non-ionic since highly negatively charged bitumen

droplets are detrimental for air bubble attachment. Natural surfactants are usually negatively charged and the high potential on bitumen surface would increase the double layer forces with air bubbles.

Thirdly, the two blocks of the copolymer should be water soluble around 20 to 25 °C, so the polymer can be recovered with process water after the tailings discharged to tailings pond. Finally, the copolymers can't have very high molecular weight since high molecular weight polymers may act as flocculants and lower the froth quality.[54, 55]

The proposed procedure of using these temperature switchable non-ionic block copolymers to oil sands extraction process is shown in Figure 17.

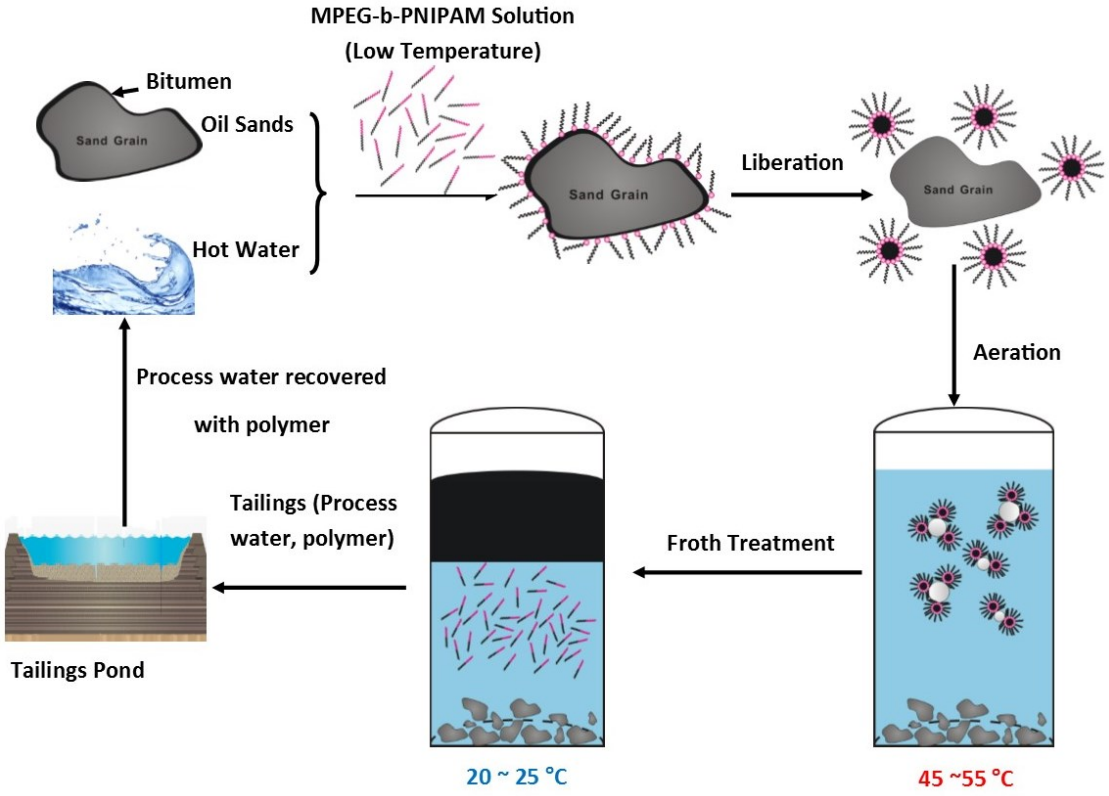

Figure 17. Proposed procedure of using these temperature switchable non-ionic block copolymers to oil sands extraction process.

In this work, we synthesized MPEG2000-*b*-PNIPAM$_{50}$, MPEG750-*b*-PNIPAM$_{35}$ by ATRP (atom transfer radical polymerization) method and applied these temperature switchable non-ionic block copolymers into modified Denver cell extraction test. Further tests of the polymers' functions like bitumen liberation flow visualization cell (BLFVC), induction time measurement were also conducted and the preliminary results proved our design concept.

Chapter 5. Materials and Methods

5.1 Materials

5.1.1 Chemicals Used for Synthesis.

Methoxy poly (ethylene glycol) (MPEG) with two different average molecular weight, M_n = 750 g mol^{-1} and 2000 g mol^{-1} (flakes), 2-bromoisobutyryl bromide (≥98%), N,N,N,N″,N″-pentamethyldiethylene-triamine (PMDETA, ≥99%), were purchased from Aldrich and used without further purification unless otherwise noted. Triethylamine (TEA, ≥ 99%), N,N-dimethylformamide (DMF, ≥99.5%), dichloromethane (DCM, anhydrous, ≥99.8%), n-heptane, diethyl ether (anhydrous, ≥99.0%), CuBr (98%) and 4-(dimethylamino) pyridine (4-DMAP) and N-isopropylacrylamide (NIPAM) were purchased from Fisher Scientific and used without further purification unless otherwise noted. CuBr was stirred in 30% acetic acid aqueous solution for 2 hrs and washed by water, ethanol and diethyl ether following the named sequence. The purified CuBr was then dried under vacuum and stored in round bottom flask in argon atmosphere. All water used in experiments was purified with a Millipore Milli-Q system, and the resistivity was approximately 18.2 MΩ cm. Argon (PP 4.8 GP-529325) from PRXAIR was used in all of the atom transfer radical polymerization syntheses.

5.1.2 Oil Sands Ore Sample

The oil sands ore samples (SUNP210) were supplied by Suncor and the basic information is showed in Table 1.

The composition of the oil sands ore was determined by the Soxhlet Dean-Stark apparatus.[56, 79] To

obtain fine solids content, we collected the solids from the Dean-Stark apparatus and wet-screened the solids by a 44 μm sieve and both above- and under-sieve products were then dried in an oven. The two portions of solids were weighed accurately and the fines content could be calculated by dividing the mass of the under-sieve solids by the mass of the total solids.

Table 1. Composition (wt. %) of Oil Sands Ore.

Name	Bitumen (%)	Water (%)	Solids (%)	Fines - 44 μm (%)
SUNP210	**10.0**	**2.6**	**86.8**	**21.5**

5.1.3 Process water

Process water was supplied by Syncrude. And the basic information of the process water is listed in Table 2.

Table 2. Concentration of Major Ions in the Plant Recycle Process (Syncrude, Aurora; Research EXP pilot, March3, 2009) Water of pH 7.7.

Major ion	Ca^{2+}	Mg^{2+}	K^{+}	Na^{+}
Concentration (ppm)	**50.5**	**27.3**	**34.0**	**940.0**

5.1.4 Bitumen sample

Vacuum Distillation Unit Feed bitumen was obtained from Syncrude Canada Ltd, Dec 22, 2004 and was used for induction timer measurement.

5.2 Synthesis of Temperature Switchable Block Co-polymer MPEG-*b*-PNIPAM

5.2.1 Synthesis of 2-bromopropionate MPEG2000 Macroinitiator (MPEG2000-Br)

The macroinitiator was prepared according to the procedure published by several groups with

some modifications (Scheme 2).[72, 78, 80, 81] Briefly, the monomethyl ether of poly (ethylene glycol) reacted with 2-bromoisobutyryl bromide and gave an ester with C-Br bond which is an active center for further functionalization.

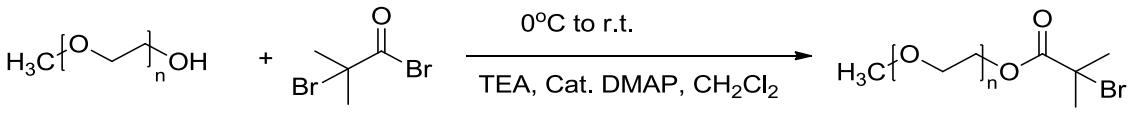

Scheme 2. Synthesis of macroinitiator 2-bromopropionate MPEG2000.

MPEG2000 (M_n = 2000 g mol^{-1}) 10.0 g (5.0 mmol), 4-(dimethylamino) pyridine (4-DMAP) 100 mg were pre-weighed into a 300 ml flame dried three-neck round bottom flask. Then the flask was purged with argon three times. The flask was then charged with 30 ml of anhydrous CH_2Cl_2 and was cooled to 0 °C. Triethylamine (TEA, 6.0 mmol, 0.84 ml) was pre-dried by CaH_2 and was added into flask dropwise through syringe. The mixture was stirred at 0 °C for another 15 min. 2-bromoisobutyryl bromide (6.0 mmol, 0.75 ml) was dissolved into addition funnel by 20 ml anhydrous CH_2Cl_2 and the solution was added into the flask dropwise in 15 min. After the addition of 2-bromoisobutyryl bromide, the mixture's temperature was slowly raised to room temperature and the reaction was stirred overnight. The reaction mixture was then filtered through an alumina gel (gel size 300 nm) packed column three times to remove triethylamine hydrobromide salt. Then the clear solution was concentrated by rotation evaporator and precipitated in cold diethyl ether for three times. Finally, the precipitation of 2-bromopropionate MPEG2000 was filtered, collected and subjected to high vacuum to get dried.

5.2.2 Synthesis of 2-bromopropionate MPEG750 Macroinitiator (MPEG750-Br)

2-bromopropionate MPEG750 was synthesized using similar method. MPEG750 (M_n = 750 g mol^{-1}) 3.75 g (5.0 mmol), 4-(dimethylamino) pyridine (4-DMAP) 100 mg were pre-weighed into a 300 ml flame dried three-neck round bottom flask. Then the flask was purged with argon three times. The flask was then charged with 30 ml of anhydrous CH_2Cl_2 and cooled to 0 °C. Triethylamine (TEA, 6.0 mmol, 0.84 ml) was pre-dried by CaH_2 and was added into flask dropwise through syringe. The mixture was stirred at 0 °C for another 15 min. 2-bromoisobutyryl bromide (6.0 mmol, 0.75 ml) was dissolved into addition funnel by 20 ml anhydrous CH_2Cl_2 and the solution was added into the flask dropwise in 15 min. After the addition of 2-bromoisobutyryl bromide, the mixture's temperature was slowly raised to room temperature and the reaction was stirred overnight. The reaction mixture was washed with bicarbonate saturated solution and filtered through an alumina gel (gel size 300 nm) packed column three times. Then the clear solution was concentrated by rotary evaporator and subjected to high vacuum to get dried.

5.2.3 Synthesis of MPEG-*b*-PNIPAM by Atom Transfer Radical Polymerization (ATRP)

The connection of the PNIPAM block onto the macroinitiator MPEG-Br was achieved by using conventional atom transfer radical polymerization (ATRP) with some modifications (Scheme 3).[78, 80, 81]

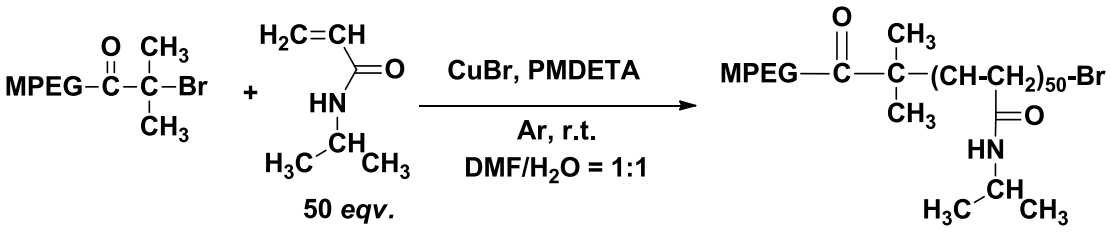

Scheme 3. Synthesis of MPEG2000-*b*-$PNIPAM_{50}$.

N-isopropyl acrylamide (NIPAM) was recrystallized three times in hexane to remove the inhibitor inside before use. CuBr was stirred in 30% acetic acid aqueous solution for 2 hrs and washed in the sequence of water, ethanol and diethyl ether, and dried. Milli-Q water and DMF were mixed in 1:1 ratio and purged with argon in a rubber sealed flask for 30 min before use. NIPAM (5.65 g, 50 mmol), MPEG2000 macroinitiator (MPEG2000-Br) (1.0 mmol, 2.15 g) were added to a 300 mL three-neck round bottom flask under stirring by stir bar. Pre-deoxygenated DMF/H_2O solvent mixture (30 mL, volume ratio of DMF: H_2O = 1:1) was transferred into the three-neck round bottom flask by syringe. After NIPAM and MPEG-Br were completely dissolved, the mixture was degassed by three freeze-pump-thaw cycles. The flask was then filled with argon and immersed in water bath to be kept at 20 °C.

In order to make the catalyst initiate the reaction, pre-purified CuBr (0.142 g, 1 mmol) was weighed into a 25 ml vial and sealed by a rubber septum. The vial was then purged with argon for 15 min. Then N,N,N,N″,N″-pentamethyldiethylene-triamine (PMDETA, 0.21 ml, 1 mmol) and 1 ml degased Milli-Q water was added into the vial and the mixture was purged under argon for another 15 min.

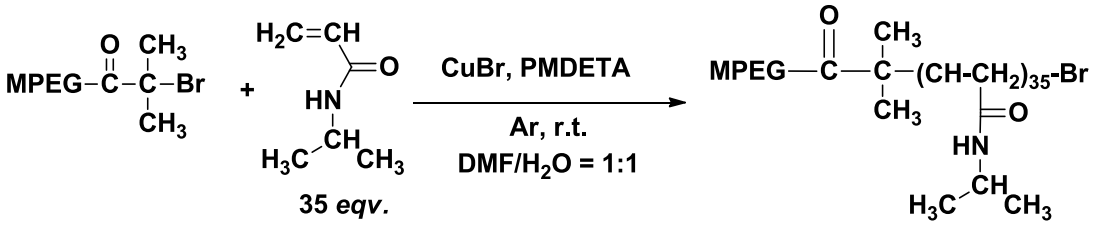

Scheme 4. Synthesis of MPEG750-*b*-$PNIPAM_{35}$.

The well mixed catalyst was added into the three-neck round bottom flask dropwise by a syringe and the reaction system was kept under argon atmosphere in water bath at 20 °C. After the addition

of the catalyst, the polymerization started quickly and the viscosity of the mixture went up. The reaction was stirred overnight and the polymerization was terminated by purge into air. The mixture was then transferred into a dialyzing tube with a molecular weight cut-off of 3500 and purified by dialyzing against deionized water for 3 days. Finally, the solid product was isolated by lyophilization of the clear solution inside the dialyzing tube. 2-bromopropionate MPEG750-*b*--PNIPAM$_{35}$ was synthesized using similar method (Scheme 4).

5.2.4 ^{1}H NMR Spectroscopy and FT-IR Spectroscopy

The chemical structure of the macroinitiator MPEG-Br and MPEG-*b*-PNIPAM block copolymers were confirmed by both ^{1}H NMR and FT-IR. The number-average molecular weights (M_n) of the copolymers were also determined by ^{1}H NMR.

5.2.5 Interfacial Tension Measurement by Du Noüy Ring Method

Kruss-12 Tensionometer was used to measure the interfacial tension between polymer solution and HPLC grade toluene in a temperature range from 20 °C to 50 °C.

5.2.6 Turbidity Measurement

The synthesized polymers were made into solution and their turbidities were measured from 20 °C to 60 °C by using Micro100 Laboratory Turbidimeter from HF Scientific. The turbidimeter was calibrated by standard samples with turbidity of 0.02 NTU, 10.0 NTU and 1000 NTU before the measurement of new samples.

5.2.7 Size Measurement of Polymer Species in Aqueous Solution

Zetasizer Nano-ZS (Malvern Instruments Ltd., Worcestershire, U.K.) was used to measure the polymers' size in aqueous solution at different temperature. 173° backscatter (NIBS default) model was chosen to process the measurement and each test was run 3 times with 6 measurements.

5.2.8 Bitumen Flotation

The bitumen flotation tests were processed by following the literature with some modification.[16, 51, 56, 79, 82] Basically, the oil sands extraction tests were conducted in a Denver flotation cell with a 1-L volume. And the stainless-steel cell has a water jacket which was connected to a water bath to keep at a certain temperature. A stainless-steel impellor was connected to a 1/2 HP Baldor Industrial Motor and used as the agitator to make slurry. The stirring speed is measured by a tachometer. Air was added into the slurry through the impellor's shaft and the flow rate of the air bubble was controlled and measured by a digital flowmeter. The schematic of the Denver flotation cell is shown in Figure 18.[16]

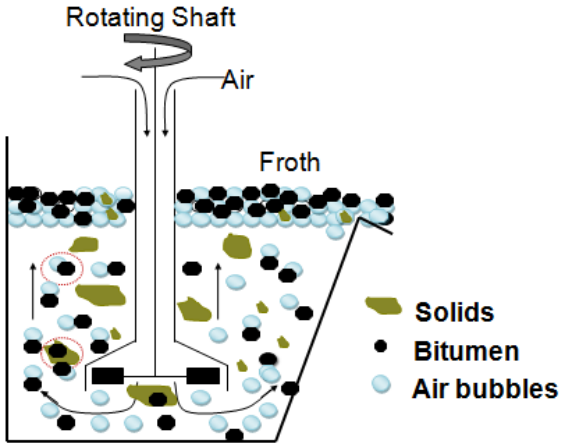

Figure 18. Schematic of Denver flotation cell.[31]

Prior to each test, frozen oil sands ores were allowed to thaw at room temperature for 24 h. Then the 500 g thawed ore was added into the flotation cell with 250 mL of process water together with pre-dissolved synthesized polymer and 0.25 g NaOH at 80 °C, leading to slurry at 50±1 °C. After agitating the oil sands slurry at the rate of 800 rpm for 5 min, the water bath pre-set at 50 °C was attached to the Denver cell to maintain the slurry was processed at 50 °C. The air flow rate was kept at 150 mL/min and the slurry was conditioned for 5 min. Then 800 mL process water pre-heated to 50 °C was added into the cell and the slurry was agitated at the same speed for another 10 min without air addition. Then the primary bitumen froth was collected into a pre-weighed cellulose thimble A. Then the secondary froth was collected into another pre-weighed thimble B after another 10 min agitation at the same agitating speed with air addition at 150 mL/min air flow rate. After collecting the froth, the remained slurry in the Denver cell was discharged as tailings and the primary and secondary froth collected was further analyzed by using Dean Stark analysis to determine the mass of bitumen, water and solids in the froth.

5.2.9 Dean Stark Analysis

Dean Stark analysis is the most common method used to determine the mass amount of bitumen, solid and water, which can be used to evaluate bitumen recovery and froth quality from bench-scale flotation.[51, 83] The cellulose thimble (Fisher Scientific) with collected bitumen froth from Denver flotation cell was placed in a steel wire holder, which was hung on the glass adaptor between the flask and Dean Stark trap. The thimble was covered by a mesh lid on the top and the condenser was connected to the trap. This assembly was then put into an extraction flask, and a condenser was connected aside with the trap (Figure 19).

Around 200 mL toluene was poured into the extraction flask and was heated up to evaporate.

Toluene vapor was condensed by the condenser and dripped into the trap. The water was also heated to evaporate and condensed by condenser and collected by Dean Stark trap. Due to the higher density of the condensed water, it sank in the bottom of the trap while the condensed toluene stay on the top and flowed back to the thimble and extracted the bitumen from the froth into the extraction flask. The inorganic solids was remained in the thimble.[16]

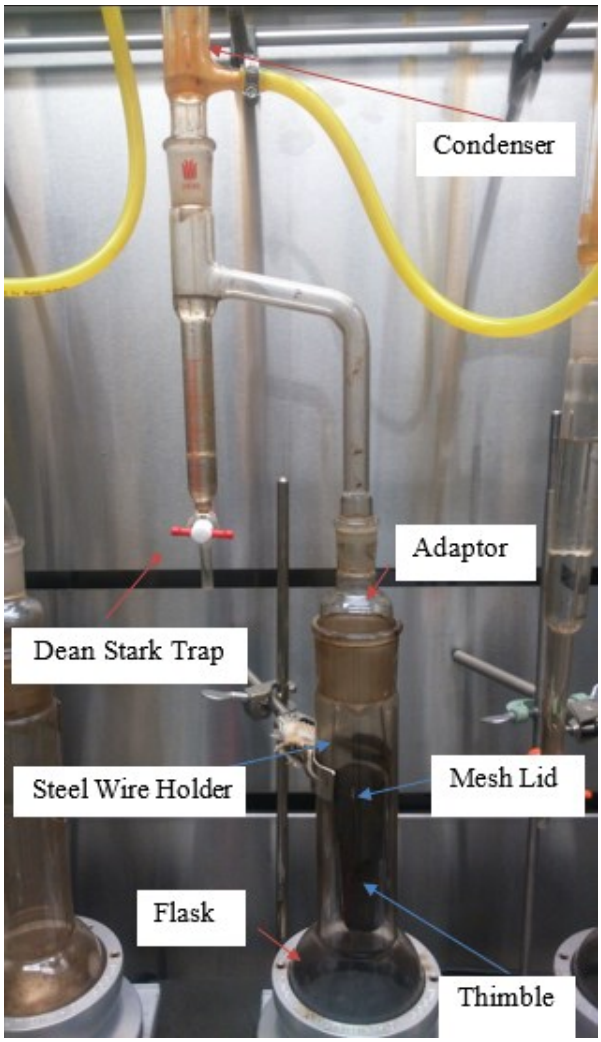

Figure 19. Dean Stark Apparatus

Typically, there are two phenomena indicating the complete of the analysis: (1) The toluene dripping from the thimble bottom is clear; and (2) No water droplet is condensed from the condenser. With the satisfaction of the two phenomena, heat was removed and the whole system

was cooled down to room temperature. The thimbles were then vacuum dried over night with the solids inside. A small plastic bottle was used to collect the water in the trap, and the mass of the water was weighed. The toluene-bitumen solution in the flask was then transferred into a 250-mL volumetric flask and diluted to 250 mL precisely. The bitumen solution was then well mixed and 5 mL of diluted bitumen solution was taken using a pipette and sprayed evenly on a filter paper. The paper was then hung up in the fume hood for 20 minutes, and the mass difference of the filter paper before and after absorbing 5 ml bitumen solution was measured to determine the mass of bitumen in the froth. From the Dean Stark analysis, the bitumen recovery **R**, bitumen/solids ratio (**B/S**) and bitumen/water ratio (**B/W**) were calculated by the formula listed below.

$$\mathrm{R} = \frac{Mass\ of\ Bitumen\ Recovered}{Mass\ of\ Bitumen\ in\ Oil\ Sands} \times 100\% \quad [10]$$

$$\mathrm{B/S} = \frac{Mass\ of\ Bitumen\ Recovered}{Mass\ of\ Solid\ Inside\ the\ Froth} \times 100\% \quad [11]$$

$$\mathrm{B/W} = \frac{Mass\ of\ Bitumen\ Recovered}{Mass\ of\ Water\ Inside\ the\ Froth} \times 100\% \quad [12]$$

5.2.10 Liberation Cell Test

A bitumen liberation test of the oil sands ores was taken in a bitumen flow visualization cell (BLFVC, Figure 20) developed by our group and the detailed operation procedure was described elsewhere.[51, 73, 74]

Briefly, the oil sands ore samples were thawed at room temperature for 24 h and around 1 g of the ore sample was packed into a glass sample holder. Then the glass sample holder with oil sands were carefully placed on an O-ring in the packet of the cell and capped with a steel plate with a diamond shape hole in the center. Then the oil sands sample was patted and flattened to get a good

flat surface. The sample holder was mounted on the cell by a set of screws and the cell was sealed by a glass slide and metal cover pressed on the glass slide by four screws. The cell was kept at 50 ℃ by the built-in heating plate. Polymers synthesized were dissolved into process water and pre-heated to 50 ℃ to pass through the cell by a peristaltic pump during the experiments. The bitumen liberation process was monitored by stereo microscope (Olympus SZX 10, Japan) and the videos of the liberated oil sands ores were taken by the CCD camera at a speed of 10 frames/s with set exposure time of 50.00 ms and magnification of 0.64mm/pixel. By analyzing the subsequent extracted frames of the video by software image pro plus 6.0 with a certain interval, we can calculate the so-called bitumen liberation degree as illustrated in the flowchart in Figure 21.[16]

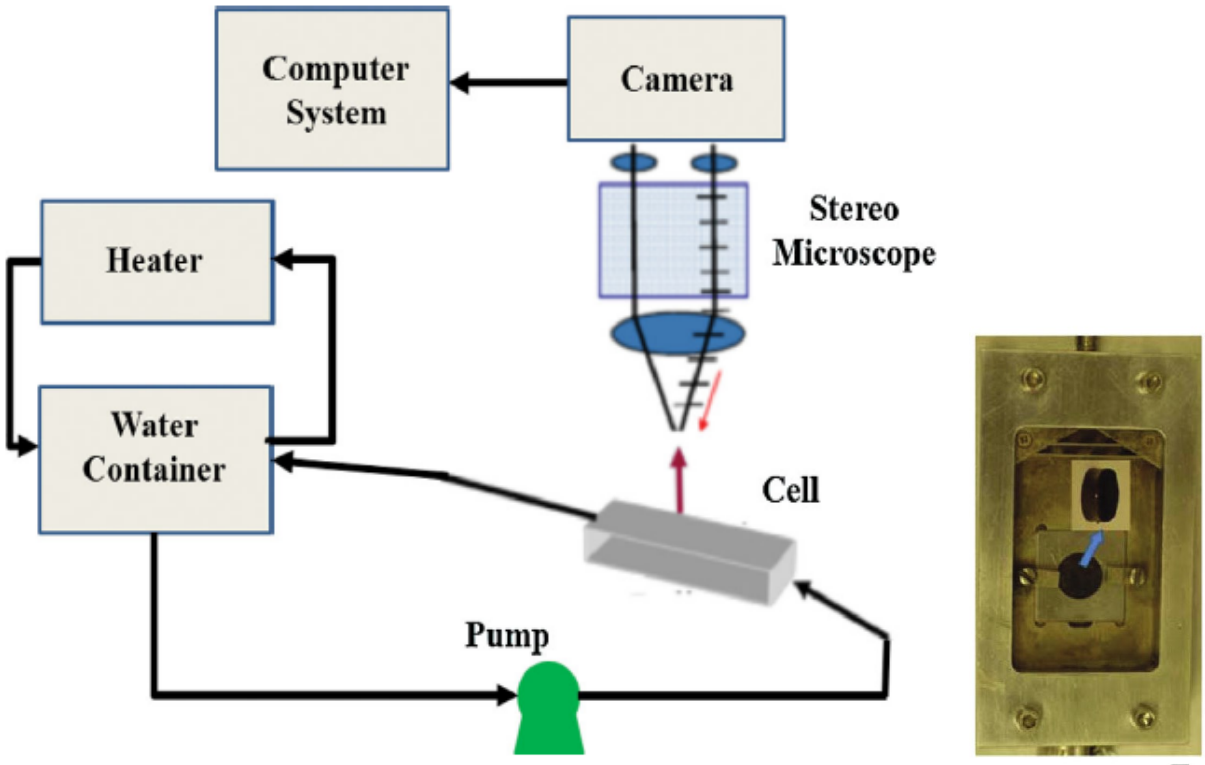

Figure 20. Schematic flow diagram of liberation cell and figure of liberation cell.[73, 74]

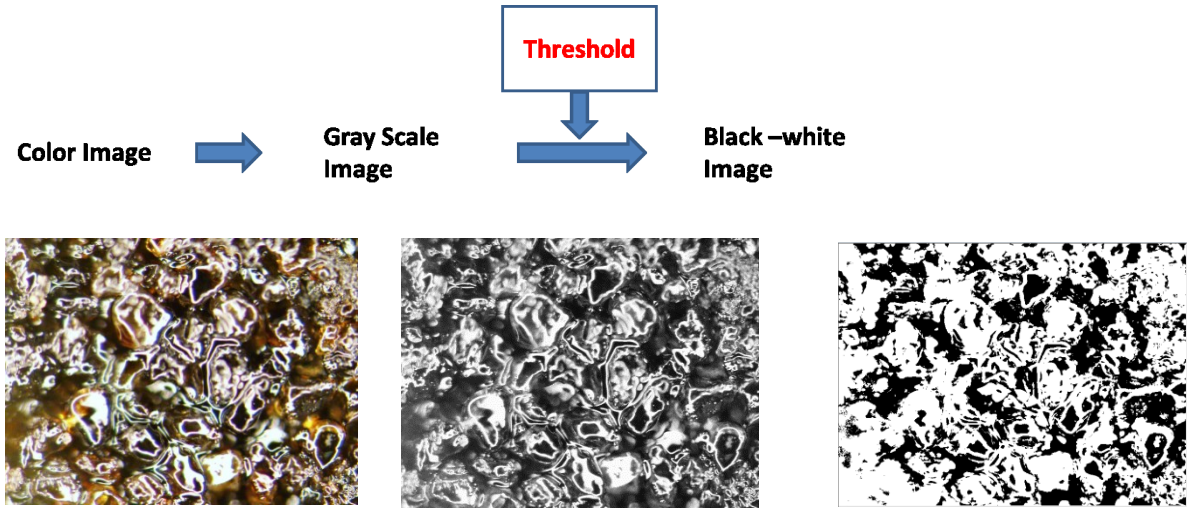

Figure 21. Liberation cell test.

Briefly, the analysis of the pictures are described as follows:

The color image was extracted by a certain time interval and converted to "gray scale 8" format firstly by using image analysis software-Image-pro.[72-73] And then the threshold was applied to the gray scale image by Image-pro. Each pixel in the grey scale image contains a specific value according to its color, ranging from 0 (representing the pure black) to 255 (pure white). Here, we set 80 as the threshold of our ore sample, which means the pixel with a value above 80 was convert to white and considered as liberated area without bitumen coverage while the pixel with a value below 80 was converted to black and considered as unliberated area. The degree of bitumen liberation (DBL) is then defined as:

$$DBL(\%) = \frac{A_0 - A}{A_0} \times 100\% \qquad [13]$$

In this formula, A_0 is designated as the area of black pixels in the image captured at time zero (practically, that is the time tight before the fluid was pumped into the cell), and A is the area of black pixels at the time of analysis. As the area of black pixels decreases, the DBL increase, which is easily to understand as more bitumen separated from sand grains and more sands exposed.

As the CCD camera was focused on the top surface of the flattened ore samples, the liberated bitumen droplets in the field of view above the flat plane would be out of the focus of the camera, and hence would be shown blurred or otherwise carried away by the flowing process water. Therefore, bitumen droplets in the images were the drops attached on solids (sand) surfaces, not the ones liberated and attached to the top window of the cell. Each test was repeated at least three times with good repeatability.

5.2.11 Induction Time Measurement

A custom-built induction timer in our lab was used to determine the effect of synthesized polymer on aeration process of bitumen extraction. The detailed operation procedure can be found elsewhere and the apparatus was showed in Figure 22.[16, 51, 59]

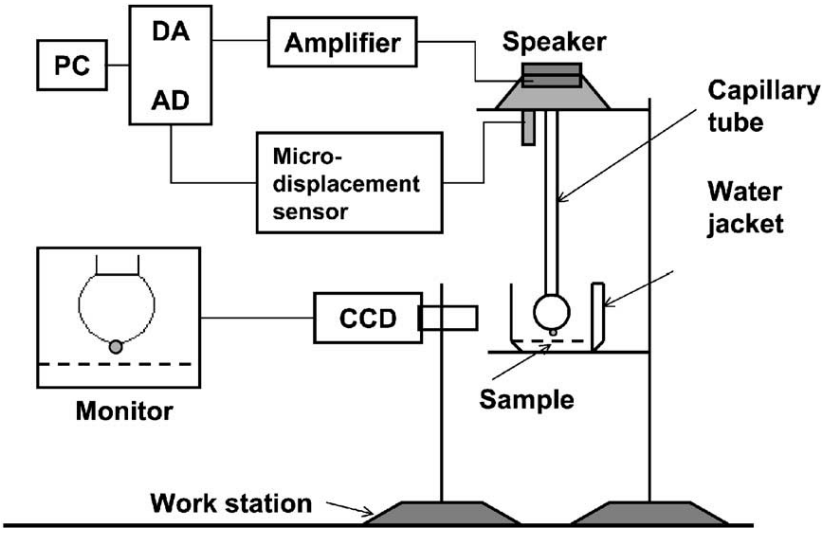

Figure 22. Apparatus of induction timer measurement. [59]

Briefly, the induction time of bitumen-air bubble attachment was defined as the minimum time required of an air bubble in contact with bitumen for the bubble to attach to the bitumen surface.[59] The vacuum distillation unit feed was placed into a half sphere shape pocket of a Teflon disk and

the surface was made flat by razor blade.[16] The sample was then heated to around 35 ℃ and was allowed to relax for 15 min with a glass cap on the top. We can get a flat and mirror-shinning bitumen surface, and the sample was then placed into a cubic glass cell with testing solution which had already been heated to 50 ℃. The cubic glass cell was held by a three-axial translation stage with portable heating plate and the solution was kept at 50 ℃. A clean glass capillary tube was connected to the diaphragm of a speaker above the translation stage. The displacement, approaching speed and duration of the capillary tube at the set displacement can be adjusted by the speaker which was controlled by a computer through a charge amplifier. In our tests, all the air bubbles were generated to a bubble diameter of 1.5 mm by a micro syringe and the initial gap between air bubble and bitumen surface was set as 0.4 mm. The approaching speed of the air bubble to the bitumen surface was set at 40 mm/s and different contact time between air bubble and bitumen surface can be set through computer and tested. The approach-contact-retract cycle were recorded by a CCD camera equipped with a macro lens. By setting a given contact time, the approach-contact-retract cycle was repeated for 20 times and the percentage of contacts that made attachment was calculated. And the contact time that leads to 50 % of attachment was defined as the induction time.

5.2.12 Recoverability Test of Synthesized Polymers

As designed in Chapter 3, we expected the polymers used can be recovered after the extraction and can be reused together with process water. We anticipate to establish a method to determine how much polymer we used could go back into the water phase when the temperature cooled down to room temperature. We first measured a series of concentrations of MPEG-*b*-PNIPAM aqueous solution's turbidity from 50 °C to 20 °C. With the standard curve of concentration *vs.* turbidity at a

certain temperature, we can easily correlate a measured turbidity of the polymer solution to the polymer's concentration at that temperature. Considering the color of bitumen may have huge impact on the turbidity measurement, we invoked HPLC grade toluene as oil phase. 1 ml of toluene was mixed with 24 ml polymer solution and settled at test temperature for 12 h. The aqueous phase's turbidity was then measured at the same temperature and the concentration of polymer can be calculated by the standard curve of concentration *vs.* turbidity. By comparing the concentration change of polymer in the water solution, the percentage of recovered polymer could be calculated when we switched the temperature.

Chapter 6. Results and Discussions

6.1 Characterization of Synthesized Temperature Switchable Polymers

6.1.1 Characterization of MPEG2000-*b*-PNIPAM$_{50}$

The successful synthesis of macroinitiator MPEG2000-Br was confirmed by both IR spectrum and ^{1}H NMR spectrum (Figure 23, Figure 24).

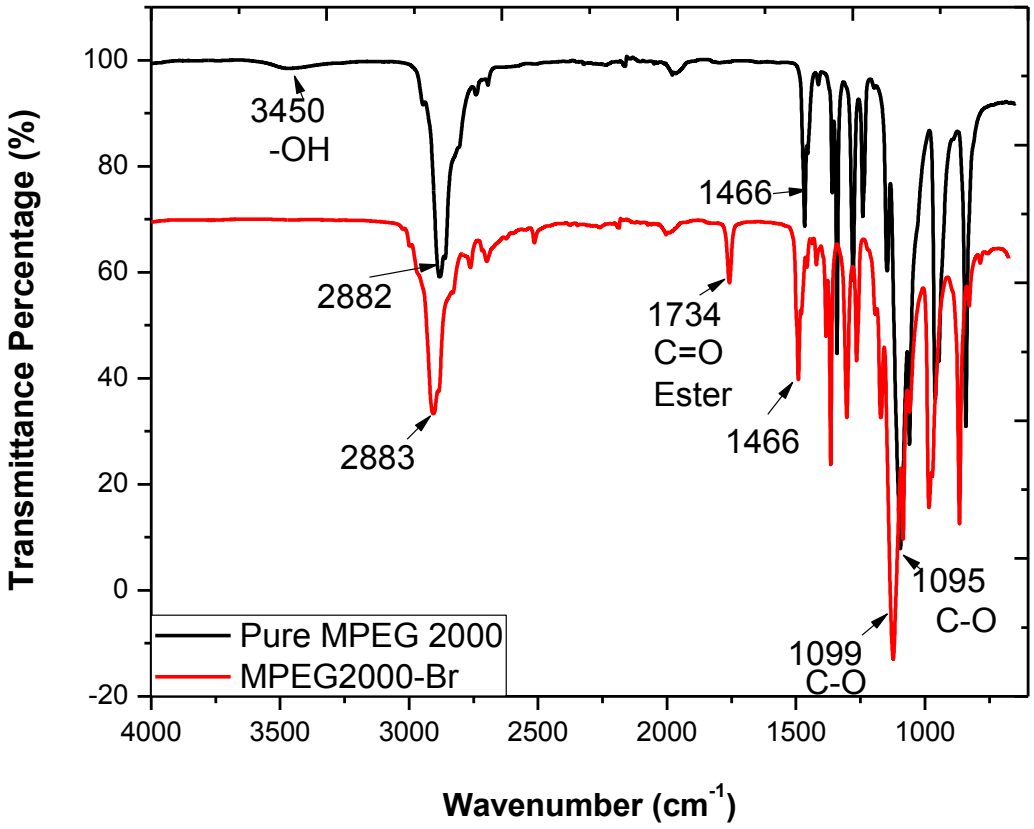

Figure 23. IR Spectrum of pure MPEG2000 and macroinitiator MPEG2000-Br.

By comparing the IR spectrum of MPEG2000 and MPEG2000-Br shown in Figure 23, we couldn't find any absorption at 3450 cm^{-1} for hydroxyl group in the IR spectrum of macroinitiator

MPEG2000-Br while its spectrum did show a new peak at 1734 cm^{-1} which is typically a characteristic absorption of aliphatic ester's carbonyl group.

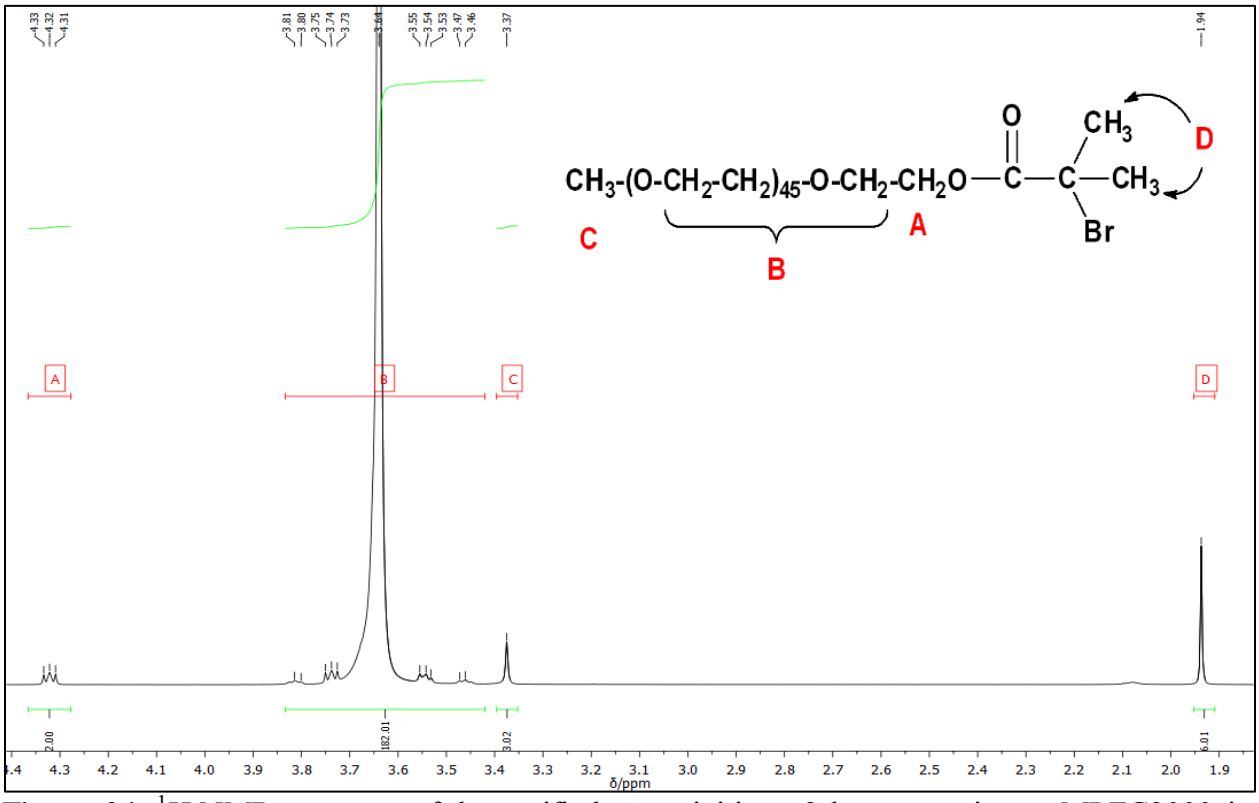

Figure 24. ^{1}H NMR spectrum of the purified macroinitiator 2-bromopropionate MPEG2000 in $CDCl_3$.

From the ^{1}H NMR spectrum of MPEG2000-Br we can easily infer that the hydroxyl group in MPEG2000 was esterified and the signal at 4.32 ppm in ^{1}H NMR was assigned to the geminal protons of the CH_2 attached to the ester group's oxygen. It could be concluded that the macroinitiator was successfully synthesized and well purified. More importantly, in ^{1}H NMR, each type of proton in the sample has its corresponding peak in the spectrum and the integral value of each peak is proportional to that type of proton's number in the sample. We assigned all the peaks in ^{1}H NMR to the protons noted in MPEG2000-Br and the assignments were shown in Figure 24. By comparing the integral number of peak A, B and C, we can conclude the average

repeating unit number of ethylene oxide (-CH_2CH_2O-) for MPEG2000-Br is 46. And the average molecular weight is 2056, which is nearly the same as the number (M_n~2000) given by chemical supplier.

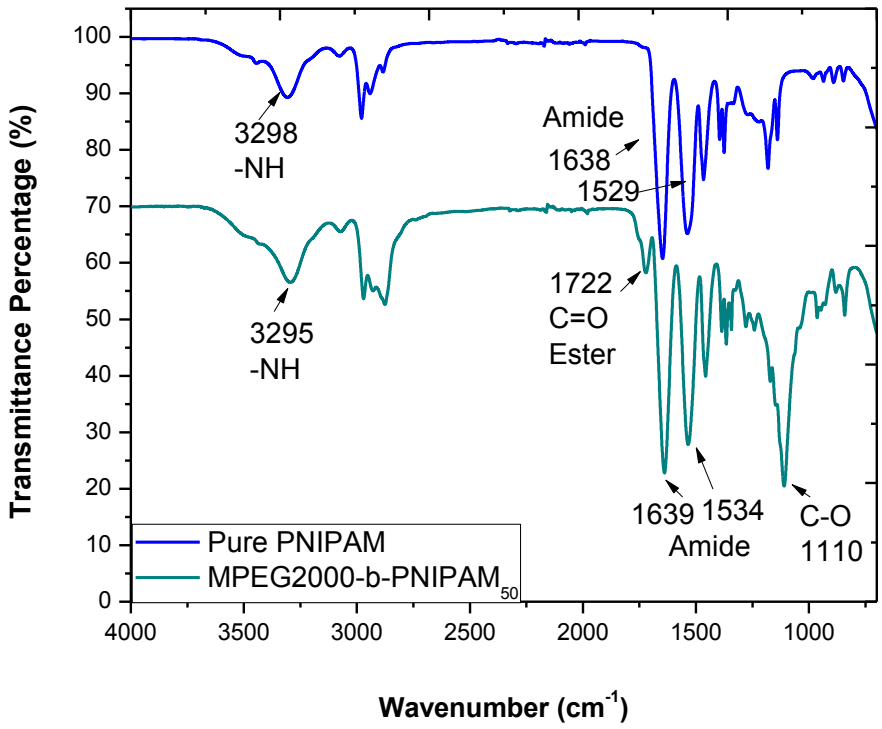

Figure 25. IR spectrum of pure PNIPAM and MPEG2000-*b*-$PNIPAM_{50}$.

With the macroinitiator in hand, we conducted the ATRP reaction with a [Initiator]: [NIPAM] =1:50 and got IR spectrum (Figure 25) and ^{1}H NMR spectrum (Figure 26) of the purified product. The assignment of the peaks in ^{1}H NMR spectrum was shown in Figure 26 with the synthesized polymer structure.

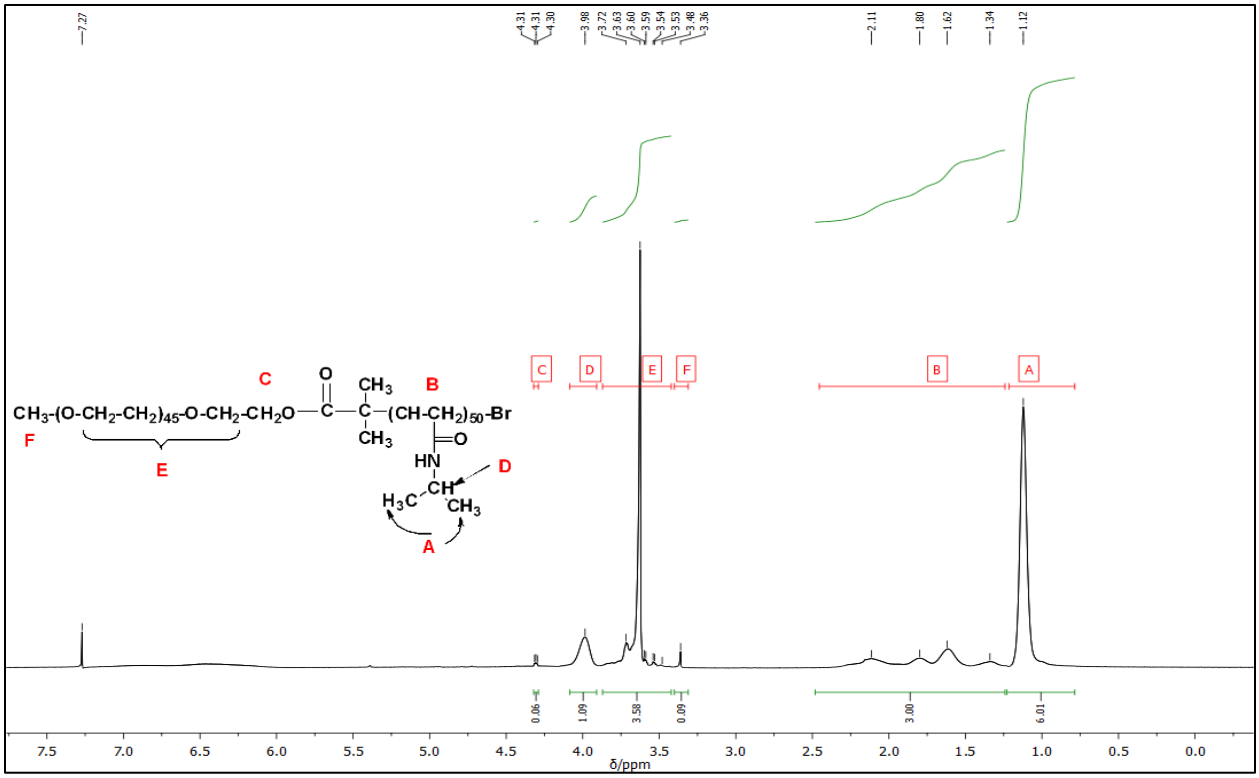

Figure 26. ^{1}H NMR spectrum of the purified polymer MPEG2000-*b*-PNIPAM$_{50}$ in $CDCl_3$.

By comparing the IR spectrum of MPEG2000-*b*-PNIPAM with pure PNIPAM and macroinitiator MPEG-Br, we could easily conclude that the PNIPAM block was successfully connected to the macroinitiator 2-bromopropionate MPEG2000 since the copolymer's IR spectrum showed amide absorption peak (1639 cm^{-1} and 1534 cm^{-1}) coming from PNIPAM block, ester carbonyl absorption peak (1722 cm^{-1}) coming from the ester linkage and strong C-O absorption peak (1100 cm^{-1}) coming from the MPEG2000 fragment. By comparing the C=O absorption of the macroinitiator and MPEG2000-*b*-PNIPAM carefully, we noticed that the carbonyl's absorption shifted from 1734cm^{-1} towards the lower wavenumber at 1722cm^{-1} in the IR spectrum due to the substitution of the Br atom to a long polymer block PNIPAM. Furthermore, we can also calculate the polymerization degree (repeating unit number) of PNIPAM block by calculating the ratio of

peaks' integral numbers showed in the copolymer's ^{1}H NMR spectrum since the peak area's integral is proportional to the assigned protons' number.[84] As aforementioned, MPEG2000 portion has a predetermined M_n of 2056 by the ^{1}H NMR of macroinitiator 2-bromopropionate MPEG2000 and the MPEG block roughly has 46 repeating units of -CH_2CH_2O-. Signal **E** was assigned to the protons of repeating units of -CH_2CH_2O- and signal **A** was assigned to the protons of the two geminal methyl groups. By calculating the integral of peak **E** and peak **A**, we can easily calculate the repeating unit numbers' ratio between -CH_2CH_2O- and NIPAM is:

$$\frac{(3.58 + 0.06)/4}{6.01/6} = 0.91$$

The result indicates that the repeating units of -CH_2CH_2O- and NIPAM have a ratio of 0.91:1. As we have calculated the repeating unit number of MPEG block is 46, we can conclude that the repeating unit number of NIPAM is 50.5 and the polymer's structure is roughly MPEG2000-*b*-$PNIPAM_{50}$. And the number-average molecular weight of the synthesized copolymer is M_n = 7816.

6.1.2 Characterization of MPEG750-*b*-$PNIPAM_{35}$

The chemical structure of the macroinitiator MPEG750-Br and block copolymer MPEG750-*b*-$PNIPAM_{35}$ were confirmed by both ^{1}H NMR and FT-IR. The number-average molecular weight (M_n) of the copolymer was also determined by ^{1}H NMR.

The successful synthesis of macroinitiator MPEG750-Br was confirmed by both ^{1}H NMR spectrum and IR spectrum. From Figure 27 we can easily find hydroxyl group in MPEG was

esterified and the signal at 4.26 ppm was assigned to the geminal protons of the CH_2 attached to the ester group's oxygen.

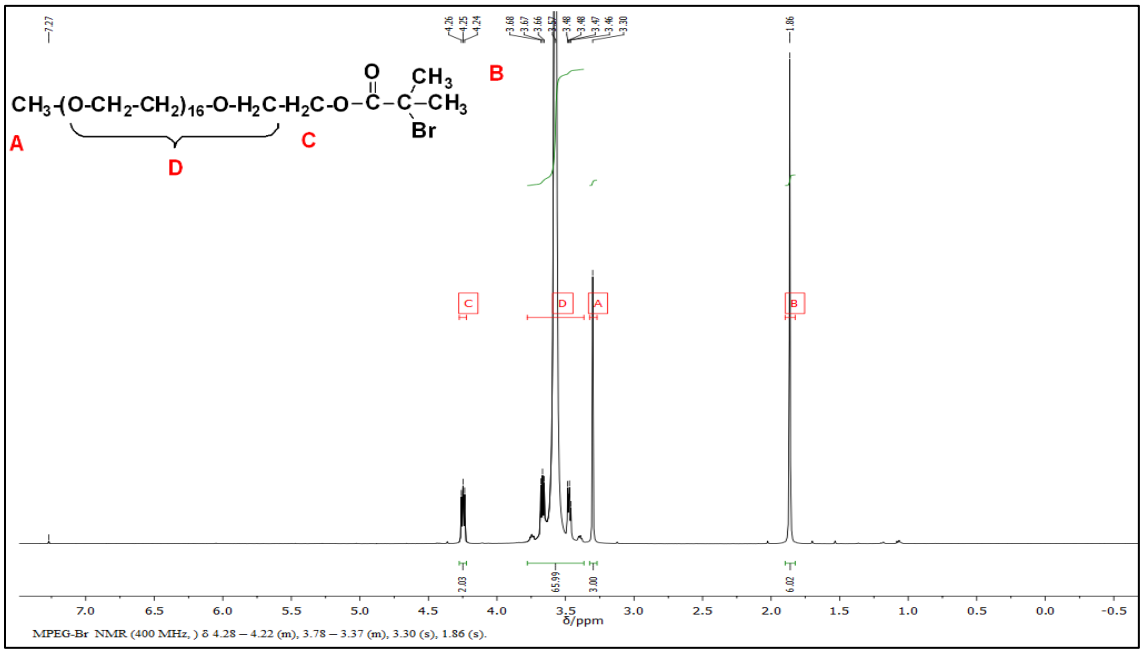

Figure 27. ^{1}H NMR spectrum of the purified macroinitiator 2-bromopropionate MPEG750 in $CDCl_3$.

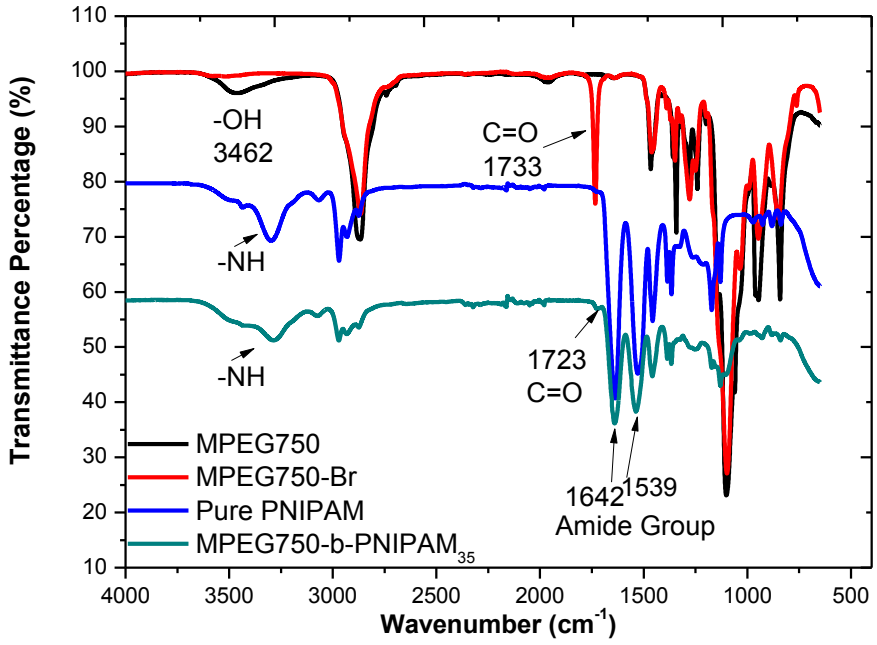

Figure 28. IR spectra of pure PNIPAM, pure MPEG750, macroinitiator MPEG750-Br and synthesized polymer MPEG750-*b*-PNIPAM$_{35}$.

By comparing the IR spectrum of MPEG750 and MPEG750-Br shown in Figure 28, we can see the absorption at 3462 cm^{-1} for hydroxyl group in MPEG750 but there is no -OH peak showed in spectrum of macroinitiator MPEG750-Br. And the spectrum of MPEG750-Br showed a new peak at 1733 cm^{-1} which is typically a characteristic absorption of aliphatic ester carbonyl. It could be concluded that the macroinitiator MPEG-Br was successfully synthesized and purified. More importantly, as the integral of each peak in ^{1}H NMR is proportional to the proton number that it represents, by comparing the integral number, we can calculate the average repeating units number of ethylene oxide for each MPEG750-OH chain is 17. And the average molecular weight of MPEG is 764, which is nearly the same as the number (M_n~750) given by chemical supplier.

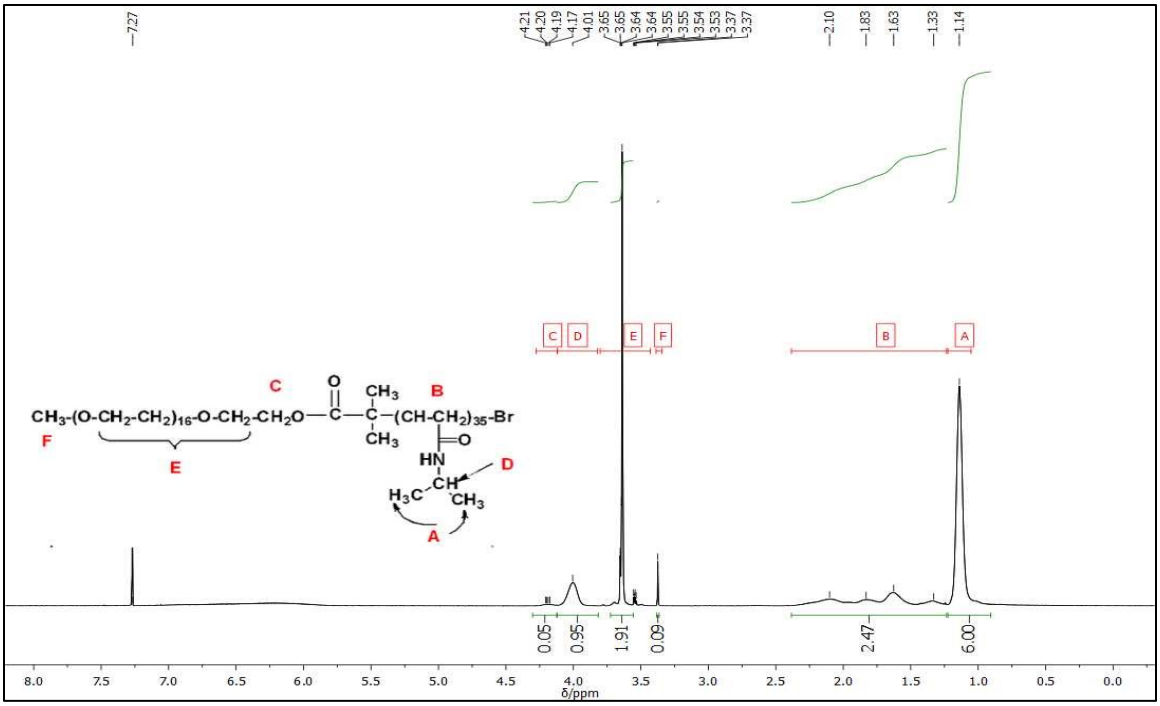

Figure 29. ^{1}H NMR spectrum of the purified polymer MPEG750-*b*-PNIPAM$_{35}$ in $CDCl_3$.

With the macroinitiator MPEH750-Br in hand, we conducted the ATRP reaction with a ratio of [Initiator]: [NIPAM] =1:35 and got the ^{1}H NMR spectrum and IR spectrum of the purified product. The assignment of the peaks of the ^{1}H NMR spectrum was shown in Figure 29 with the synthesized polymer structure. By comparing the IR spectrum of MPEG750-*b*-PNIPAM with pure PNIPAM and macroinitiator MPEG-Br in Figure 28 we can easily conclude that the PNIPAM block was successfully connected to the macroinitiator 2-bromopropionate MPEG750 since the synthesized polymer's IR spectrum showed amide absorption coming from PNIPAM block (1642 cm^{-1}, 1539 cm^{-1}), ester carbonyl absorption (1723 cm^{-1}) coming from the ester linkage and C-O absorption at around 1100 cm^{-1} coming from the MPEG750 fragment. By comparing the C=O absorption of the macroinitiator and MPEG750-*b*-PNIPAM carefully, we could notice that the carbonyl's absorption peak shifted from 1733cm^{-1} towards the lower wavenumber at 1723 cm^{-1} in

the IR spectrum and it was due to the substitution of the Br atom into a long PNIPAM block. Furthermore, we can also calculate the polymerization degree (repeating unit number) by the ratio of peaks' integrals showed in the copolymer's ^{1}H NMR spectrum since the peaks area is proportional to the assigned protons' population. As MPEG750 has a predetermined M_n of 764 based on the analysis of the ^{1}H NMR of macroinitiator 2-bromopropionate MPEG750, the MPEG part roughly has 17 repeating units of -CH_2CH_2O-. Signal **E** was assigned to the protons of repeating units of -CH_2CH_2O- and signal **A** was assigned to the protons of the two geminal methyl groups, which are shown in Figure 31. By determining the integrals of peak **E** and peak **A**, we can easily calculate the repeating units' ratio between -CH_2CH_2O- and N-isopropyl acrylamide is:

$$\frac{1.91/4}{6.00/6} = 0.48$$

The result indicates that the repeating units of -CH_2CH_2O- and NIPAM have a ratio of 0.48:1. As we have calculated the repeating unit number of MPEG is 17, we can conclude that the repeating unit number of N-isopropyl acrylamide is 35, the polymer's structure is MPEG750-*b*-$PNIPAM_{35}$ and the number-average molecular weight of the synthesized copolymer is M_n =4785.

6.2 Interfacial Tension Measurement of the Polymer Solution

The block copolymer MPEG2000-*b*-$PNIPAM_{50}$ and MPEG750-*b*-$PNIPAM_{35}$'s aqueous solution were made into 50 ppm (polymer mass/water mass). The interfacial tension between pure toluene and polymer solution was measured at different temperature to test our design of taking advantage of the switchable property of the polymers. Du Noüy Ring method was used to measure the interfacial tension and the results are shown in Figure 30.

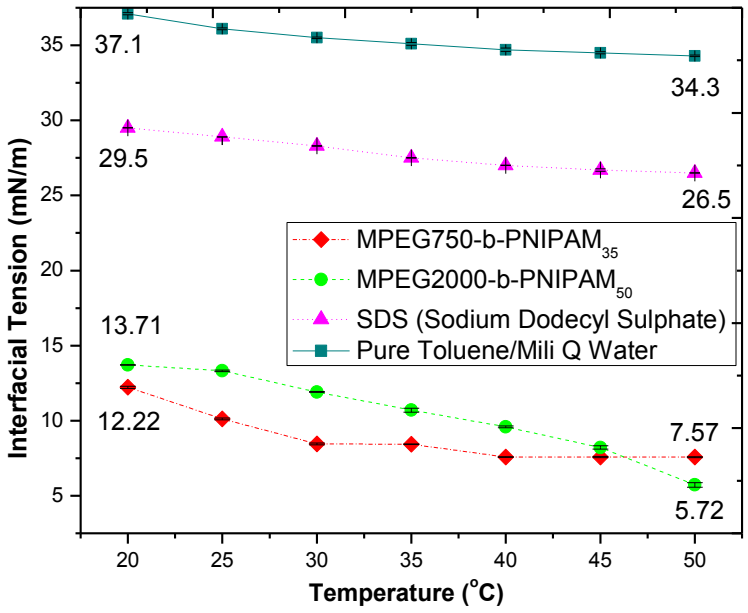

Figure 30. Interfacial tension between polymer solution and pure toluene. MPEG750-*b*-PNIPAM$_{35}$, MPEG2000-*b*-PNIPAM$_{50}$, and SDS were all made into aqueous solutions with concentration of 50 ppm (mass of solute/mass of water).

By analyzing the data, we could find the synthesized polymers showed good interfacial activity comparing with commercially available surfactant SDS (sodium dodecyl sulfate) at the same concentration (50 ppm). Also, the synthesized polymers showed noteworthy interfacial tension changes with temperature changes. Briefly, the synthesized polymers showed better interfacial activity at water and toluene interface when temperature went up from 20 °C to 50 °C. And this may due to the PNIPAM block in the copolymer changed from hydrophilic to more hydrophobic and the copolymers were amphiphilic when temperature went up, which was showed in our design.

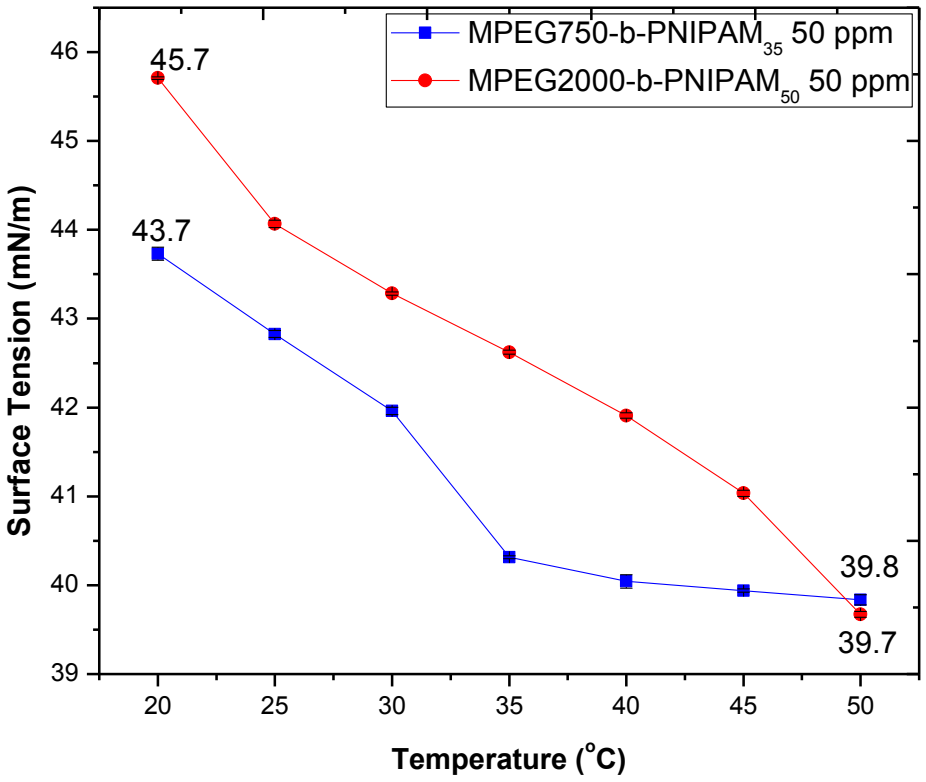

Figure 31. Surface tension of polymer solution. MPEG750-*b*-PNIPAM$_{35}$, MPEG2000-*b*-PNIPAM$_{50}$ were both made into aqueous solutions with concentration of 50 ppm (mass of solute/mass of water).

6.3 Surface Tension Measurement of Two Polymers

The surface tension of the two polymer solutions were also measured at different temperature and the results are shown in Figure 31.

Although the surface tension of both polymer solution decreased, the changes were not as much as the interfacial tension between toluene and water. These results indicate the PNIPAM block may

have different conformation at different interface. When the copolymer is at water/toluene interface, the PNIPAM block may partially dissolved.

6.4 Turbidity Measurement of Synthesized Polymers

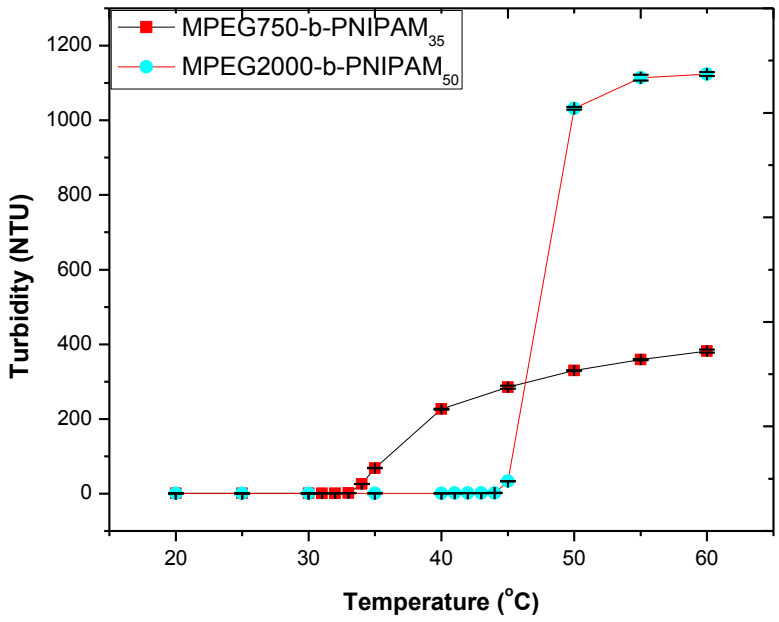

Figure 32. Turbidity MPEG2000-*b*-PNIPAM$_{50}$ 1000 ppm solution, MPEG750-*b*-PNIPAM$_{35}$ 1000 ppm solution with temperature change.

The turbidities of synthesized polymers were measured by using Micro100 Laboratory Turbidimeter from HF Scientific and the results are shown in Figure 32.

From Figure 32, we can find the cloud point of MPEG2000-*b*-PNIPAM$_{50}$ and MPEG750-*b*-PNIPAM$_{35}$ were at 45 °C and 34 °C respectively. For pure PNIPAM polymer, the cloud point is around 32°C.[70, 71] We may conclude that the connection of the water soluble block of

MPEG to PNIPAM made the cloud point go up, in another words, it changed the LCST of PNIPAM by connecting the second block to it. And it seems that the higher the ethylene oxide/NIPAM repeating unit ratio, the higher the cloud point temperature. A plausible explanation is that the longer water soluble part (MPEG block) made the entire polymer molecule more hydrophilic and less easily to precipitate out from the solution.

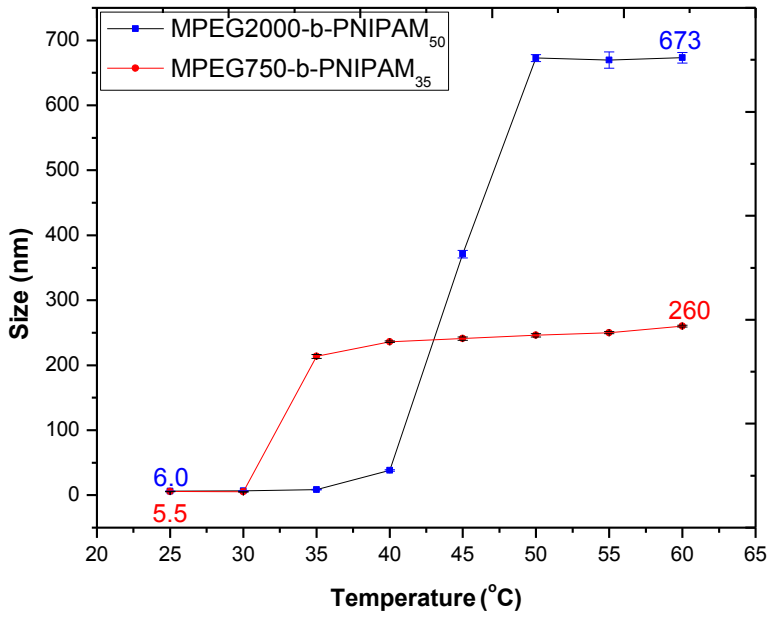

Figure 33. Species size of MPEG2000-*b*-PNIPAM$_5$ 1000 ppm solution and MPEG750-*b*-PNIPAM$_{35}$ 1000 ppm solution at different temperature, the micelles formed above its LCST.

6.5 Polymer Species Size in Aqueous Solution

The polymer species' size were measured at different temperature by Zetasizer Nano-ZS (Malvern Instruments Ltd., Worcestershire, U.K.). The results are shown in Figure 33.

The results showed that both polymer may form miscells after the temperature raised above their LCST respectively. From the results showed in Figure 33, we may infer that MPEG2000-*b*-PNIPAM$_{50}$ formed bigger micells than MPEG750-*b*-PNIPAM$_{35}$ since MPEG2000-*b*-PNIPAM$_{50}$ has more repeating units and longer chains than MPEG750-*b*-PNIPAM$_{35}$.

6.6 Bitumen Flotation Test

The bitumen floatation test was conducted using Denver flotation cell. Each test was repeated three times to calculate the average number of results. In the test with polymer addition, 50 mg polymer was added and mixed with 1050 ml process water in total, which gave us a polymer solution with roughly 50 ppm polymer concentration based on water mass (Table 3).

Table 3. Addition of polymer in flotation tests.

Test Group	A	B	C
Polymer Added	No Polymer	MPEG2000-*b*-PNIPAM$_{50}$	MPEG750-*b*-PNIPAM$_{35}$
Polymer Mass	0	50 mg	50 mg

By comparing the results shown in Figure 33, we could find that both MPEG2000-*b*-PNIPAM$_{50}$ and MPEG750-*b*-PNIPAM$_{35}$ increased of bitumen recovery by around 15% after their addition in flotation slurry. And these results gave us a preliminary proof of the feasibility of our design. However, after we carefully analyzed other parameters to evaluate the extraction, we found that polymer MPEG2000-*b*-PNIPAM$_{50}$ lowered the froth quality significantly in terms of the Bitumen/Water ratio (Figure 34) and Bitumen/Solid ratio (Figure 35). In the test with

MPEG2000-*b*-PNIPAM$_{50}$ addition, the Bitumen/Solids ratio and Bitumen/Water ratio were 2.08 and 0.29 comparing to 2.63 and 0.35 respectively in the conditions without polymer. It indicates that copolymer MPEG2000-*b*-PNIPAM$_{50}$ may bring more solids, salts and water into the bitumen froth, which is detrimental to froth treatment and downstream refinery processing.[85, 86]

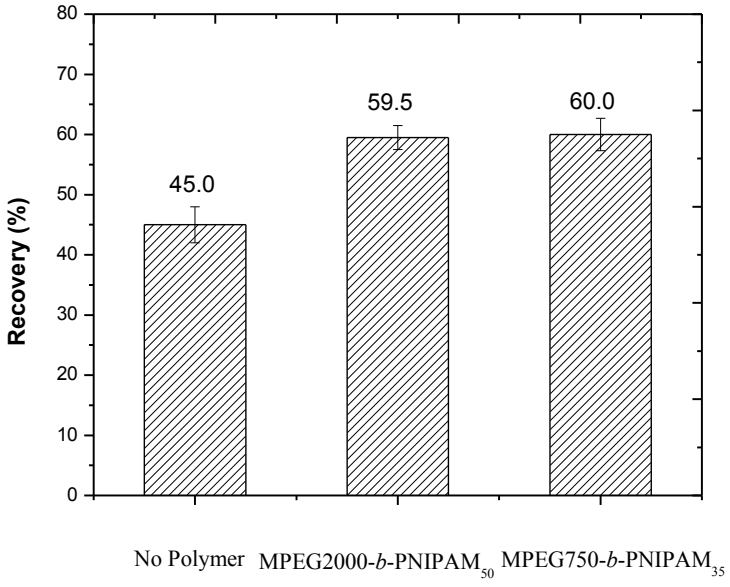

Figure 34. Recovery of bitumen in extraction tests.

On the other hand, after the addition of MPEG750-*b*-PNIPAM$_{35}$ into the extraction process, the froth collected had nearly the same quality as the froth we got from the extraction test without polymer addition. It seemed that the copolymer with shorter chain length showed better performance than its longer analogue. Previously, it has been reported that the addition of high molecular weight of PNIPAM into extraction process made the froth quality decrease as high molecular weight PNIPAM would facilitate the attachment of fine solids to bitumen droplets and, hence, could cause severe slime coating consequently. It is plausible that the longer PNIPAM chain in MPEG2000-*b*-PNIPAM$_{50}$ could attach to and collect more solids and stick to bitumen

surface.[53]

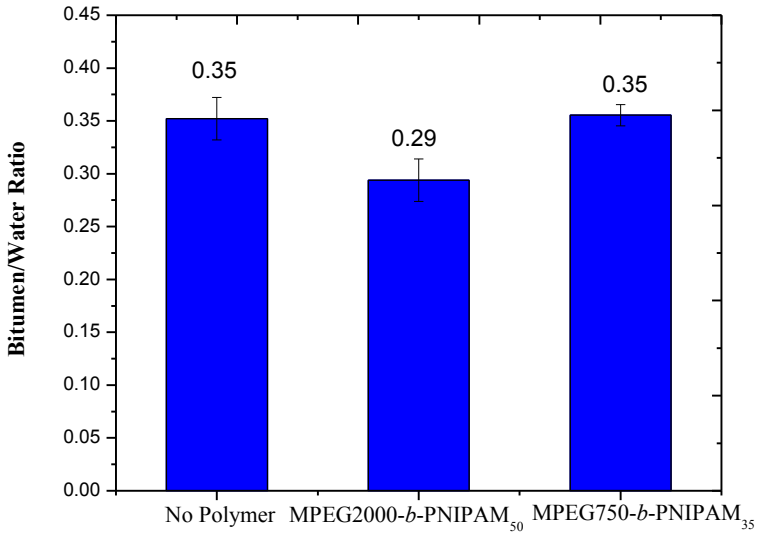

Figure 35. Bitumen/Solids ratio of froth collected in extraction tests.

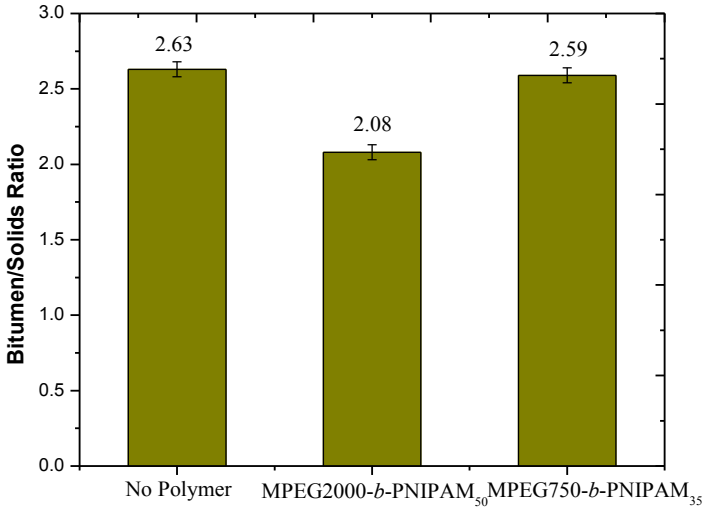

Figure 36. Bitumen/Water ratio of froth collected in extraction tests.

We then screened the optimized dosage of the polymer MPEG750-*b*-PNIPAM$_{35}$ for the extraction. Each group of test has three parallel trials.

Table 4. Polymer dosage effect on Denver flotation cell bitumen extraction.

Test Group	1	2	3	4	5
Polymer Mass	0	25 mg	50 mg	100 mg	200 mg

The results in Figure 37 showed the bitumen recovery didn't change too much when the polymer concentration was over 50 ppm. And the froth quality decreased a little bit in terms of Bit/Solid ratio (Figure 38) and Bit/Water ratio (Figure 39). In order to save chemicals and lower the cost, the further tests were all done under 50 ppm polymer concentration.

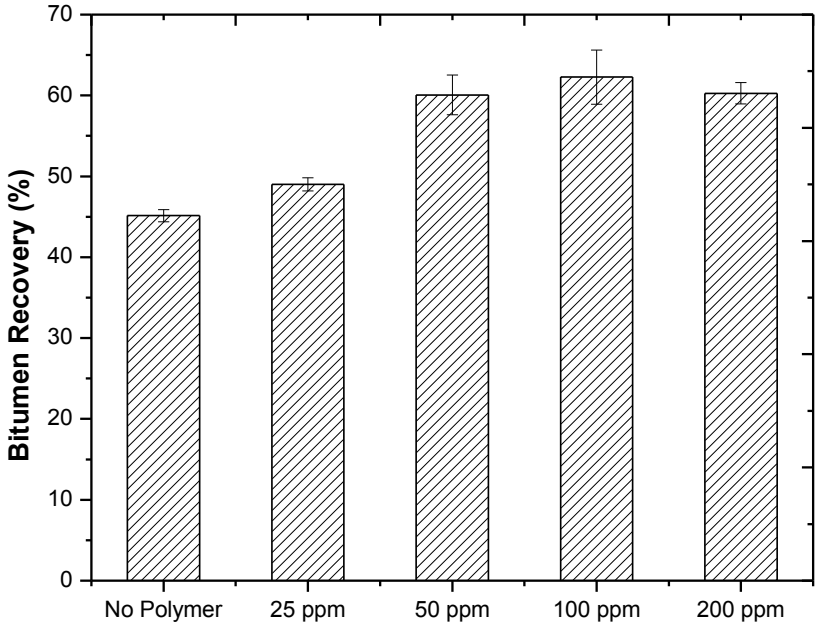

Figure 37. Bitumen recovery with different dosage of MPEG750-*b*-PNIPAM$_{35}$.

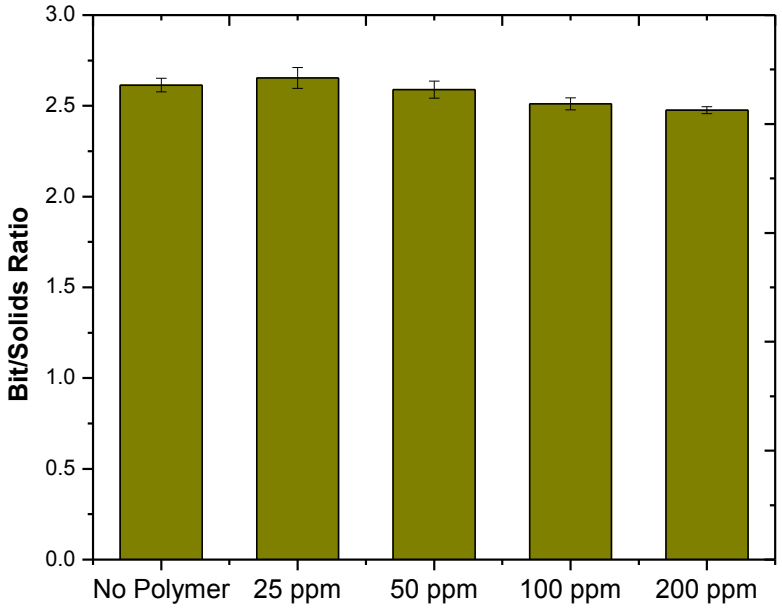

Figure 38. Bit/Solids ratio with different dosage of MPEG750-*b*-PNIPAM$_{35}$.

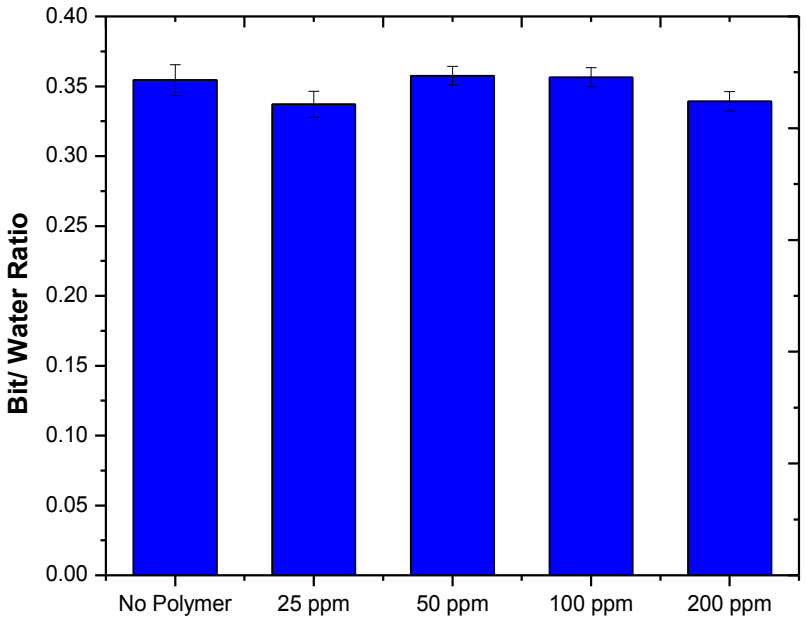

Figure 39. Bit/Water ratio with different dosage of MPEG750-*b*-PNIPAM$_{35}$.

6.7 Liberation Cell Test

The oil sands ore samples were subjected to liberation cell tests under different liberation temperatures in process water (pH=7.7) with or without polymer addition. Videos were taken from our self-built BLFVC and were analyzed according to the method aforementioned in experiment section. As an example, the pictures of bitumen liberation test at different time with 50 ppm MPEG750-*b*-PNIPAM$_{35}$ at 50 °C were shown in Figure 40. By analyzing the videos taken from liberation tests, we got the DBL% *vs.* time curve shown in Figure 41 and Figure 42. The addition of copolymer MPEG2000-*b*-PNIPAM$_{50}$ and MPEG750-*b*-PNIPAM$_{35}$ facilitated the liberation of bitumen from oil sands at both 20 °C and 50 °C. Both liberation speed and final liberation degree increased. The results may due to the polymer's good interfacial activity of lowering the interfacial tension between bitumen and sand grains, especially at higher temperature, at which the block copolymers were more amphiphilic. These liberation tests provide good evidence to prove our design shown at the beginning.

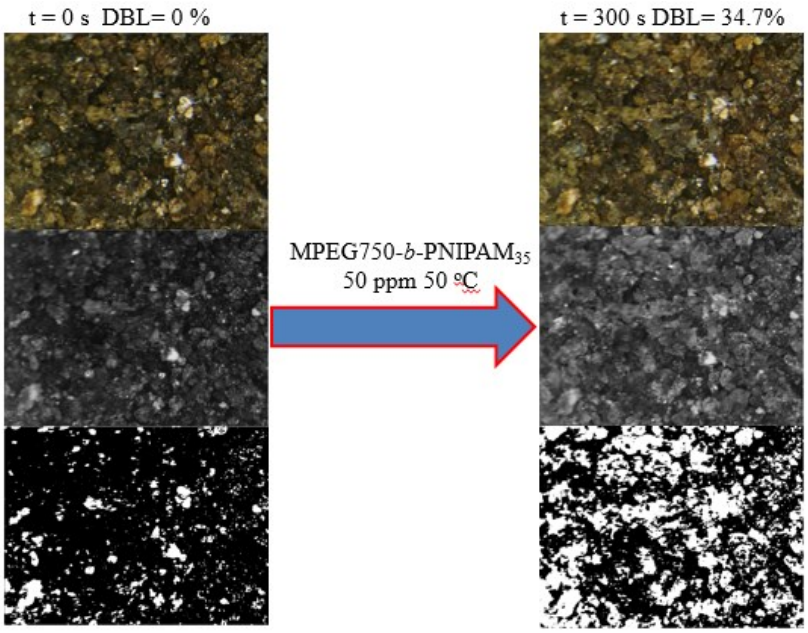

Figure 40. Bitumen liberation with 50 ppm MPEG750-*b*-PNIPAM$_{35}$ at 50 °C (pH=7.7).

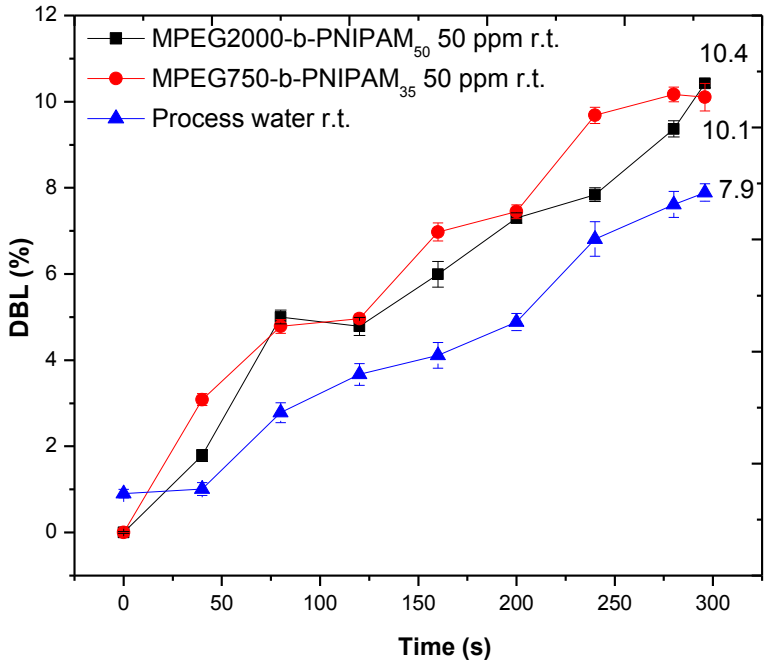

Figure 41. DBL vs. time for liberation cell tests at 20 °C. (pH=7.7)

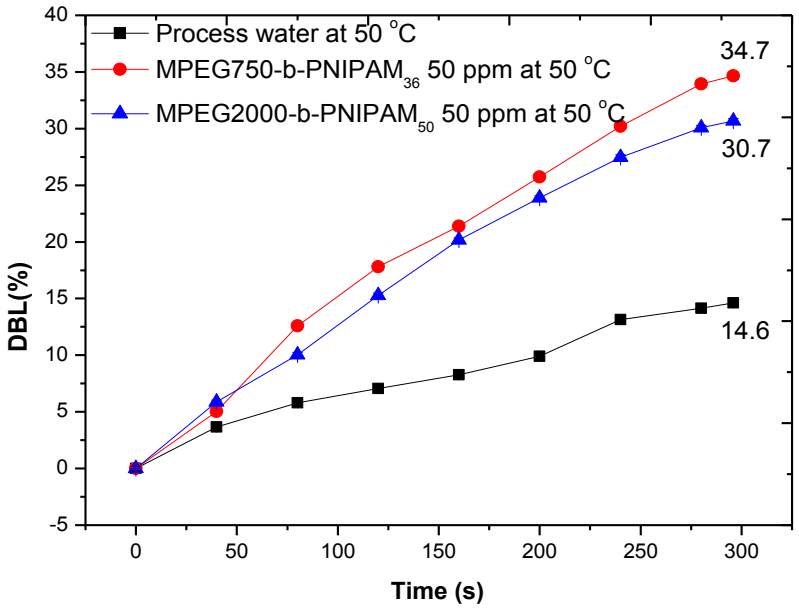

Figure 42. DBL *vs.* time for liberation cell tests at 50 °C. (pH=7.7)

6.8 Induction Time Measurement

In order to understand our copolymer's impacts on both liberation and aeration stages respectively, we measured induction time through bitumen-air bubble attachment. In our test, vacuum distillate bitumen supplied by Syncrude Canada Ltd. was used and the induction time for bitumen-air bubble attachment was defined as the contact time that leads to 50 % of attachment. The measurements were conducted at 50 °C in process water with or without polymer addition and the results are shown in Figure 43.

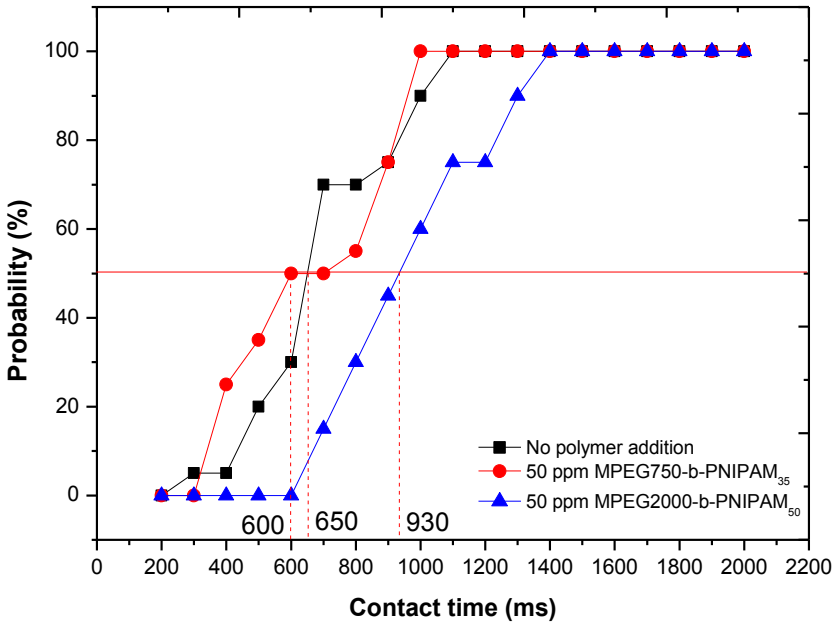

Figure 43. Probability *vs.* contact time for bitumen-air bubble attachment induction time measurement at 50 °C.

When the tests were done in process water without polymer, the induction time was 650 ms while the addition of polymer MPEG750-*b*-PNIPAM$_{35}$ gave an induction time around 600 ms. It showed that the addition of MPEG750-*b*-PNIPAM$_{35}$ reduced the induction time a little. However,

in typical extraction process, as caustic was added into slurry, it would increase the pH of slurry and facilitate the ionization of natural surfactant inside the bitumen. Typically, the addition of sodium hydroxide would produce more anionic surfactant attached to bitumen surface and significantly increase the induction time due to the increase of repulsion force from negatively charged bitumen surface and air-bubble.[51] Comparing with classical caustic, MPEG750-*b*--PNIPAM$_{35}$ showed fairly good performance. It is plausible that the interfacial active polymer covers both bitumen surface and air bubble, which leads to less repulsive electrical double layer force when they approach to each other. In the case of MPEG2000-*b*-PNIPAM$_{50}$ the induction time increased quite a lot to 930 ms, which may due to the longer polymer chain of MPEG2000 in the copolymer which led to more steric hindrance for air bubble attachment.

6.9 Recoverability Test of Synthesized Polymer

We expected the polymer used during extraction process could be recovered after the extraction and could be reused together with process water, so we designed experiments to determine the amount of polymer we could recover from aqueous phase when the temperature cooled down to the temperature lower than its LCST. At a given temperature, the turbidity of MPEG750-*b*-PNIPAM$_{35}$ solution has a linear correlation with polymer's concentration in a concentration range. The correlation of turbidity *vs.* temperature for different concentration of polymer solutions were plotted in Figure 44. We got linear correlation equations of turbidity *vs.* polymer concentration at different temperatures respectively (Figure 45 and Figure 46 showed two example of the linear fit equation at 50 ^{o}C and 25 ^{o}C).

With the standard curves and equations of polymer concentration vs. turbidity at a certain temperature, we could easily correlate a measured turbidity of polymer aqueous solution to its

polymer concentration at that temperature. As the color of bitumen may have huge impact on the turbidity measurement, we invoked HPLC grade toluene as organic phase to test the recoverability of the polymer. Basically, 24 ml of 250 ppm MPEG750-*b*-PNIPAM$_{35}$ polymer solution and 1 ml toluene were well mixed in a vial, and the mixture was settled at test temperature for 12 h. The turbidity of the aqueous phase was then measured at the same temperature and the concentration of polymer in aqueous phase can be calculated by the linear fit equation of polymer concentration vs. turbidity. The linear fit equation of MPEG750-*b*-PNIPAM$_{35}$'s concentration vs. turbidity at different temperature and the calculated polymer concentrations based on the measured turbidity in the recoverability test are listed in Table 5. By comparing the polymer concentration change in aqueous phase, we can calculate the percentage of recovered polymer when we change the temperature.

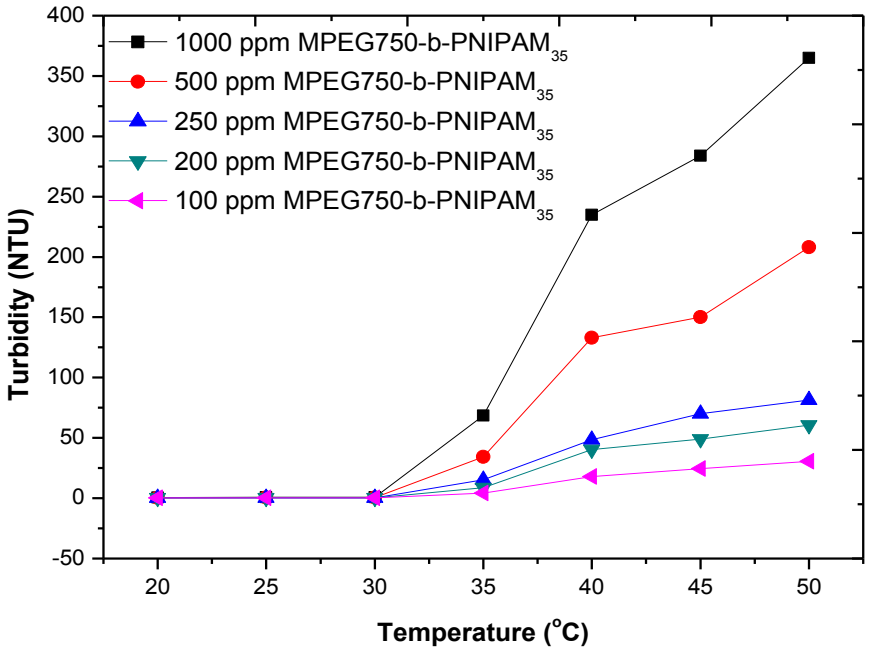

Figure 44. Turbidity *vs.* temperature for different concentration of MPEG750-*b*-PNIPAM$_{35}$ solutions.

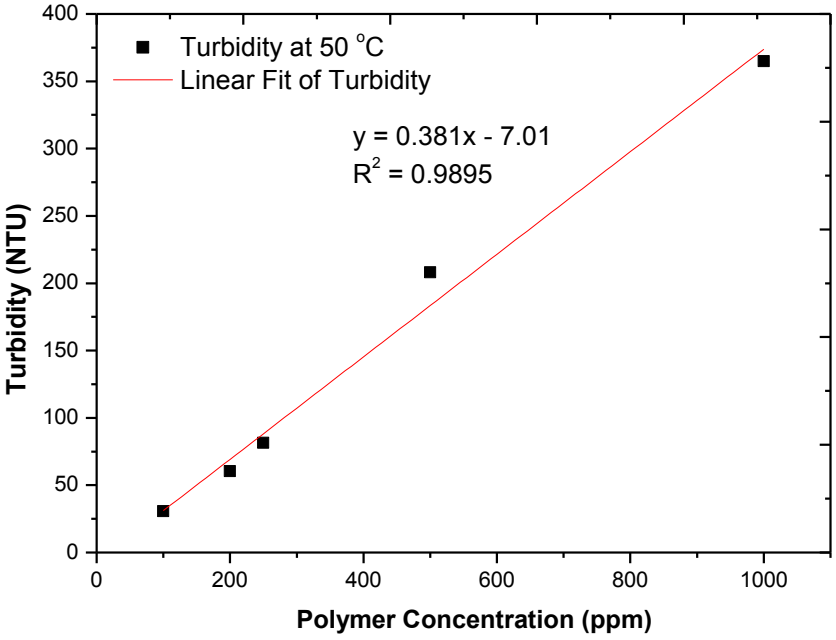

Figure 45. Turbidity *vs*. MPEG750-*b*-PNIPAM$_{35}$ concentration at 50 °C.

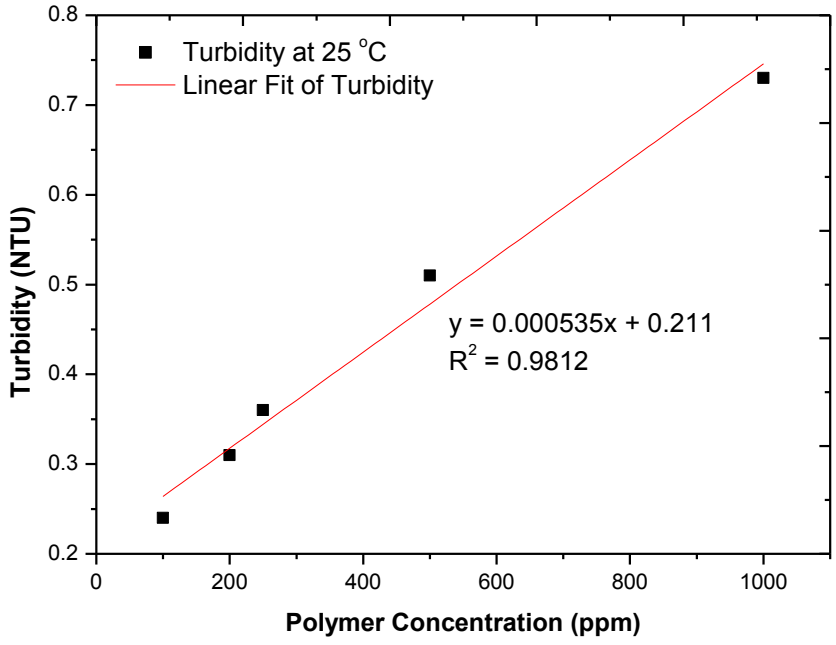

Figure 46. Turbidity *vs*. MPEG750-*b*-PNIPAM$_{35}$ concentration at 25 °C.

Table 5. Linear fit equations at different temperature.

Temperature/°C	Turbidity(y) *vs.* Conc.(x)	Turbidity Measured /NTU	Polymer Conc.(x)/ppm
50	y= 0.381x- 7.01	**50.9**	**152**
45	y = 0.291x - 3.84	**44.5**	**166**
40	y = 0.247x - 6.26	**34.5**	**166**
35	y = 0.0727x - 3.63	**12.5**	**222**
30	y = 0.000629x + 0.218	**0.37**	**242**
25	y = 0.000535x + 0.211	**0.34**	**241**

We define R as:

$$R = \frac{\text{Polymer concentration in aqueous at T}}{\text{Original polymer concentration in aqueous phase}} \times 100\% \qquad [13]$$

From Figure 47 and Figure 48 we could easily conclude that when the temperature went down, more and more MPEG750-*b*-PNIPAM$_{35}$ dissolved back into aqueous phase since the PNIPAM block turned to more hydrophilic. When the temperature was at 50 °C, only 60.8% of polymer remained in the aqueous phase. However, when the temperature was cooled down to 25~30 °C, around 97% percent of polymer dissolved back into the aqueous phase, which proved that the polymer is potentially recoverable and could be reused along with process water. However, as the real bitumen extraction and froth treatment system are more complicated than pure toluene/water system, we can only state that our polymer is potentially feasible in practical system.

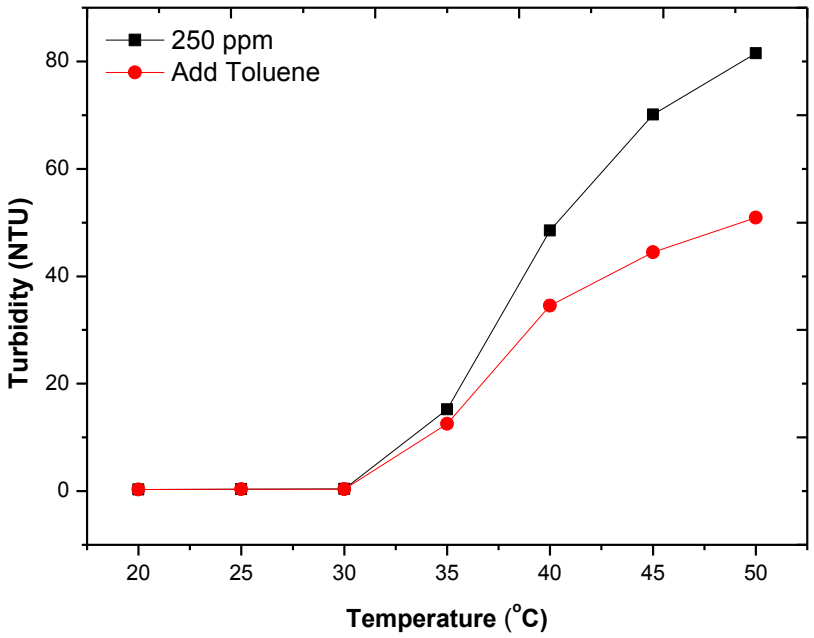

Figure 47. Turbidity *vs.* temperature with/without toluene addition.

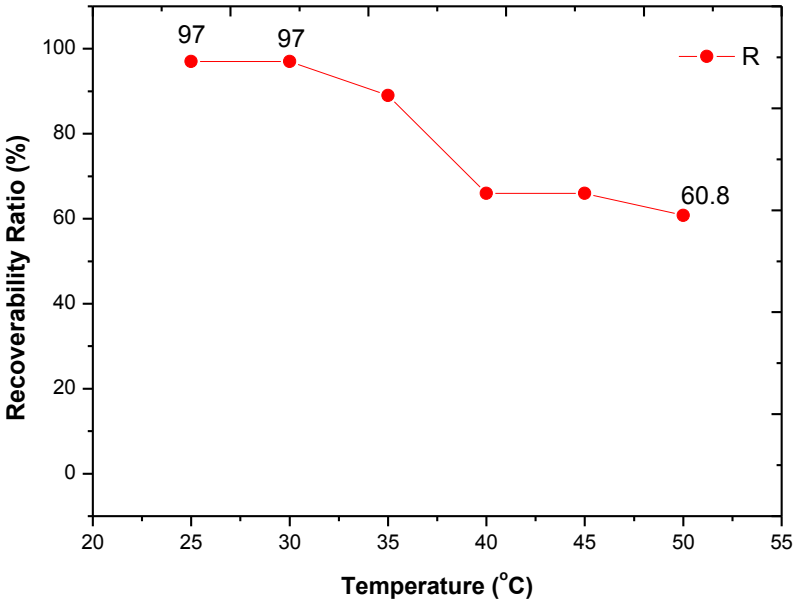

Figure 48. Recoverability of MPEG750-*b*-PNIPAM$_{35}$ ratio *vs.* temperature with toluene addition.

Chapter 7. Conclusions

Based on the technics of current oil sands extraction process and the property of temperature switchable polymers, we designed and synthesized two types of temperature switchable non-ionic block copolymers MPEG2000-*b*-PNIPAM$_{50}$ and MPEG750-*b*-PNIPAM$_{35}$ by taking advantage of the hydrophilicity of MPEG block and switchable property of PNIPAM block. The non-ionic block copolymers were synthesized by ATRP method with functionalized MPEG as macroinitiator and the block copolymers' structure were confirmed by both ^{1}H NMR and IR.

The non-ionic block copolymers showed good interfacial activity between toluene and water. And their interfacial activity showed noteworthy dependence on temperature changes which confirmed our design concept on "switchable".

The application of the two polymers to Denver cell tests showed that polymers could help increase the recovery of bitumen. However, with longer polymer chains and higher molecular weight, MPEG2000-b-PNIPAM$_{50}$ gave poor froth quality in bitumen extraction which may due to its higher probability of flocculating solids comparing with low molecular weight analogous MPEG750-*b*-PNIPAM$_{35}$.

Further liberation cell tests of the two polymers showed that they both facilitate the liberation process by increasing the liberation rate and DBL.

Induction timer measurements showed that MPEG750-*b*-PNIPAM$_{35}$ didn't help too much to lower the induction time comparing to blank test. However, by comparing with classical caustic additive like NaOH, MPEG750-*b*-PNIPAM$_{35}$ revealed fairly good performance.[51] It may due to the reduction of repulsive double layer force by using non-ionic polymer, leading to an enhanced drainage and rupture of thin water films between bitumen and air bubbles during the attachment

process.[16, 36, 44, 50, 87] On the contrary, MPEG2000-*b*-PNIPAM$_{50}$ polymer solution increased the induction time between air bubbles and bitumen surfaces, which may be due to the steric hindrance originate from the longer polymer chains.

The recoverability test of MPEG750-*b*-PNIPAM$_{35}$ between pure toluene and water phase showed that it has good switching property, which was one of the main goals in our design. When temperature cooled down from 50 ^{o}C to 20 ~ 25 ^{o}C, most of the polymer in oil phase could dissolve back into aqueous phase, which is potentially feasible to recover and reuse the polymer together with process water.

The preliminary results proved the feasibility of our design of taking advantage of temperature switchable non-ionic block copolymers to facilitate oil sands extraction process with recoverable material and less environmental impact.

Chapter 8. Future Work

Present work and results are still limited to lab test without further plant practical examination. And the mechanism study is still ongoing. The Future work may undergo in the following aspects.

1. Current polymers are not systematically synthesized, we should evaluate the influence of the length of each block. The following are the polymers should be synthesized, so we can evaluate the influence from the length of each block and the ratio between the two blocks, *etc.*

   MPEG750-*b*-PNIPAM$_{17}$ (repeating unit ratio = 1:1), MPEG750-*b*-PNIPAM$_{52}$ (repeating unit ratio = 1:3); MPEG2000-*b*-PNIPAM$_{100}$ (repeating unit ratio = 1:2), MPEG2000-*b*-PNIPAM$_{150}$ (repeating unit ratio = 1:3). One of the important things need to be notify here is the ligand selection for the ATRP reaction as it has huge influence on the polymerization degree of the PNIPAM block.
2. We also expect it would be more helpful if our polymer can leave bitumen/water interface and dissolve back into water phase, since that will leave bitumen droplets without covered by any surfactants and the bitumen droplet should be more hydrophobic. The more hydrophobic bitumen droplets should be more easily attached and that would enhance bitumen aeration stage. The idea should be evaluate by induction timer measurement. One should conduct the induction time test slightly below the LCST of polymer and make the polymer dissolve back to water and observe if that would reduce induction time.
3. Investigate the interaction between the polymers and bitumen, polymers and clays through AFM. The interactions between bitumen droplets, clays and air bubbles are the majority players in oil sands extraction. The chemical addition usually can affect more than one interactions. As macroscale measurements cannot give too many details of the interactions

between them. By using AFM could give better understanding of what is going on between these colloidal systems.

4. Langmuir–Blodgett trough measurement. Langmuir trough can be used to compress monolayers of molecules on the surface of a substance (*e.g.* water). It can measure the surface phenomena due to the compression. We believe the polymer solution may form a thin layer of film in water surface. The characterization of the film would be very important for the characterization of the polymer and may give more information to discover the mechanism.
5. Brewster's angle measurement of the polymer solution. Brewster's angle is an angle of incidence at which light with a particular polarization is perfectly transmitted through a transparent dielectric surface, with no reflection. With this measurement, one can characterize the surface property after the polymer addition.
6. Calculation of the polymer adsorbed at interface.

   Surface excess is the difference between the amount of a component actually present in the system, and that which would be present in a reference system if the bulk concentration in the adjoining phases were maintained up to a chosen geometrical dividing surface.[87] And the amount of surfactant adsorbed per unit area can be calculated from surface or interfacial tension measurements based on the Gibbs adsorption equation.

   At constant temperature:

$$\Gamma = -\frac{1}{RT}\left(\frac{d\gamma}{dlnC}\right)_T$$

   Based on the data we got of the interfacial tension between Toluene and MPEG2000-*b*--PNIPAM$_{50}$ at different concentration at 20 ^{o}C.

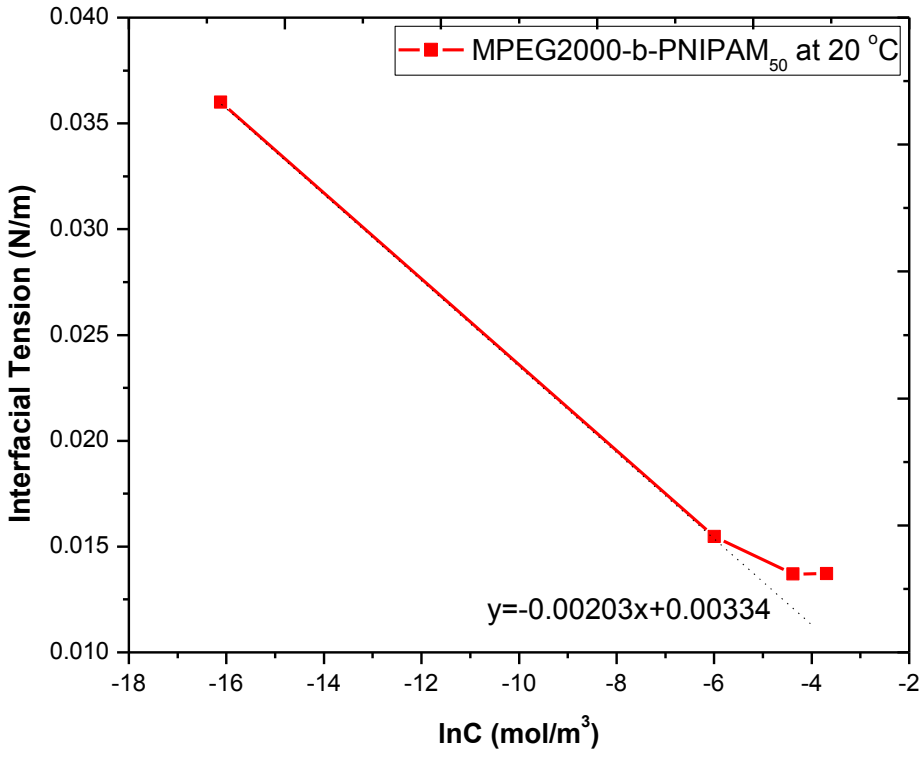

$$\Gamma = -\frac{1}{8.314 \times 298} \times \frac{(-0.00203)mol}{m^2} = 8.19 \times 10^{-7}\ mol/m^2$$

The data are still limited and more tests need to be done to calculate the Gibbs excess for each polymer at different temperatures. By doing this calculation, we can have better ideal how the polymer switch with temperature change, especially how the surface excess correlate with its surface activity.

7. Try to connect other temperature switchable polymer to MPEG, *e.g.*: 2-(2-methoxyethoxy) ethyl methacrylate. There are many types of polymers reported having temperature responsible property and we should screen other candidates for new copolymers.

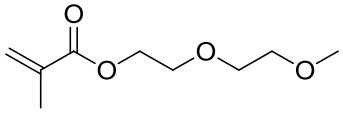

8. Apply the polymer for a pilot extraction process. Apply the polymer to larger scale process, recover the process water after the extraction.

Reference

1. H.Masliyah, J.; Czarnecki, J. A.; Xu, Z., Handbook on theory and practice o bitumen recovery from Athabasca Oil Sands. **2011,** 1, 2.
2. http://www.pythongroup.ca/mining-news/article/id/54.
3. Takamura, K., Microscopic structure of Athabasca oil sand. *The Canadian Journal of Chemical Engineering* **1982,** 60, (4), 538-545.
4. Masliyah, J.; Zhou, Z. J.; Xu, Z.; Czarnecki, J.; Hamza, H., Understanding Water-Based Bitumen Extraction from Athabasca Oil Sands. *The Canadian Journal of Chemical Engineering* **2004,** 82, (4), 628-654.
5. Canada, N. R., Energy Markets Fact Book **2014**, 20-25.
6. Hein, F.; Cotterill, D., The Athabasca Oil Sands — A Regional Geological Perspective, Fort McMurray Area, Alberta, Canada. *Natural Resources Research* **2006,** 15, (2), 85-102.
7. Facts about Alberta's Oil Sands and Its Industry. In Alberta Department of Energy: 2002.
8. Clark, K., The separation of the bitumen from Alberta bituminous sands. *Can. Inst. Min. Metall. Bull* **1929,** 22, 1385-1395.
9. Clark, K., Hot-water separation of Alberta bituminous sand.[High recovery of oil with low sand content obtained with 10 percent water; small air bubbles float oil; too much air floats sand]. *Trans. Can. Inst. Min. Metall.* **1944,** 47.
10. Clark, K., The hot water washing method for recovery of oil from the Alberta tar sands. *Can Oil Gas Ind* **1950,** 3, (6), 46-49.
11. Clark, K., Athabasca Oil Sands–Fundamentals Affecting Development. *Can. Pet* **1966,** 7, 18-21.
12. Clark, K.; Pasternack, D., Hot water seperation of bitumen from Alberta bituminous sand. *Industrial & Engineering Chemistry* **1932,** 24, (12), 1410-1416.
13. Barillas, J. L. M.; Dutra Jr, T. V.; Mata, W., Reservoir and operational parameters influence in SAGD process. *Journal of Petroleum Science and Engineering* **2006,** 54, (1–2), 34-42.
14. Kisman, K. E.; Yeung, K. C., Numerical Study of the SAGD Process in the Burnt Lake Oil Sands Lease. In Society of Petroleum Engineers.
15. Medina, M., SAGD: R&D for unlocking unconventional heavy-oil resources. *The Way Ahead* **2010,** 6, (2), 9.
16. Chen, T. Effect of Salinity on the Warm Water-Based Processing of Mineable Oil Sands. University of Alberta, 2015.
17. H.Masliyah, J.; Czarnecki, J. A.; Xu, Z., Handbook on theory and practice o bitumen recovery from Athabasca Oil Sands. **2011,** 1, 26.
18. H.Masliyah, J.; Czarnecki, J. A.; Xu, Z., Handbook on theory and practice o bitumen recovery from Athabasca Oil Sands. **2011,** 1, 25.
19. Chalaturnyk, R. J.; Don Scott, J.; Özüm, B., MANAGEMENT OF OIL SANDS TAILINGS. *Petroleum Science and Technology* **2002,** 20, (9-10), 1025-1046.
20. Dai, Q.; Chung, K. H., Hot water extraction process mechanism using model oil sands. *Fuel* **1996,** 75, (2), 220-226.
21. Jain, A. K.; Ahmed, K.; Ortiz-volcan, J. L.; Al-Khamees, W., Water Analysis - A Key Tool for Reservoir Monitoring Under Cyclic Steam Stimulation. In Society of Petroleum Engineers.

22. Sheng, J. J., Cyclic Steam Stimulation. *Enhanced Oil Recovery Field Case Studies* **2013**, 389-412.
23. Heidari, M.; Hejazi, S.; Farouq Ali, S. In *SAGD Performance with Temperature Dependent Properties-An Analytical Approach*, SPE Annual Technical Conference and Exhibition, 2015; Society of Petroleum Engineers: 2015.
24. Sheng, J. J., SAGD for Heavy Oil Recovery. *Enhanced Oil Recovery Field Case Studies* **2013**, 413-445.
25. Mohammadpoor, M.; Torabi, F., Comprehensive experimental study and numerical simulation of vapour extraction (VAPEX) process in heavy oil systems. *The Canadian Journal of Chemical Engineering* **2015,** 93, (11), 1929-1940.
26. Sheng, J. J., *In-situ* Combustion *Enhanced Oil Recovery Field Case Studies* **2013**, 447-540.
27. La, H.; Guigard, S. E., Extraction of hydrocarbons from Athabasca oil sand slurry using supercritical carbon dioxide. *The Journal of Supercritical Fluids* **2015,** 100, 146-154.
28. Everett, D. H., *Basic principles of colloid science*. Royal Society of Chemistry: 1988.
29. Butt, H.-J.; Graf, K.; Kappl, M., *Physics and chemistry of interfaces*. John Wiley & Sons: 2006.
30. H.Masliyah, J.; Czarnecki, J. A.; Xu, Z., Handbook on theory and practice o bitumen recovery from Athabasca Oil Sands. **2011,** 1, 53-60.
31. Young, T., An essay on the cohesion of fluids. *Philosophical Transactions of the Royal Society of London* **1805**, 65-87.
32. Gouy, M., Sur la constitution de la charge electrique a la surface d'un electrolyte. *J. Phys. Theor. Appl.* **1910,** 9, (1), 457-468.
33. Gouy, G., Phys. 9, 457 (1910). *Ann. Phys.(Paris)* **1917,** 7, 163.
34. Debye, P.; Hückel, E., De la théorie des électrolytes. i. abaissement du point de congélation et phénomènes associés. *Physikalische Zeitschrift* **1923,** 24, (9), 185-206.
35. Chapman, D. L., LI. A contribution to the theory of electrocapillarity. *The London, Edinburgh, and Dublin Philosophical Magazine and Journal of Science* **1913,** 25, (148), 475-481.
36. H.Masliyah, J.; Czarnecki, J. A.; Xu, Z., Handbook on theory and practice o bitumen recovery from Athabasca Oil Sands. **2011,** 1, 81-104.
37. Lin, K.-W.; Lu, C.-L.; Hsu, T.; Chin, S.; Yen, A., Micro/Nano Lithography Sub-20nm node photomask cleaning enhanced by controlling zeta potential.
38. Werway, E.; Overbeek, J. T. G., Theory of Stability of Lyophobic ColloidsElsevier. *Amsterdam-New York* **1948**, 34.
39. Derjaguin, B.; Landau, L., The theory of stability of highly charged lyophobic sols and coalescence of highly charged particles in electrolyte solutions. *Acta Physicochim. URSS* **1941,** 14, 633-52.
40. Derjaguin, B., On the repulsive forces between charged colloid particles and on the theory of slow coagulation and stability of lyophobe sols. *Transactions of the Faraday Society* **1940,** 35, 203-215.
41. Israelachvili, J. N., *Intermolecular and surface forces: revised third edition*. Academic press: 2011.
42. Russel, W.; Saville, D.; Schowalter, W., Colloidal dispersions. Cambridge monographs on mechanics and applied mathematics. In Cambridge University Press, Cambridge: 1989.
43. Trefalt, G.; Borkovec, M. Overview of DLVO Theory. http://www.colloid.ch/index.php?name=dlvo

44. H.Masliyah, J.; Czarnecki, J. A.; Xu, Z., Handbook on theory and practice o bitumen recovery from Athabasca Oil Sands. **2011,** 1, 289-316.
45. Takamura, K.; Chow, R. S., A Mechanism For Initiation of Bitumen Displacement From Oil Sand.
46. Lelinski, D.; Drelich, J.; Miller, J. D.; Hupka, J., Rate of bitumen film transfer from a quartz surface to an air bubble as observed by optical microscopy. *Canadian journal of chemical engineering* **2004,** 82, (4), 794-800.
47. Adamson, A. W.; Gast, A. P., Physical chemistry of surfaces. **1967**.
48. Mao, L.; Yoon, R.-H., Predicting flotation rates using a rate equation derived from first principles. *International Journal of Mineral Processing* **1997,** 51, (1–4), 171-181.
49. Rabinovich, Y. I.; Yoon, R. H., Use of Atomic Force Microscope for the Measurements of Hydrophobic Forces between Silanated Silica Plate and Glass Sphere. *Langmuir* **1994,** 10, (6), 1903-1909.
50. Yoon, R. H.; Luttrell, G. H., The Effect of Bubble Size on Fine Particle Flotation. *Mineral Processing and Extractive Metallurgy Review* **1989,** 5, (1-4), 101-122.
51. Flury, C.; Afacan, A.; Tamiz Bakhtiari, M.; Sjoblom, J.; Xu, Z., Effect of caustic type on bitumen extraction from Canadian oil sands. *Energy & Fuels* **2013,** 28, (1), 431-438.
52. Li, H.; Long, J.; Xu, Z.; Masliyah, J. H., Synergetic Role of Polymer Flocculant in Low-Temperature Bitumen Extraction and Tailings Treatment. *Energy & Fuels* **2005,** 19, (3), 936-943.
53. Long, J.; Li, H.; Xu, Z.; Masliyah, J. H., Improving Oil Sands Processability Using a Temperature-Sensitive Polymer. *Energy & Fuels* **2011,** 25, (2), 701-707.
54. Li, H.; Long, J.; Xu, Z.; Masliyah, J. H., Effect of molecular weight and charge density on the performance of polyacrylamide in low-grade oil sand ore processing. *The Canadian Journal of Chemical Engineering* **2008,** 86, (2), 177-185.
55. Li, H.; Long, J.; Xu, Z.; Masliyah, J. H., Novel polymer aids for low-grade oil sand ore processing. *The Canadian Journal of Chemical Engineering* **2008,** 86, (2), 168-176.
56. Wang, L.; Dang-Vu, T.; Xu, Z.; Masliyah, J. H., Use of Short-Chain Amine in Processing of Weathered/Oxidized Oil Sands Ores. *Energy & Fuels* **2010,** 24, (6), 3581-3588.
57. Dai, Q.; Chung, K. H., Bitumen—sand interaction in oil sand processing. *Fuel* **1995,** 74, (12), 1858-1864.
58. H.Masliyah, J.; Czarnecki, J. A.; Xu, Z., Handbook on theory and practice o bitumen recovery from Athabasca Oil Sands. **2011,** 1, 79-104.
59. Gu, G.; Xu, Z.; Nandakumar, K.; Masliyah, J., Effects of physical environment on induction time of air–bitumen attachment. *International Journal of Mineral Processing* **2003,** 69, (1), 235-250.
60. Ozum, B., Method for extraction of bitumen from oil sands using lime. In Google Patents: 2011.
61. Masliyah, J.; Czarnecki, J.; Xu, Z., Handbook on Theory and Practice of Bitumen Recovery from Athabasca Oil Sands. *Vol. II. Theoretical basis* **2010**, 374-386.
62. Klimpel, R. R.; Fee, B. S., Recovery of petroleum from tar sands. In Google Patents: 1992.
63. Humphreys, R. D., Tar sands extraction process. In Google Patents: 1999.
64. Sury, K. N., Low temperature bitumen recovery process. In Google Patents: 1990.
65. Allcock, G.; Siy, R.; Spence, J.; Sury, K., Cold dense slurrying process for extracting bitumen from oil sand. In Google Patents: 1999.

66. Ozum, B., Method for improving bitumen recovery from oil sands by production of surfactants from bitumen asphaltenes. In Google Patents: 2011.
67. Hall, J. B.; Russo, A., Process for extracting oil from tar sands. In Google Patents: 1990.
68. Globus, A. R., Process for recovery of bituminous material from tar sands. In Google Patents: 1978.
69. Beetge, J. H.; Kasongo, T.; Komishke, B. D.; Li, H.; Long, J.; Masliyah, J. H.; Venter, J.; Wang, S.; Xu, Z., Processing aids for enhanced hydrocarbon recovery from oil sands, oil shale and other petroleum residues. In Google Patents: 2005.
70. Heskins, M.; Guillet, J. E., Solution Properties of Poly(N-isopropylacrylamide). *Journal of Macromolecular Science: Part A - Chemistry* **1968,** 2, (8), 1441-1455.
71. Schild, H. G., Poly(N-isopropylacrylamide): experiment, theory and application. *Progress in Polymer Science* **1992,** 17, (2), 163-249.
72. Yang, B.; Duhamel, J., Extraction of Oil from Oil Sands Using Thermoresponsive Polymeric Surfactants. *ACS Applied Materials & Interfaces* **2015,** 7, (10), 5879-5889.
73. He, L.; Zhang, Y.; Lin, F.; Xu, Z.; Li, X.; Sui, H., Image analysis of heavy oil liberation from host rocks/sands. *The Canadian Journal of Chemical Engineering* **2015,** 93, (6), 1126-1137.
74. Srinivasa, S.; Flury, C.; Afacan, A.; Masliyah, J.; Xu, Z., Study of Bitumen Liberation from Oil Sands Ores by Online Visualization. *Energy & Fuels* **2012,** 26, (5), 2883-2890.
75. Wang, W.; Zhou, Z.; Nandakumar, K.; Masliyah, J. H.; Xu, Z., An induction time model for the attachment of an air bubble to a hydrophobic sphere in aqueous solutions. *International Journal of Mineral Processing* **2005,** 75, (1), 69-82.
76. Lutz, J.-F.; Hoth, A., Preparation of Ideal PEG Analogues with a Tunable Thermosensitivity by Controlled Radical Copolymerization of 2-(2-Methoxyethoxy)ethyl Methacrylate and Oligo(ethylene glycol) Methacrylate. *Macromolecules* **2006,** 39, (2), 893-896.
77. Özdemir, C.; Güner, A., Solubility profiles of poly(ethylene glycol)/solvent systems, I: Qualitative comparison of solubility parameter approaches. *European Polymer Journal* **2007,** 43, (7), 3068-3093.
78. Zhu, K.; Jin, H.; Kjøniksen, A.-L.; Nyström, B., Anomalous Transition in Aqueous Solutions of a Thermoresponsive Amphiphilic Diblock Copolymer. *The Journal of Physical Chemistry B* **2007,** 111, (37), 10862-10870.
79. Bulmer, J. T.; Starr, J., Syncrude Analytical Methods for Oil Sand and Bitumen Processing. In Alberta Oil Sands Technology and Research Authority (AOSTRA): Edmonton, Alberta, Canada, 1979.
80. Chen, J.; Liu, M.; Gong, H.; Huang, Y.; Chen, C., Synthesis and Self-Assembly of Thermoresponsive PEG-b-PNIPAM-b-PCL ABC Triblock Copolymer through the Combination of Atom Transfer Radical Polymerization, Ring-Opening Polymerization, and Click Chemistry. *The Journal of Physical Chemistry B* **2011,** 115, (50), 14947-14955.
81. Lee, S. B.; Russell, A. J.; Matyjaszewski, K., ATRP Synthesis of Amphiphilic Random, Gradient, and Block Copolymers of 2-(Dimethylamino)ethyl Methacrylate and n-Butyl Methacrylate in Aqueous Media. *Biomacromolecules* **2003,** 4, (5), 1386-1393.
82. Zhou, Z.; Kasongo, T.; Xu, Z.; Masliyah, J., Assessment of Bitumen Re c overy from the Athabasca Oil Sands Using a Laboratory Denver Flotation Cell. *The Canadian Journal of Chemical Engineering* **2004,** 82, (4), 696-703.
83. Dean, E. W.; Stark, D. D., A Convenient Method for the Determination of Water in Petroleum and Other Organic Emulsions. *Journal of Industrial & Engineering Chemistry* **1920,** 12, (5), 486-490.

84. Hong, C.-Y.; You, Y.-Z.; Pan, C.-Y., Synthesis and characterization of well-defined diblock and triblock copolymers of poly(N-isopropylacrylamide) and poly(ethylene oxide). *Journal of Polymer Science Part A: Polymer Chemistry* **2004,** 42, (19), 4873-4881.
85. Peng, J.; Liu, Q.; Xu, Z.; Masliyah, J., Novel Magnetic Demulsifier for Water Removal from Diluted Bitumen Emulsion. *Energy & Fuels* **2012,** 26, (5), 2705-2710.
86. Lopetinsky, R.; Masliyah, J.; Xu, Z., *Solids‐stabilized emulsions: A review, in Colloidal Particles at Liquid Interfaces*. Cambridge University Press: 2006.
87. Luttrell, G. H.; Yoon, R. H., A hydrodynamic model for bubble—particle attachment. *Journal of Colloid and Interface Science* **1992,** 154, (1), 129-137.

Appendix

A1. Size Measurement of Polymer Solution

A1.1 MPEG750-*b*-PNIPAM$_{35}$ 1000 ppm

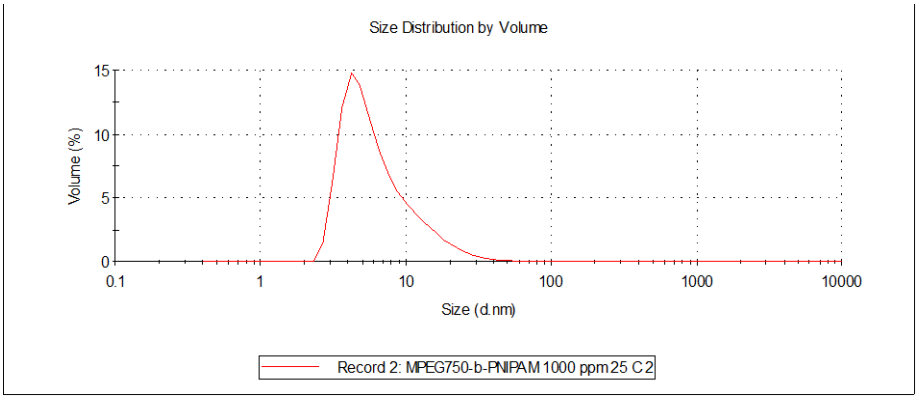

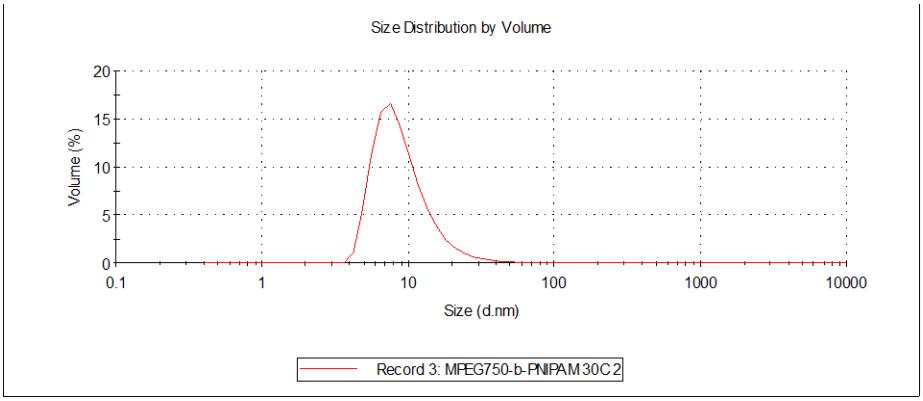

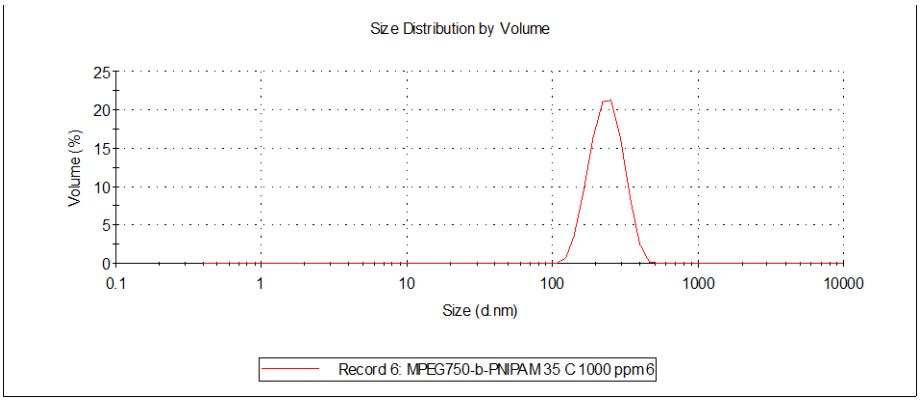

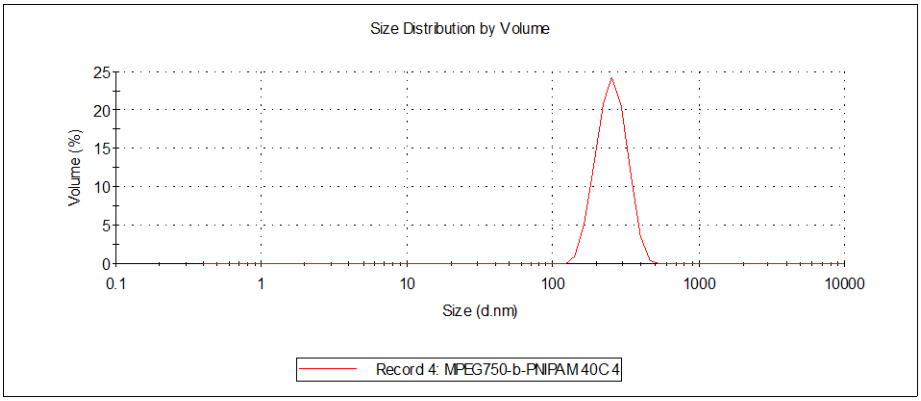
Size Distribution by Volume
Volume (%)
25
20
15
10
5
0
0.1
1
10
100
1000
10000
Size (d.nm)
Record 4: MPEG750-b-PNIPAM 40C 4

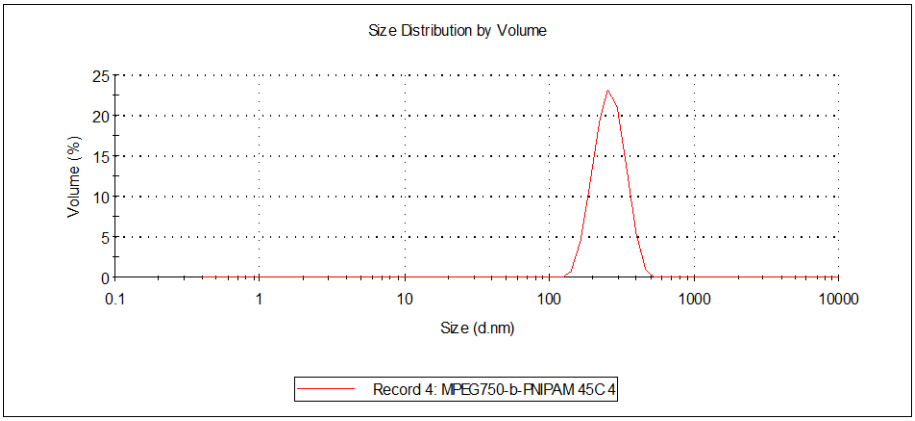
Size Distribution by Volume
Volume (%)
25
20
15
10
5
0
0.1
1
10
100
1000
10000
Size (d.nm)
Record 4: MPEG750-b-PNIPAM 45C 4

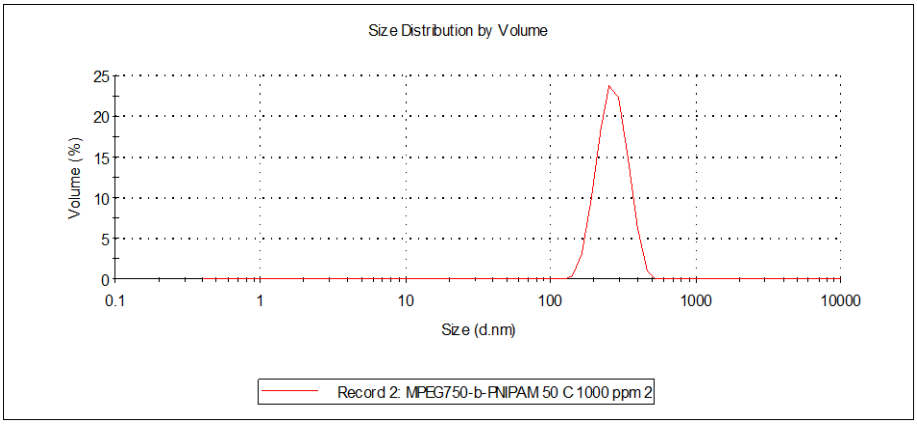
Size Distribution by Volume
Volume (%)
25
20
15
10
5
0
0.1
1
10
100
1000
10000
Size (d.nm)
Record 2: MPEG750-b-PNIPAM 50 C 1000 ppm 2

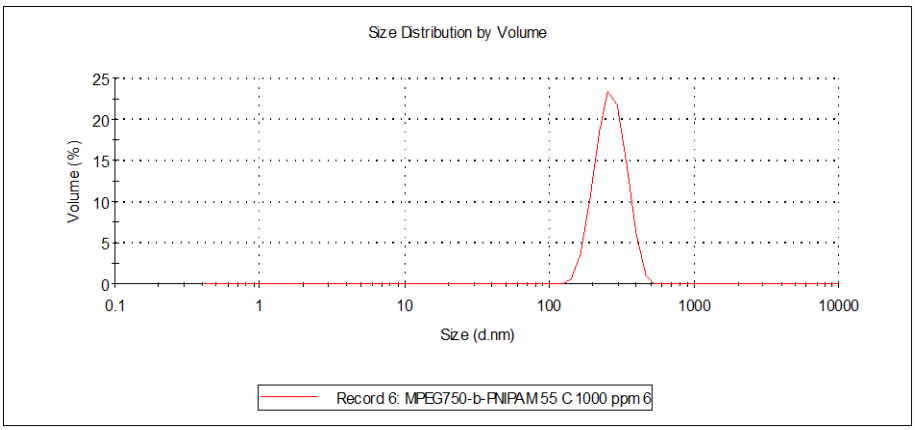

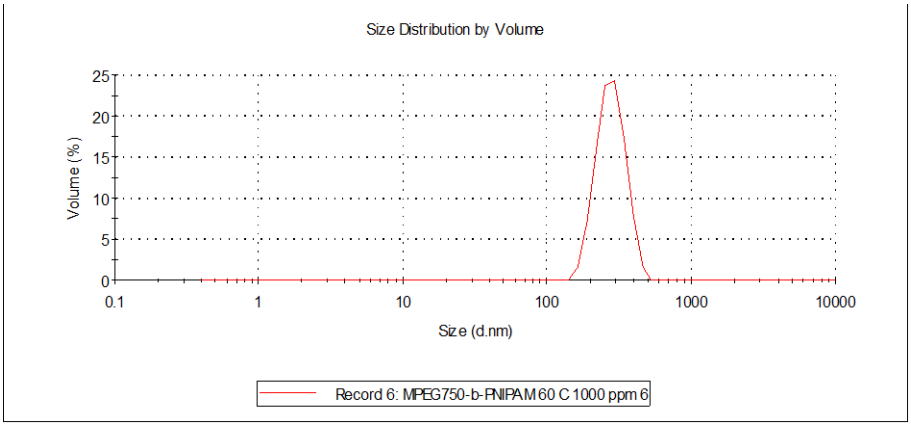

A1.1 MPEG2000-*b*-PNIPAM$_{50}$ 1000 ppm

25 °C

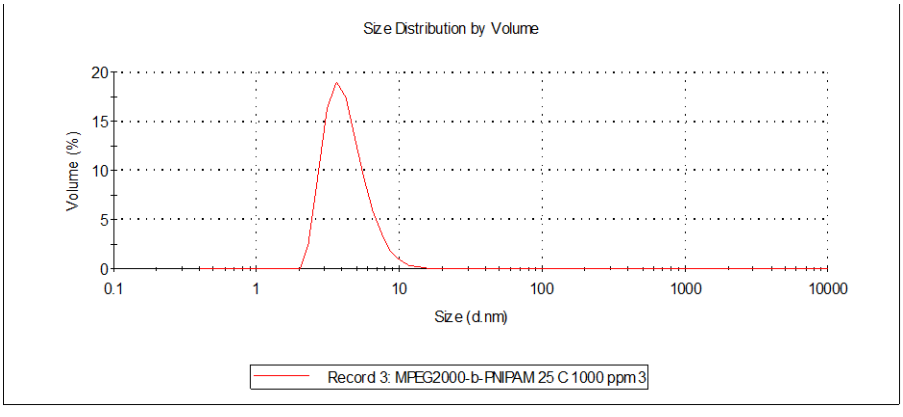

30 °C

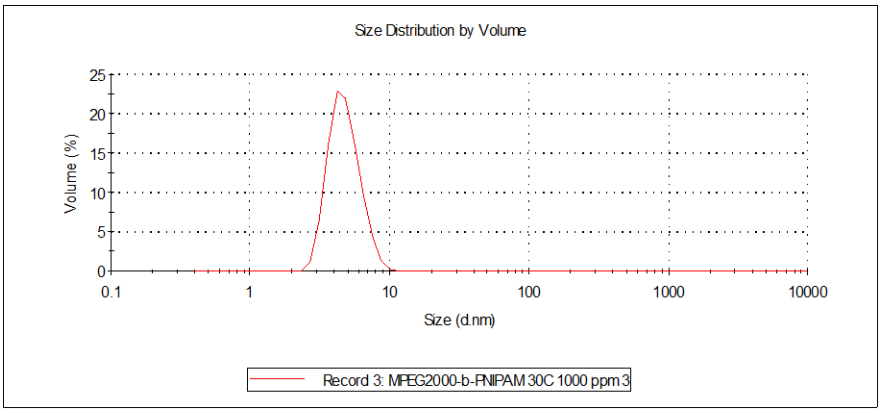
Size Distribution by Volume
Volume (%)
25
20
15
10
5
0
0.1
1
10
100
1000
10000
Size (d.nm)
Record 3: MPEG2000-b-PNIPAM 30C 1000 ppm 3

35 °C

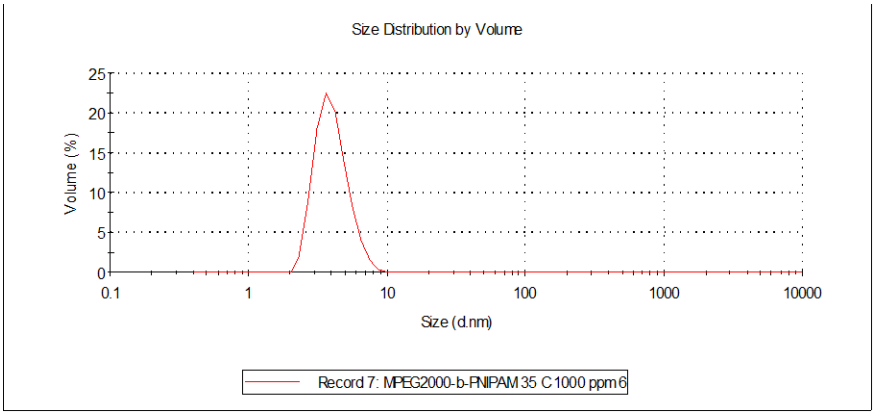
Size Distribution by Volume
Volume (%)
25
20
15
10
5
0
0.1
1
10
100
1000
10000
Size (d.nm)
Record 7: MPEG2000-b-PNIPAM 35 C 1000 ppm 6

40 °C

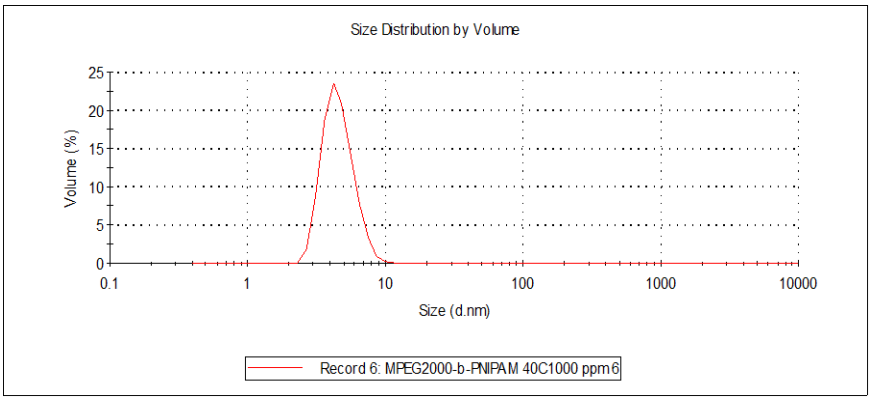
Size Distribution by Volume
Volume (%)
25
20
15
10
5
0
0.1
1
10
100
1000
10000
Size (d.nm)
Record 6: MPEG2000-b-PNIPAM 40C1000 ppm 6

45 °C

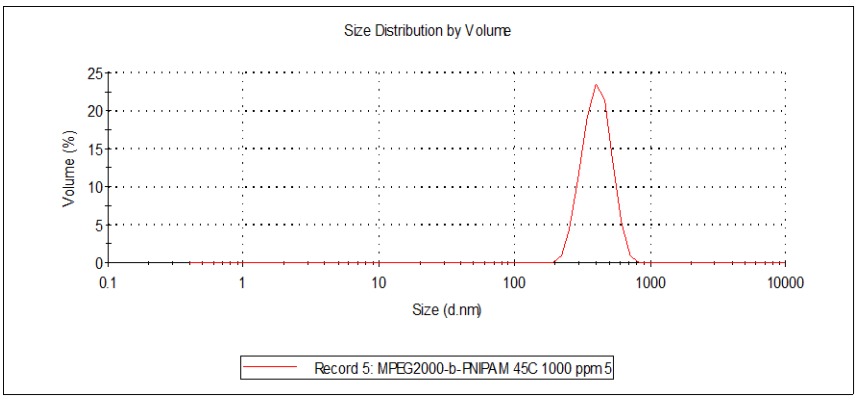
Size Distribution by Volume
Volume (%)
25
20
15
10
5
0
0.1
1
10
100
1000
10000
Size (d.nm)
Record 5: MPEG2000-b-PNIPAM 45C 1000 ppm 5

50 °C

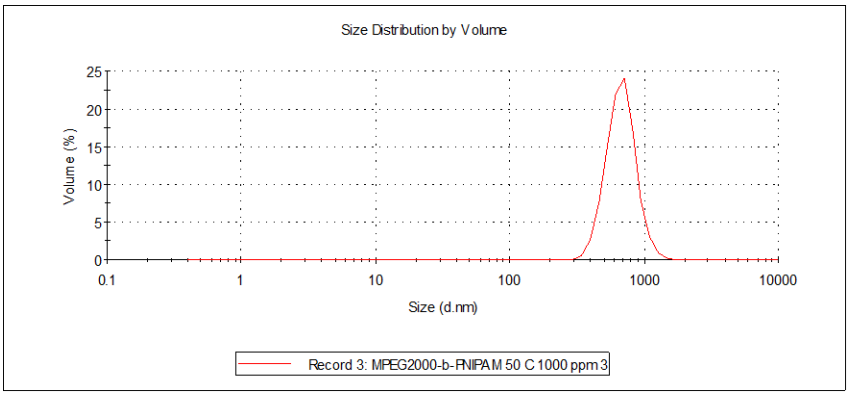
Size Distribution by Volume
Volume (%)
25
20
15
10
5
0
0.1
1
10
100
1000
10000
Size (d.nm)
Record 3: MPEG2000-b-PNIPAM 50 C 1000 ppm 3

55 °C

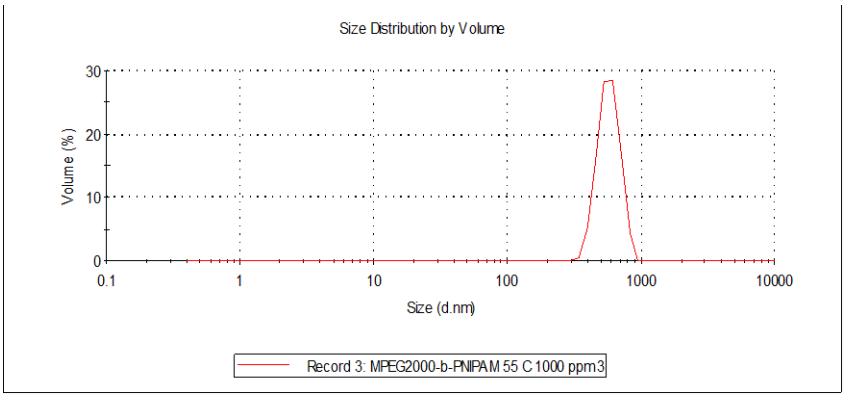
Size Distribution by Volume
Volume (%)
30
20
10
0
0.1
1
10
100
1000
10000
Size (d.nm)
Record 3: MPEG2000-b-PNIPAM 55 C 1000 ppm 3

60 °C

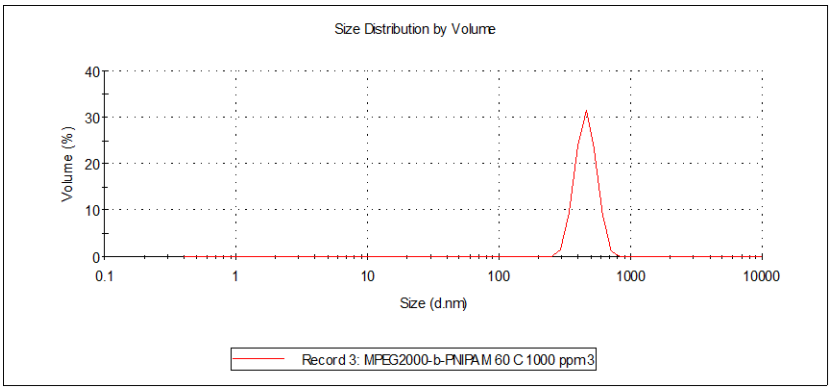

A2. Recoverability Test and Related Equations

Correlation between turbidity and MPEG750-*b*-PNIPAM$_{35}$ concentration at different temperature.

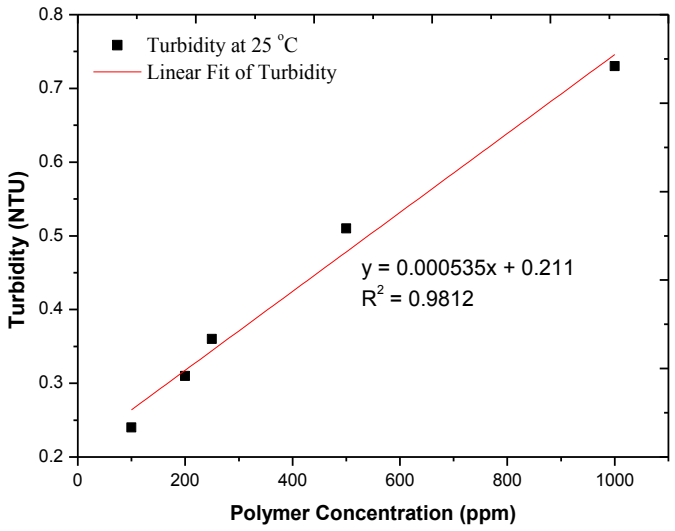

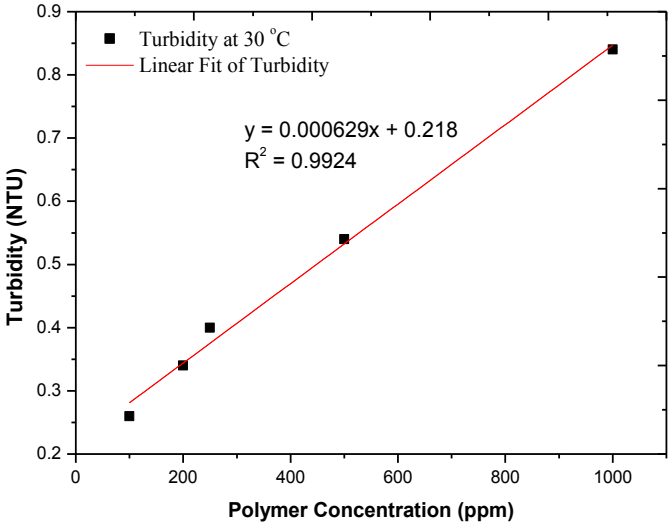
Turbidity at 30 °C
Linear Fit of Turbidity
y = 0.000629x + 0.218
R2 = 0.9924
Turbidity (NTU)
Polymer Concentration (ppm)
0.2
0.3
0.4
0.5
0.6
0.7
0.8
0.9
0
200
400
600
800
1000

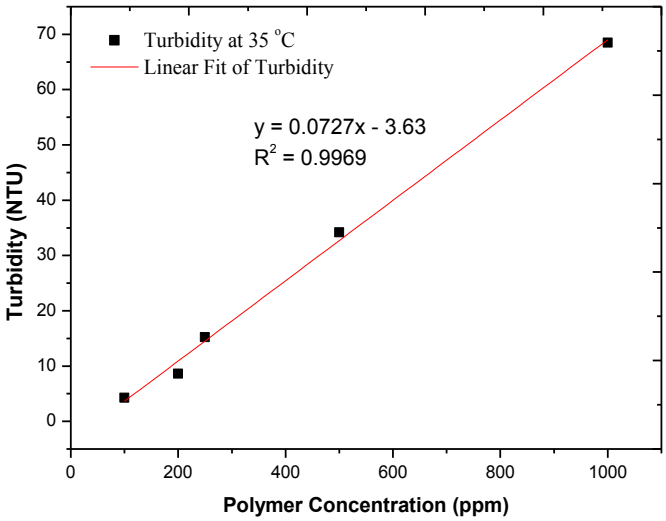
Turbidity at 35 °C
Linear Fit of Turbidity
y = 0.0727x - 3.63
R2 = 0.9969
Turbidity (NTU)
Polymer Concentration (ppm)
0
10
20
30
40
50
60
70
0
200
400
600
800
1000

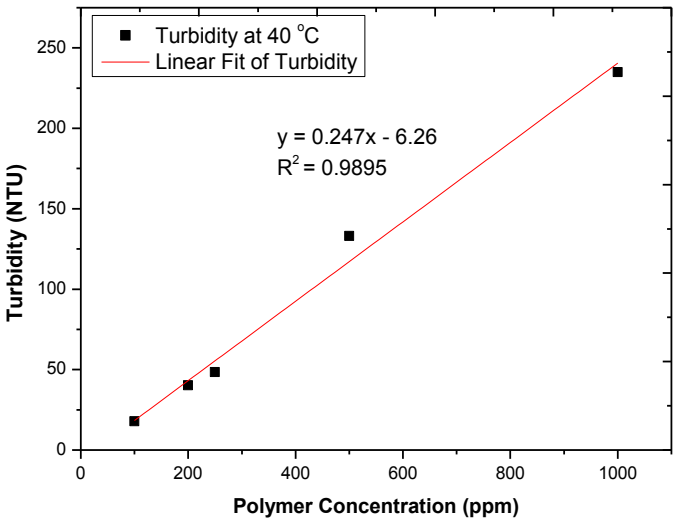
Turbidity at 40 °C
Linear Fit of Turbidity
y = 0.247x - 6.26
R2 = 0.9895
Turbidity (NTU)
Polymer Concentration (ppm)
0
50
100
150
200
250
0
200
400
600
800
1000

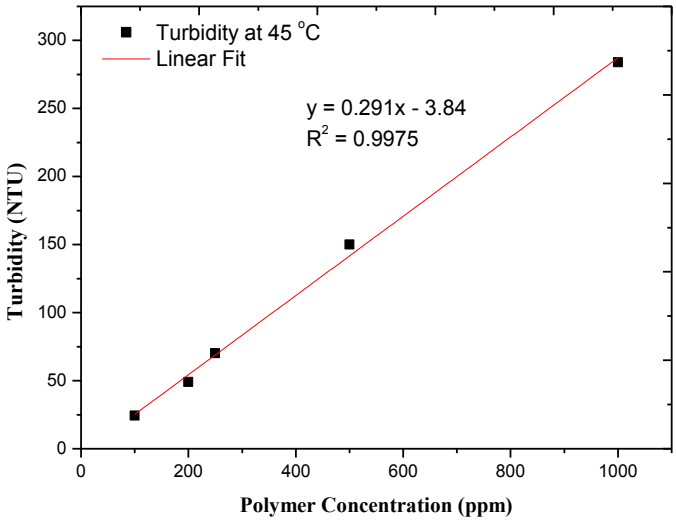
Turbidity at 45 °C
Linear Fit
y = 0.291x - 3.84
R2 = 0.9975
Turbidity (NTU)
Polymer Concentration (ppm)
0
50
100
150
200
250
300
0
200
400
600
800
1000

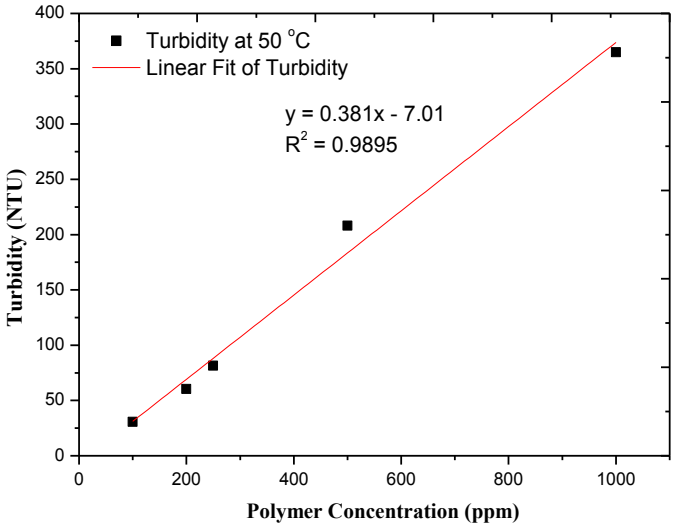
Turbidity at 50 °C
Linear Fit of Turbidity
y = 0.381x - 7.01
R2 = 0.9895
Turbidity (NTU)
Polymer Concentration (ppm)
0
50
100
150
200
250
300
350
400
0
200
400
600
800
1000